NASA SP-96

Significant Achievements in

Satellite Meteorology 1958-1964

NATIONAL AERONAUTICS AND SPACE ADMINISTRATION

NASA SP-96

Significant Achievements in

Satellite Meteorology 1958-1964

Scientific and Technical Information Division 1966
NATIONAL AERONAUTICS AND SPACE ADMINISTRATION
Washington, D.C.

FOR SALE BY THE SUPERINTENDENT OF DOCUMENTS, U.S. GOVERNMENT PRINTING OFFICE, WASHINGTON, D.C., 20402 - PRICE 60 CENTS

Foreword

THIS VOLUME IS ONE OF A SERIES which summarize the progress made during the period 1958 through 1964 in discipline areas covered by the Space Science and Applications Program of the United States. In this way, the contribution made by the National Aeronautics and Space Administration is highlighted against the background of overall progress in each discipline. Succeeding issues will document the result from later years.

The initial issue of this series appears in 10 volumes (NASA Special Publications 91 to 100) which describe the achievements in the following areas: Astronomy, Bioscience, Communications and Navigation, Geodesy, Ionospheres and Radio Physics, Meteorology, Particles and Fields, Planetary Atmospheres, Planetology, and Solar Physics.

Although we do not here attempt to name those who who have contributed to our program during these first 6 years, both in the experimental and theoretical research and in the analysis, compilation, and reporting of results, nevertheless we wish to acknowledge all the contributions to a very fruitful program in which this country may take justifiable pride.

HOMER E. NEWELL
Associate Administrator for
Space Science and Applications, NASA

Preface

THROUGHOUT HISTORY, man's ability to live and work successfully has been, in a large measure, weather dependent. Consequently, he has always tried to predict the future course of weather, in order to be better prepared for its severity and marked changes. Man has been successful in adapting to his local weather by means of proper clothing, housing, and air conditioning. More recently he has been successful in actually modifying the weather, though on a limited scale. For example, man has dissipated fog over airports to permit aircraft to take off and land. He has enclosed a huge volume in a manmade structure (the Harris County Domed Stadium in Houston) so that he might control the weather within that structure. In the last few decades man has been turning to the more ambitious possibilities of controlling weather on a regional and even a global basis. These have included proposals for increasing precipitation over a watershed, for modifying or redirecting the course of damaging hurricanes, and for changing the climate of substantial portions of the Earth.

It is clear, however, that reliable weather prediction and weather control are not possible without a good understanding of the atmosphere's behavior. Without this understanding, weather prediction becomes random in character and weather-control efforts become indeterminate, since they would lack a scientific basis for implementation and evaluation. (For example, there would be no standard of what would have occurred naturally.) Just as understanding is required for reliable prediction and weather-control efforts, an adequate description of the state of the atmosphere is a prerequisite for acquiring the necessary understanding. Thus, it follows that, in fact, observations adequate in number and in quality are at the root of scientific weather prediction and weather control.

The importance of proper information concerning the state of the atmosphere is related to the worldwide character of weather and the extent and rapid rate of movement of storms. Weather prediction thus becomes dependent both on the availability of adequate information about the state of the atmosphere and on the rapid communication of this information to the user.

During the last century, the technological developments that improved weather observation systems have acted as catalysts to the acceleration of

meteorology as a science. In this regard, space technology appears to be emerging as the current major catalyst. Rockets and satellites not only have provided new vehicles for carrying meteorological instruments; they have provided something perhaps more important—an opportunity for a new view of the atmosphere. With rockets, we can sample the atmosphere directly at altitudes never before attained. With satellites, we can look down at the atmosphere and observe its motion and phenomena on a global basis, rather than upward from discrete points on the surface. Further, we can measure the energy input from the Sun without the filtering effect of the atmosphere.

During the past 6 years, NASA, together with the Department of Commerce and the Department of Defense, has been applying space technology to the problem of satisfying the full data observation requirements of meteorology. This document describes the efforts along these lines and the scientific results that have ensued.

There were two significant discoveries very early in the NASA meteorological program. First was the demonstration that the Earth's cloud cover was highly organized on a global scale. Coherent cloud-cover systems were found to extend over thousands of miles, and were related to other systems of similar dimensions. In this manner, the integrated character of the atmosphere on a global scale was clearly shown. Second, weather systems were directly identified by their cloud structure, and so it was possible to identify and locate important atmospheric phenomena such as fronts, storms, hurricanes, cloud fields, and so forth, and chart their courses on a daily basis with extreme accuracy.

Cloud-cover observation began with the launch of Tiros I, on April 1, 1960, and, with the exception of a few short intervals, has been continuous since that date. In fact, since June 19, 1962, meteorological satellites have at all times provided cloud-cover observations.

The most spectacular observations have been those of tropical storms and hurricanes. For example, in calendar year 1964, there were 63 tropical storms in meteorological records. Of these, meteorological satellites observed and tracked 46, and 18 of these were located and identified by meteorological satellite before they were noted in the forecast bulletins issued by cognizant forecasting centers. Of these tropical storms observed in 1964, 7 were hurricanes and 17 were typhoons. Cloud pictures also aided in the delineation of jetstreams and shear lines, and furnished mesoscale-cloud features in areas between regular surface observational sites. The weather-satellite data have been applied to nonmeteorological problems, such as the location and movement of sea ice, the freezeup and breakup of ice in major rivers and lakes, and the variation and extent of snow cover,

swamps, and flooded areas. The weather-satellite data have also been used in following changes in the detail of many geographical features.

The applications described above were based on the TV cloud pictures provided during sunlight only. Measurements of infrared radiation in selected wavelengths have provided some cloud-cover data at night, from which the height of the cloud tops could be inferred. Further, infrared radiation measurements have been used to determine the temperature of the surface of the Earth and of distinctive (radiating) layers of the atmosphere. Refinement and extension of these satellite-borne techniques are expected to produce some of the most valuable new atmospheric data.

Satellites to date do not replace the capability of rockets to take measurements directly in the atmosphere. Thus, meteorological sounding-rocket data have continued to provide important new facts independently. For instance, the rocket data have indicated the existence of different circulation patterns below and above 80 kilometers, suggesting the possibility of different physical mechanisms sustaining the motions. Further, the annual cycle of circulation in the 30- to 60-kilometer region has been shown to include a summer period of east wind and a slightly longer winter period of stronger west winds.

In preparing this document, there has been an undeniable sense of potential, as well as past, achievement. The first-generation experiments and hardware have shown what we can and should provide for measurements for both research and operations. TOS, the Tiros Operational Satellite system, is about to be implemented as the first Weather Bureau operational meteorological-satellite system. Already, improvements to this system are being contemplated, and new types of experiments are being designed that will permit an even greater step forward in future operational satellites. Much has been achieved, and we are confident that there is much more that we can expect to achieve in the future. Meteorology is a science that has application to all mankind, and thus the efforts in meteorological satellites and sounding rockets represent one of the most directly beneficial, peaceful uses of space.

The entire staff of Meteorological Programs, Office of Space Science and Applications, participated in writing this comprehensive report, which describes the significant achievements in the areas of meteorological satellites and meteorological sounding rockets during the past 6 years. The Aeronomy and Meteorology Division, NASA Goddard Space Flight Center, and the National Weather Satellite Center, Weather Bureau, Department of Commerce, provided numerous references that formed the basis of the document. This assistance and the subsequent constructive review of the final document by these groups are gratefully acknowledged.

The collection of the material and its organization and editing were done under the direction of William C. Spreen, Program Manager, Meteorology and Meteorological Soundings Branch, with the assistance of Robert H. McQuain, Staff Engineer, Meteorological Flight Projects Branch, and George P. Tennyson, Jr., Staff Scientist, Meteorology and Meteorological Soundings Branch. The Preface was written by Morris Tepper, Director, Meteorological Programs, Office of Space Science and Applications.

Contents

chapter 1

Introduction

STATUS OF METEOROLOGICAL OBSERVATIONS PRIOR TO 1958

TRADITIONALLY, METEOROLOGISTS have been handicapped by having only a fragmentary knowledge of the state of the atmosphere at a given time. Since the establishment of national meteorological services, in the mid-19th century, observing networks have expanded greatly both geographically and in altitude, particularly since World War II. Still this does not provide sufficient information to describe the atmosphere fully. The vast, sparsely populated land areas of the globe, and the oceans, which cover more than seven-tenths of the Earth's surface, are virtually silent areas as far as meteorological observations are concerned.

Early meteorologists recognized that particular atmospheric motions produced distinct patterns of weather, and so it became necessary to observe and describe the basic atmospheric motions. The first weather charts covered an area of several thousand square kilometers and were restricted to surface observations taken more or less simultaneously at prescribed times. The more these charts were studied and used as a basis for hypothesis, weather analysis, and prediction, the stronger became the realization that for full understanding of atmospheric processes, it was necessary to have knowledge of their interaction, vertically and horizontally, over hemispheric dimensions. The world radiosonde network developed as a result of this. Each radiosonde station twice (and at some locations, four times) daily sends aloft balloons carrying observing equipment that provides information on atmospheric wind, pressure, temperature, and moisture. This vertical sampling of the atmosphere is effective to about 30-kilometer altitude.

While these radiosonde stations have provided a considerable extension of observations into the vertical, little was added to the geographical coverage. It is generally agreed by meteorologists that ideal observation requires measurement of wind, temperature, pressure, and water-vapor content, as well as measurement of heat budget and the concentration of the principal absorbers and emitters of radiation (CO_2, H_2O, and O_3), on a global grid of about 250 to 300 kilometers, from the surface up to 100 kilometers. Meteorologists usually consider the atmosphere below about 100 kilometers as a more or less homogeneous, electrically neutral fluid in

motion. Above this elevation, the nature and the distribution of the individual particles become important, as well as the effect of external influences. However, the conventional surface and upper-air balloon meteorological observations provide adequate coverage over less than 10 percent of the Earth's surface, and only up to about 30 kilometers. This coverage could be expanded somewhat, but economic and physical limitations prohibit adequate global measurements with the conventional techniques. The solution to this problem awaited recent advances in space technology.

RELATION TO SPACE TECHNOLOGY

Experimental sounding-rocket observations in the 1950's demonstrated the feasibility of studying the atmosphere structure above 30 kilometers and also the advantages of viewing the atmosphere from an orbiting space platform. NASA undertook to help solve the meteorological observational problem as part of its mission as set forth in the Space Act, enacted by Congress on July 29, 1958. This act established NASA and provided the charter for its activities in space, including programs in the field of meteorology. The following objectives, here excerpted from the act, are the primary foundation on which the Office of Space Science and Applications (OSSA) meteorological program is built:

> The expansion of human knowledge of phenomena in the atmosphere and space. . . .
>
> The preservation of the role of the United States as a leader in aeronautical and space science and in the application thereof to the conduct of peaceful activities within and outside the atmosphere. . . .
>
> Cooperation by the United States with other nations and groups of nations in work done pursuant to this act and in the peaceful application of the results thereof.

The first of these includes the scientific objective of the OSSA meteorological program. However, it is significant to note that it does not refer to forecasting or weather prediction per se, but rather to the broader task of "expansion of human knowledge of phenomena in the atmosphere." The two other objectives, which concern the image, influence, and leadership of this Nation in the world community, have also guided the program in the past and will continue to do so in the future.

In 1962, Congress recognized the potential of the meteorological satellites developed by NASA for weather analysis and forecasting operations of the Department of Commerce and other agencies. In the Supplemental Appropriations Act of 1962 and thereafter, Congress provided funds and authorized the U.S. Weather Bureau to operate a system for the continuous observation of worldwide meteorological conditions from satellites and for the collection, processing, and dissemination of data for use in weather analysis and forecasting.

OBJECTIVES OF THE METEOROLOGICAL PROGRAM

The overall objective of the meteorological satellite and sounding-rocket program is to provide the space technology that, together with more conventional observational techniques, will increase our knowledge and understanding of the Earth's atmosphere, improve our ability to forecast the weather over extended time periods, and provide a basis for weather-modification experiments.

In addition, as part of the broad national space effort, this objective may be extended to apply to the systematic exploration of the atmospheres of other planets, in a manner similar to the systematic investigation of the Earth's atmosphere.

In more specific terms, the meteorological program objectives are as follows:

Developing Satellite Capability for Identifying and Tracking of Storms

The first and most dramatic application of the meteorological-satellite system has been the identification and tracking of known meteorological phenomena, such as hurricanes, typhoons, and frontal systems. Initially, the satellite-data coverage was limited in area; however, a global-coverage capability has now been demonstrated. It will be increased in scope in succeeding years to fulfill operational requirements. The capability of the satellite to view clouds during the night has also been demonstrated. In addition, to identify and track storms of short duration and significant severity and to observe other critical and rapidly changing meteorological phenomena, a satellite having a more nearly continuous observational capability must be developed. Initial experiments on board satellites at synchronous altitude will determine the level of difficulty of this objective.

Developing Satellite Capability as Part of a Global Weather System

The long-range objective of the satellite observing system is to provide data for global meteorology. Weather forecasts more complex in character or for longer time periods than those involved in the daily identification and tracking of discrete storms require consideration of the atmosphere as a system defined by the measurements of temperature, wind, and moisture. Models have been developed that describe the atmosphere in this manner and there are computers capable of performing the calculations. However, the required quantitative data are not available, and the character and extent of the data-sparse areas are such that it is impractical to provide these observations merely by extending the conventional methods.

The satellite's capability for scanning the entire Earth can be utilized to obtain the required quantitative data. The satellite can be employed two

ways: first, as a sensor platform in itself; second, as an integral part of a system for obtaining, referencing, and reporting measurements taken by automatic sensing platforms located within the atmosphere.

As a sensor platform, the satellite is limited to viewing the atmosphere at a distance and from above. Thus, it must rely on the measurement of the electromagnetic radiation from the atmosphere and the Earth. Infrared radiometers and spectrometers can provide temperature measurements of the Earth's surface and of cloud tops, and an estimate of the vertical distribution of temperature. Microwave techniques can measure surface temperature and characteristics despite the presence of clouds.

Unfortunately, not all of the necessary quantitative measurements can be made remotely from the satellite. Some, at least for the foreseeable future, must be measured within the atmosphere itself. This will require automatic instrument platforms within the atmosphere, including balloons floating at a constant-pressure altitude, fixed and floating buoys, and automatic land stations. Suitable equipment can be readily included in a satellite to interrogate these platforms, receive and record the data with the time and location of the platforms, and deliver this information to a central station. This information can then be fed to automatic computing machines.

Advanced Meteorological Research by Means of Space Vehicles

The meteorological satellites described above are for more or less routine observations. However, a satellite provides a powered and stabilized platform for testing new instrumentation and techniques, and for making unique research observations.

With the development of an orbiting research laboratory, it will be reasonable to consider the feasibility of including an astronaut-scientist aboard who could select particularly interesting phenomena to be studied, and calibrate and maintain equipment.

Exploration of the Atmospheric Region Between 30 and 100 Kilometers

Rocket measurements, meteor trails, and other observations made in the region above 30 kilometers indicate that this region is important to our understanding of the overall circulation of the atmosphere. However, regular observations of the upper atmosphere by the conventional radiosonde are limited in altitude to about 30 kilometers. Beyond this level, the balloon is not feasible for carrying meteorological equipment, and rocket techniques must be used.

To extend observations to locations other then rocket ranges, it will be necessary to develop economical, safe, and simplified rocket sounding systems.

The importance of the region between 30 and 100 kilometers is becoming increasingly clear. Large, significant temperature variations have been measured in this region, which probably influence the lower regions. A knowledge of the variations in this region is also required for space-vehicle design, especially for return and reentry.

chapter 2

Meteorological Satellites

BACKGROUND

THE STIMULATION OF METEOROLOGICAL ACTIVITY during World War II resulted in a great increase of synoptic weather information, especially upper-air data, from many parts of the world, and in a multiplication of new synoptic charts and forecasting techniques applicable to various weather forecasts, from a few hours to a month or more in range. The improvement in weather forecasting did not keep pace with the increase in meteorological observations because of the limited spatial distribution of the data. While the number of observing stations, and the frequency and altitude of the observations increased, the observations were concentrated in a relatively small area of the globe. The ground-based observing stations now in operation provide sufficient coverage of about 10 percent of the globe. In the remaining 90 percent, the density of observing stations is totally inadequate for the requirements of global meteorology and for the solution of long-range forecasting.

Yet the atmosphere is a single entity, in which there are important interactions, both internal and with the surface, with which the atmosphere never reaches statistical equilibrium. There is general agreement that macroscale atmospheric motions can in principle be predicted on the basis of knowledge of their spatial distribution at an initial time, the appropriate boundary conditions, the atmosphere's hydrodynamic and thermodynamic properties, and external conditions. An additional condition is the capability to define the effects of smaller scale motions, both within the atmosphere and at its interfaces, as a function of the macroscale variables.

Much effort has been spent on devising mathematical models of the atmosphere, for numerical weather prediction. However, use of these models has been hampered by an inability to describe properly the initial state of the atmosphere in global or even hemispheric terms, and to check the theoretical models against a fully identified state of the atmosphere. For example, since tropospheric disturbances propagate around the Earth in 4 or 5 days, the initial state of the atmosphere must be defined over at least a hemisphere, or preferably over the globe, for predictions of a week or more.

The solution of these problems requires progress in the understanding and measurement of atmospheric processes, including energy exchange between the atmosphere and its upper and lower boundaries; of the distributive processes and transformation mechanisms for such quantities as energy, momentum, and water vapor; and of the coupling processes between the various regions of the atmosphere. The description and prediction of the behavior of the atmosphere require the development of models of the atmosphere based on these investigations and the laws governing fluid motion. However, the lack of detailed knowledge of the initial and final conditions is the greatest single obstacle to substantial improvement in atmospheric simulation.

The conventional techniques used at surface-based observing locations could not be extended to meet the requirements of global meteorology. However, advances in space technology provided the means of obtaining atmospheric data in the quantity and quality required to define the global state of the atmosphere. In the late 1940's and early 1950's, rockets were used for experimental investigations of the atmosphere. In 1947, a V–2 rocket launched at White Sands, N. Mex., took the first successful photographs of the Earth's cloud cover, from an altitude to 110 to 165 kilometers.

From 1947 to 1950, additional V–2 and Viking rockets carried high-altitude cloud-photography experiments which led to the first serious proposal for meteorological satellites (ref. 1). In 1954, a Navy Aerobee rocket took pictures over the southwestern United States that emphasized the utility of a meteorological satellite. These pictures showed a storm that had passed onto land from the Gulf of Mexico. The complexity of this storm had remained completely undetected by conventional means. The presence of multiple circulation patterns explained previously inexplicable rains that occurred at several inland stations (ref. 2). Thus the ability of high-altitude photography to detect otherwise unknown storms was demonstrated. By mid-1958 work had begun in the Advanced Research Projects Agency (ARPA) of the Department of Defense on a meteorological satellite that was to become Tiros. On April 13, 1959, cognizance of this program was transferred to NASA.

METEOROLOGICAL-SATELLITE PROGRAM

The first Tiros was flown in April 1960, and demonstrated that cloud-cover information provided by a satellite is useful in describing atmospheric motions. It established the value of the spacecraft and supporting ground equipment developed around special sensors, such as cameras and radiation detectors. The successful operation of Tiros I opened the way toward the identification and tracking of fronts and storms from day to day, and the continuous quantitative global observation of the atmosphere.

Seven additional Tiros satellites and a Nimbus satellite have been flown between the first Tiros flight and December 1964, with improvements in lifetime and performance and increases in the capability of the satellite instruments. The data obtained from these satellites have been widely used by meteorologists for both operations and research.

The meteorological-satellite flight program to date consists of Tiros, the Tiros operational satellites (TOS), and Nimbus. The immediate objectives for these projects are as follows:

(1) Development of satellite-system equipment and techniques and satellite launchings, toward both an improved understanding of the atmosphere and the development and continued improvement of an operational meteorological-satellite system.

(2) Cooperation with the U.S. Weather Bureau in the establishment and support of an operational meteorological-satellite system.

Tiros

The Tiros project produced several major results. It demonstrated quite conclusively the feasibility of satellites as a meteorological tool, and gathered useful data that have been used in both research and operations. Tiros data are being actively studied in Government laboratories and in various universities, both in this country and in other countries. A system has been produced for acquiring and transmitting satellite information in time for operational use. Tiros has thus demonstrated a peaceful use of space technology that the peoples of the world can appreciate as a benefit to themselves.

Tiros has great operational importance. Over 1000 special storm advisories have been issued by the U.S. Weather Bureau on the basis of Tiros data, and between July 1961 and December 1964, 118 tropical storms were tracked, and 36 discovered, by the Tiros satellites.

The operational efficiency of the Tiros program hardware has been most satisfying. The record of eight successful launches out of eight attempts is clear indication of the advances in hardware reliability and in launch techniques.

One of the more recent sensory subsystems, which has received worldwide recognition, is the automatic-picture-transmission (APT) camera. This system, originally conceived for the Nimbus program, has been demonstrated successfully on Tiros VIII. The APT ground equipment consists of a simple tracking antenna, a receiver, and a facsimile reproducer, and is now commercially available. This system enables users with inexpensive ground equipment to obtain local cloud-cover pictures as the satellite passes overhead. This local cloud information gives the forecaster a "snapshot" of the weather pattern affecting his area and permits him to make more accu-

rate short-term weather predictions for air terminals, refueling operations, and other similar cloud-dependent activities.

Tiros Operational Satellites (TOS)

One of the most outstanding contributions of the meteorological satellite R&D program to date is the basis it has laid for TOS. TOS is funded and managed by the U.S. Weather Bureau and will provide cloud-cover pictures of global scope, both recorded for readout at the command-and-data-acquisition (CDA) stations and also as direct readout to local users. The two spacecraft required will be placed in sun-synchronous, near-polar orbits, with 9 a.m. and 3 p.m. daylight equatorial crossings. One spacecraft will provide recorded data and the other will provide direct-readout data. The system will be implemented early in calendar year 1966, with the launching of spacecraft based on the cartwheel Tiros design. The TOS spacecraft will use the advanced vidicon camera system (AVCS) and the APT camera, both developed for Nimbus. Systems and sensors checked out in the Tiros and Nimbus R&D program will be incorporated in future models in the TOS program.

Nimbus

The Nimbus spacecraft was originally conceived, even before the launch and operation of the first Tiros, as the second generation of meteorological satellites. It was to remedy, to the maximum extent possible, the deficiencies of Tiros. The basic objective was a fully instrumented meteorological observatory in space, to provide data for operational and research use. The stabilization system, the power system, and the sensory ring are all separate and independent. Thus, each can be replaced with an improved version, without affecting the basic design. The sensory ring is of standard modular construction so that, again, elements can be readily replaced by new versions.

There are three different sensors on Nimbus I—AVCS, High-Resolution Infrared Radiometer (HRIR), and APT. The AVCS is a three-camera array, whose information is recorded on magnetic tape for readout by the CDA stations. The AVCS is capable of providing, from the satellite at design altitude, TV cloud-cover pictures with a nominal resolution of 1 to 2 kilometers for the daylight portion of the world. Night cloud-cover observations are provided by the HRIR, whose data are also recorded on magnetic tape for readout by the CDA station. The HRIR operates in one spectral band (3.4μ–4.2μ) at a resolution of 8 kilometers. The third sensor is the APT camera, which provides direct local readout to inexpensive ground equipment when the satellite is within line of sight of the receiving antennas. The Nimbus satellites will fly and test new sensors and techniques.

TECHNOLOGICAL ACHIEVEMENTS WITH TIROS

Spacecraft Configuration

Tiros I had a very successful configuration, which has remained essentially unchanged through seven later models. This success is attributed not only to the advanced design of the spacecraft proper, and the power, control, stabilization, and communications equipment, but also to the concept of infrared- and television-experiment packages, with their data-processing subsystems.

The specific goals of the Tiros development are as follows:

(1) Develop a local-readout capability to give immediate operational use of data.
(2) Develop techniques for observation of the Earth's cloud cover and radiation budget over an increased area.
(3) Provide more frequent observation of the Earth's cloud cover and radiation budget.
(4) Develop increased accuracy of observations and of their geographical location.
(5) Optimize observation techniques with respect to launch characteristics and orbital parameters.
(6) Develop effective techniques of acquiring and processing data for both research and operations.
(7) Develop spacecraft technology that will provide a suitable basis for TOS.

The relative simplicity and surprisingly long operating lifetimes of Tiros have provided the basis for TOS. Essentially, it will consist of a Tiros satellite reoriented in a "cartwheel" configuration (fig. 1).

The first Tiros spacecraft had a polyhedral-prism configuration with 18 flat side panels, weighed from 270 to 300 pounds, depending upon the sensor complement, and was about 22 inches high and 42 inches in diameter. The sides and top of each spacecraft were covered by more than 9000 solar cells, to convert sunlight into electrical power. The bottom flat end, or base plate, which looked earthward during part of each orbit, held a majority of the satellite components, including sensors, recorders, and power, control, and communications equipment (fig. 2).

Table I lists the experiments and useful life of each of the first eight Tiros satellites. Each spacecraft carried two television cameras and some carried one or more infrared sensors, which usually looked through openings in the baseplate. Tiros VII carried an electron-temperature probe (ETP), with the circuitry necessary to measure variations in electron temperature and density with latitude and time of day. Provision was made to store the output on the infrared tape recorder until its transmission.

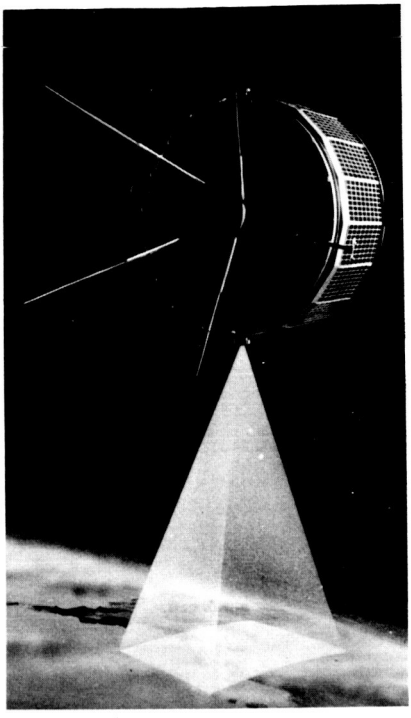

Figure 1.—The Tiros operational satellites "cartwheel" configuration.

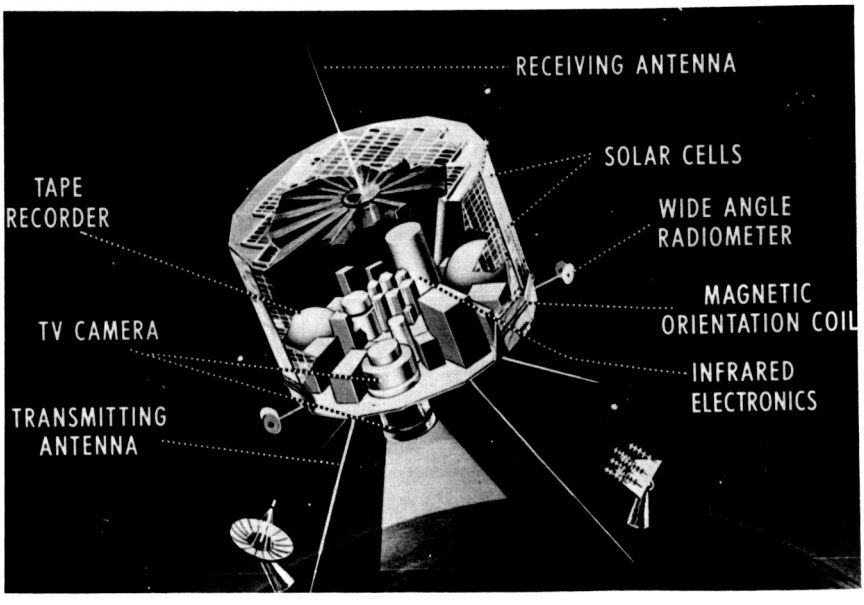

Figure 2.—First Tiros configuration and components.

Table I.—*Tiros I–VIII Flights and Sensors*

Launch date	Tiros I, April 1960	Tiros II, Nov. 1960	Tiros III, July 1961	Tiros IV, Feb. 1962	Tiros V, June 1962	Tiros VI, Sept. 1962	Tiros VII, June 1963	Tiros VIII, Dec. 1963
Useful orbital life, months	2½	10	4½	4½	10½	13	(a)	(a)
Weight, lb	263	278	285	286	287	281	298	260
Camera:								
Narrow-angle	1	1	.....	.....	.....	.....	.....	.....
Medium-angle	.....	.....	.....	1	1	1	.....	.....
Wide-angle	1	1	2	1	1	1	2	1
APT	.....	.....	.....	.....	.....	.....	.....	1
Radiometer:								
Medium-resolution	.....	1	1	1	.....	.....	1	.....
Low-resolution, wide-field	.....	1	1	1	.....	.....	.....	.....
Low-resolution, omni-directional	.....	.....	1	1	.....	.....	1	.....
Electron temperature probe	.....	.....	.....	.....	.....	.....	1	.....

[a] Operating as of Jan. 1, 1965.

Sensor Subsystems

Probably the most striking achievements of meteorological technology have been the visual results of data collected by the on-board sensor subsystems (fig. 3).

Television Camera

The major sensor accomplishment aboard Tiros has been television-camera subsystems designed to show continuous cloud-cover patterns over thousands of square miles at high resolution. The television subsystems provided both direct and remote picture-taking capabilities. The cameras were able to take pictures directly and transmit them without storage when within range of CDA stations on the ground, or to record pictures, using magnetic-tape storage, over remote areas. In the record mode, either one camera or both could be programed by ground command to take a series of pictures over prescribed remote areas and store them. Readout and reprograming were accomplished during the next pass over a CDA station.

The cameras were mounted on the baseplate of the spacecraft, with their optical axes parallel to the spacecraft spin axis. It should be noted that the camera alinement differs somewhat for Tiros *I*, the first Tiros operational

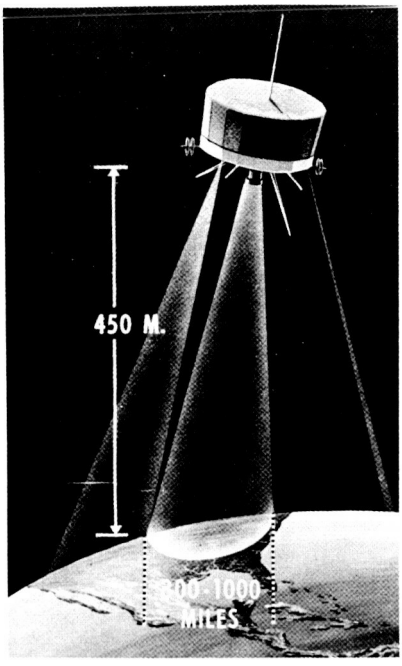

Figure 3.—Tiros sensors include two TV cameras, a multichannel scanning radiometer, and nonscanning radiometers.

satellite, which will be maneuvered into the "wheel" position, as depicted in figure 4. (It should also be pointed out here that it is customary to give spacecraft letter designations—like Tiros *I*—before launch, and change the designation to a number after launch.)

The optical sensors in the TV subsystems may be classified as narrow-angle, medium-angle, and wide-angle cameras, and as storage or nonstorage devices. Table II presents a comparison of the three classes of recording cameras and the APT camera.

The TV tubes, with the exception of the APT type, were 500-scan-line, ½-inch vidicons, with a persistence that permitted a 2-second scan with less than 20-percent degradation in picture quality. The tubes were made especially rugged for the launch and space environments, and used a long-persistency photosensitive material in the vidicon target which was specifically developed for Tiros. The seemingly long 2-second readout period was necessary to limit the video bandwidth for magnetic tape recording. The minimum interval of 10 seconds between pictures gave time to erase the target image electrically.

The video output was frequency modulated with a deviation of ± 15 kc/sec. The modulator output was fed to the tape recorder in the record mode and to the TV transmitter in the direct mode. The tape speed dur-

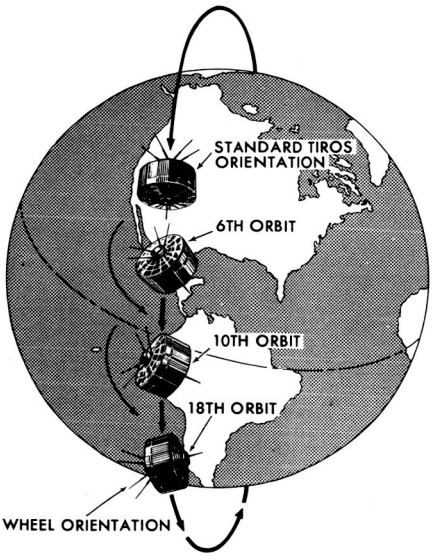

Figure 4.—Orientation of Tiros wheel configuration in orbit.

Table II.—*Tiros TV and APT Camera Parameters*

Parameter	Wide-angle camera	Medium-angle camera	Narrow-angle camera	Automatic picture transmission camera
Picture size, n. mi. [a]	700×700	420×420	70×70	800×800
Lines per frame	500	500	500	800
Frame readout time, sec	2	2	2	200
Video bandwidth, kc	62.5	62.5	62.5	2.4
Stored pictures per orbit	32	32	32	None
Percent picture overlap in the direction of motion.	50	10	None	
Peak power, watts	9	9	9	40 [b]
Lens	Elgeet, 105°, f/1.5	Tegea, 78°, f/1.8	Cinegor, 12°, f/1.8	Tegea, 105°, f/1.8

[a] Based on camera looking down vertically from a 400-nautical-mile orbit.

[b] This includes 18 watts for the camera and 22 watts for the transmitter.

ing recording and playback was 50 inches per second, with sufficient tape allotted to record 32 frames. During playback, the entire reel of 32 pictures could be read out in 100 seconds. Either of the two FM transmitters provided for relaying video data could be energized by command at any one time. Transmitted data also included Sun-angle position information that

had been previously recorded. The transmitter output was 2 watts at a carrier frequency of 235 Mc/sec.

The Tiros cameras were alined parallel to the satellite spin axis and took pictures at 10- or 30-second intervals. The latter gave 50 percent overlap of wide-angle pictures. The wide- and narrow-angle cameras have resolutions of 1½ miles and 1000 feet, respectively, at subsatellite point, and vertically cover areas of about 1200 kilometers and 100 kilometers on a side, respectively. Tiros III had no narrow-angle camera but two wide-angle cameras because of their greater value for cloud observations. The medium-angle lens used in Tiros IV, V, and VI had a 78° field of view and a 1-mile resolution.

Automatic Picture Transmission (APT) Camera

One of the newest camera sensors, the APT, provides for automatic, real-time readout of television cloud data to local viewers having inexpensive ground receiving stations. The APT was designed to provide wide-angle cloud-cover pictures. It employes a camera-vidicon arrangement designed to operate from a spin-stabilized spacecraft. The camera can take and transmit pictures on command, continuously and in real time, during the daytime orbit.

The APT system includes four major elements: the sensory housing containing the camera (fig. 5), a special 1-inch vidicon, and vidicon electronics; the video-electronics module, made up of the video detector, timing and switching circuitry, and power converters; the APT FM transmitter; and the tape recorder. The vidicon differs from other 800-scan-line vidi-

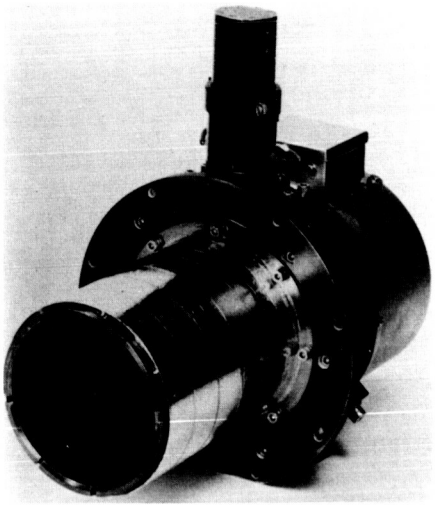

Figure 5.—**Sensory housing of automatic picture transmission (APT) system.**

cons in that it has a polystyrene layer to provide extended image-storage capability. The tube is operated through the prepare, expose, and readout phases by varying the mesh potential with respect to the target potential; i.e., the image is projected on a photoconductive layer, then transferred by potential change to the storage layer for readout. The initial operations through picture transfer require 8 seconds, with an additional 200 seconds required for slow readout at a scan rate of four lines per second. The vidicon output is amplified and applied to the video detector. Detection produces a continuous, analog readout, which is then used with a 2400-cps subcarrier to modulate the 136.950-Mc/sec APT transmitter (ref. 4).

Meteorologists are thus able to observe cloud-cover pictures of their area as the image forms on the facsimile machine at their stations. Each APT ground station can receive, depending on the satellite's elevation angle, up to three pictures during one pass, provided the satellite is within a 1500-mile radius of the station for transmission. Figure 6 shows receiving and facsimile equipment built by NASA, with antenna-position indicator, FM receiver, antenna controls, facsimile calibrator, and power supply on the left; facsimile equipment at the right.

Tiros VIII carried the first APT system, which weighed a total of 24 pounds and consumed 40 watts during transmission. This included 22 watts to operate and synchronize the solid-state 5.5-watt-output transmitter.

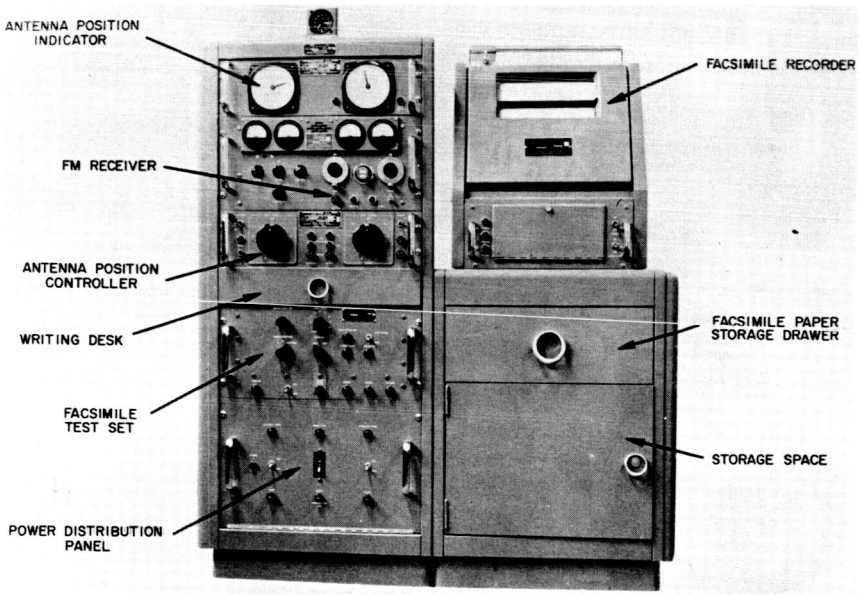

Figure 6.—Receiving and facsimile equipment for APT system.

The 5.7-millimeter, f/1.8 Tegea Kinoptic lens was able to photograph areas of about 800 miles on a side when looking directly at the Earth. The electromagnetic camera shutter permitted a 3-millisecond exposure to produce the 800-scan-line picture on the vidicon. This shutter operation had one-half the speed of previous Tiros camera operations and thus achieved higher resolution, due to a longer exposure.

Radiometers

The infrared detectors have three distinct formats. Two were designed to obtain low-resolution data, while the third obtains medium-resolution data over a relatively large area, by using an optical scanning technique. Some of the more important objectives of the IR-sensor measurements were to evaluate methods of determining the radiation balance of the atmosphere, to experiment with means of observing the cloud cover at nighttime, and to experiment with other methods of observing the structure and processes of the atmosphere (ref. 3).

Low-Resolution Infrared Radiometers (LRIR)

The LRIR devices are rigidly affixed to the main spacecraft and are nonscanning. The main difference between the two types is that one provides a more continuous view of the Earth's thermal-radiation characteristics, because the measuring elements are mounted on supports that project outward from the spacecraft body. This affords the detectors an unobstructed field of view (ref. 5). This omnidirectional LRIR is also referred to as the "University of Wisconsin Experiment." The other type of LRIR views through the baseplate.

The omnidirectional sensor has two wide-angle, low-resolution, IR-detection devices with suitable output-processing circuitry (ref. 6). Each of these has one white and one black bolometer, and the two sets are separated by 180° (fig. 7). This type of experiment was first used on Explorer VII. The bolometers are 1-inch hemispheres. The net effect of these four hemispheres is that of a white sphere and a black sphere of the same diameter isolated in space. The blackbody absorbs most of the incident radiation, while the white body is sensitive mainly to radiation whose wavelength is longer than approximately 4μ. This enables a subtraction of the direct solar radiation, with a resulting inference of the Earth's reflected radiation and the total radiation reaching the satellite. The field of view is that part of the Earth bounded by the horizon as seen from the altitude of the satellite. This sensor was used on Tiros III, IV, and VII (ref. 7).

The second type of LRIR was flown on Tiros II, III, and IV, and is often referred to as the "low-resolution, nonscanning radiometer." This device

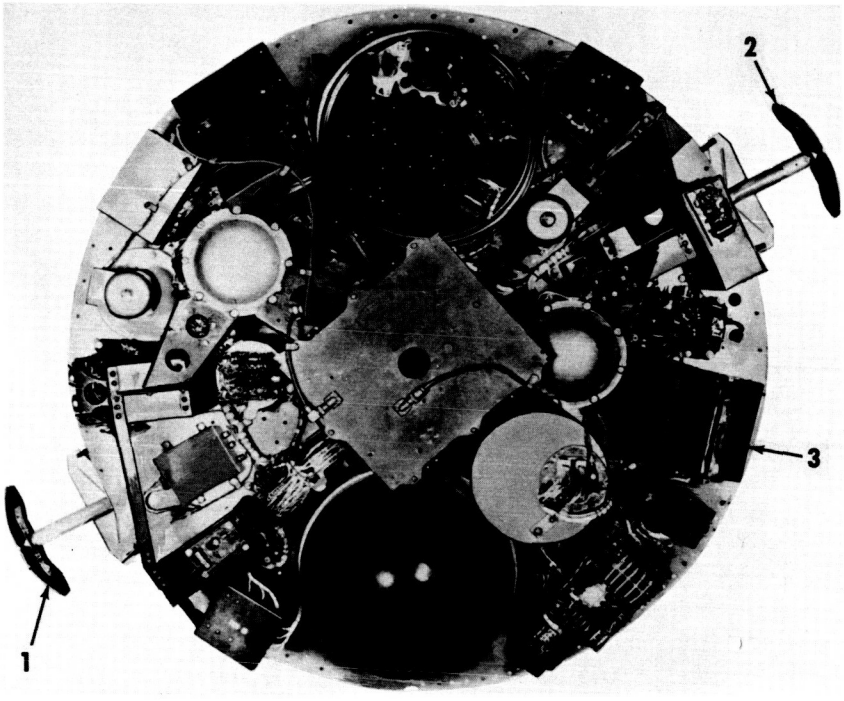

Figure 7.—**Tiros low-resolution, omnidirectional infrared radiometer (1) and (2), and medium-resolution infrared radiometer (3).**

was designed to measure the thermal and reflected solar radiation from the Earth, to permit the determination of the apparent blackbody temperatures and albedo of the Earth. It consists of two detectors mounted on the Tiros baseplate, so that the view is parallel to the spin axis (fig. 8). One detector is sensitive to the total radiation in the vicinity of the Earth (0.2μ to 50μ); the other is sensitive only to the radiation emitted by the Earth, from 5μ to 50μ.

The output of each detector is amplified, and the resulting signal is used to modulate separate audiofrequency oscillators. This modulated output is processed through the time-sharing switching circuit with the output of the scanning radiometer (ref. 8). The sensor instrument has a total weight of 46.3 grams.

Each of the LRIR devices has a 720-kilometer-diameter field of view, purposely located within the field of view of the wide-angle television cameras. The spin-stabilized Tiros satellite is space oriented, so the radiometer has its field of view filled by Earth for a maximum of one-fifth of the orbital period (ref. 9).

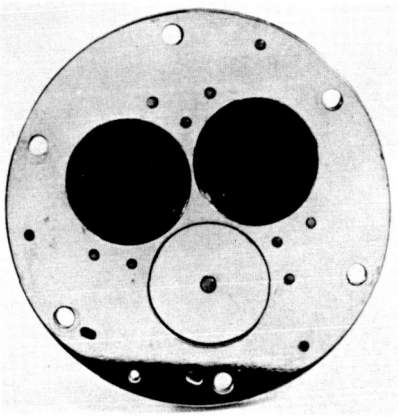

Figure 8.—Tiros low-resolution, nonscanning infrared radiometer, approximately 3 inches in diameter.

Medium-Resolution Infrared Radiometers (MRIR)

The most impressive radiometer, from the point of view of versatility, coverage, and resolution, was the scanning type used on Tiros II, III, IV, and VII (fig. 9). This measured simultaneously radiation emitted and reflected by the Earth and its atmosphere in five spectral regions. It scanned the Earth during the whole Tiros orbit. The radiometer consists of five thermistor-flake bolometers, equipped with suitable filters to provide individual channel sensitivity. These detectors view a narrow field down through the baseplate at a 45° angle to the spin axis. A reference level is obtained by having the detectors alternately look into space at a 4° to 5° angle (ref. 5). The detector location can be seen in figure 7. Each channel has the same principle of operation: the alternating voltage generated at the thermistor bolometer is proportional to the difference in radiation energy coming from two opposite directions (through the satellite wall and base) and impingent upon a chopper disk that has alternate black and mirrored halves. An individual disk simultaneously rotates at 46 rps for each of the five channels, which have almost identical output circuitry to preamplifiers and tape recorders. A block diagram of one channel of the MRIR is shown in figure 10 (ref. 10). This experiment has a 5° field of view for each channel, corresponding to a 50-kilometer resolution directly below.

Continuous radiation measurements are made through each orbit. Data are recorded on the satellite's endless loop of magnetic tape for a period of 100 minutes. Any remaining data not transmitted to the CDA stations at the end of this period are erased as new information is recorded.

The composite signal containing data from the five-channel MRIR and from other instruments is recorded on magnetic tape at the ground station

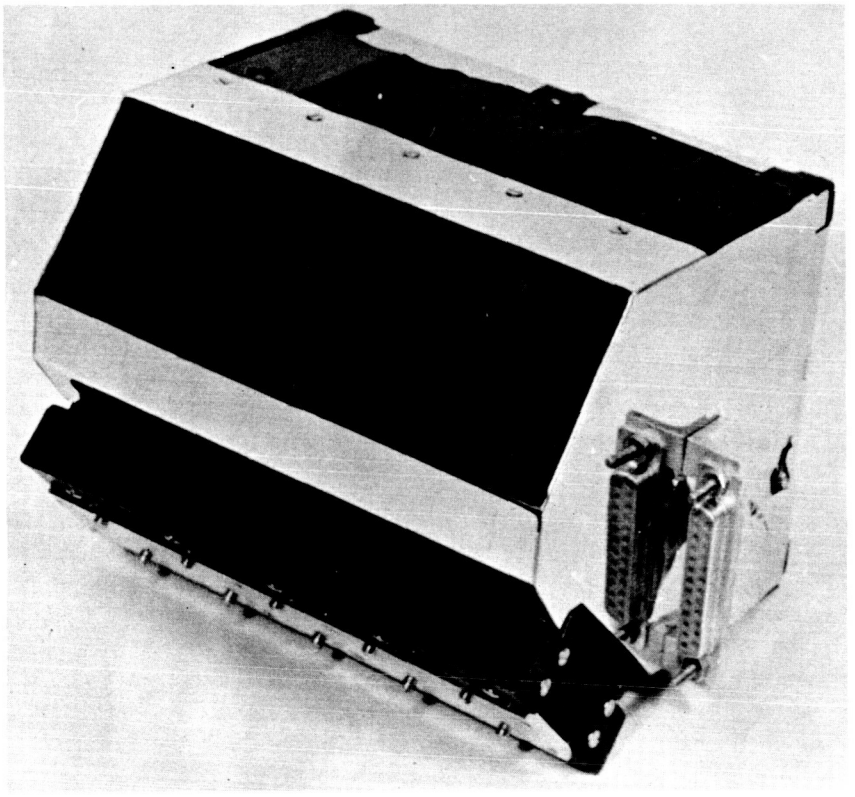

Figure 9.—**Tiros five-channel, medium-resolution infrared radiometer, approximately 6 inches wide.**

in analog format. In ground processing, the tapes are later converted into digital format for computer use.

A more advanced MRIR digital data-processing system has been developed for sequentially sampling each of the five MRIR channels and converting the readings to digital format. The data from one orbit can be stored on an eight-track, 10^7-bit-capacity digital tape recorder.

Attitude Control and Stabilization

The 263-pound, 18-sided Tiros I was launched into a nearly circular orbit by the Thor-Able rocket. A stable rotation of the satellite about its spin axis was maintained between 9 and 12 revolutions per minute. Three relatively simply devices were used to achieve dynamic spacecraft control: (*a*) spin-reduction mechanisms (yo-yo devices) to absorb excess spin energy after third-stage separation, consisting of a pair of cable-attached masses re-

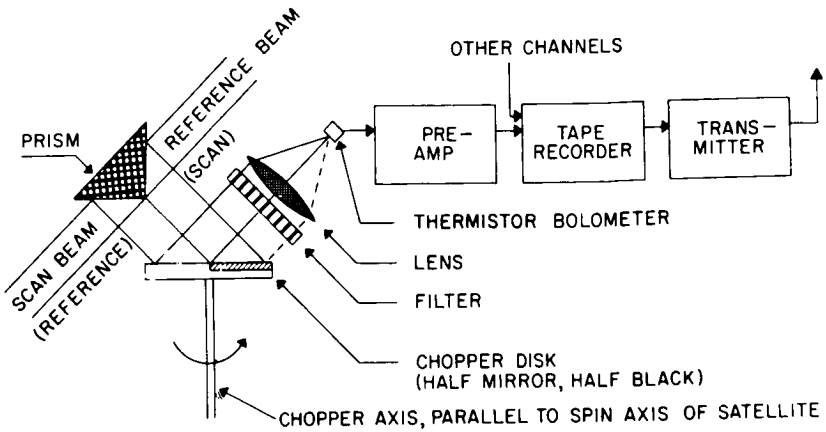

Figure 10.—**Block diagram of one channel of the Tiros medium-resolution infrared radiometer.**

leased from opposite sides of the satellite by the firing of small explosive elements (squibs); (*b*) precession dampers, consisting of variable sliding masses on vertically diametric monorails, to damp out initial satellite wobble due to precession or nutation; and (*c*) spinup rockets at diametrically opposite peripheral points, to compensate for the low spin of the satellite, caused by the reaction between the contained magnetic materials and the Earth's magnetic field.

The attitude of Tiros I had to be accurately determined for the pictures taken by on-board TV cameras. Attitude information was provided by Sun-angle sensors and horizon-scanners, for Sun-angle referencing and for spin-axis orientation, respectively. The north indicator included nine equally spaced, peripheral Sun sensors to provide data for Sun-angle calculations that located north in each picture. A horizon-scanning infrared sensor determined when the satellite field of view crossed the horizon, as in excessive dipping to one side. The resultant data beaconed to the ground helped determine the satellite space position relative to Earth (ref. 11).

An important innovation was installed in Tiros II to enable a correction of attitude. This was a magnetic attitude-control system using a simple coil around the outside lower portion of the satellite. The energized coil generated a controlled magnetic field, which interacted with the Earth's field to provide a gradual tilting or untilting in a given direction, as shown in figure 11.

The use of these basic attitude-control and stabilization techniques continued through the first eight Tiros satellites. Tiros *I* will be the first

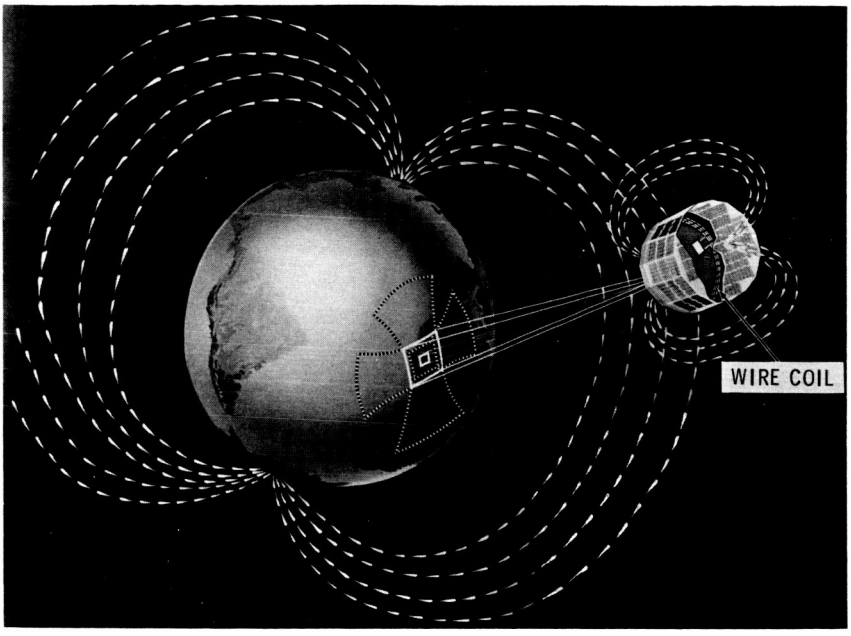

Figure 11.—**Stabilizing Tiros in orbit. The wire coil around Tiros generates a magnetic field, which interacts with the Earth's. This permits tilting of Tiros to provide the best angle for the satellite's solar cells and sensors. The patterns on Earth show how deviations in Tiros' attitude affect the angle of pictures taken by its TV cameras.**

spin-stabilized, wheel-mode satellite, and will introduce new magnetic attitude-control coils to establish three controllable dipoles, or magnetic moments, about the satellite axes. These are: (*a*) the quarter-orbit magnetic control (QOMAC), to place and keep the spin axis perpendicular to the orbital plane; (*b*) the magnetic bias control (MBC), to eliminate any residual magnetic forces and provide fine QOMAC control; and (*c*) the magnetic spin control (MASC), to vary the spin rate in response to ground commands. A dynamics controller (Dycon) programs the operation of the control coils, and other triggered mechanical functions.

Because of its wheel orientation, Tiros *I* also must use different attitude sensors. Two infrared horizon sensors will be placed in an inverted-V configuration, so that two sensors look along the V-legs toward Earth from a point on the wheel perimeter. If the satellite spin axis is not normal to the orbital plane, a yaw error signal is generated by an inequality in the pulse durations of the two sensors, and the yaw-stabilization mechanism is activated.

Power Generation and Storage

Continuous power is vital to functioning and control of the satellite, its sensors, and its data and communications systems. This power is supplied by sealed storage batteries that are periodically recharged by converted solar energy. The power loads are unique because of such factors as day-and-night sensor operations and the location of CDA stations. The latter factor also influences the type of on-board data storage and the period of satellite interrogation, which may require more power.

Solar energy is accumulated from a large number of solar cells. These cells are interconnected in various series and parallel arrangements for convenience in making power connections and protecting or bypassing groups of cells because of electrical or radiation damage. Each cell is a sandwich of alternate P/N-type semiconductor elements, with aluminum collector and radiator foils. The cells have an optical coating to improve thermal efficiency.

The first Tiros used approximately 9200 top and wall solar cells, with an average conversion efficiency of 7.5 percent, to produce an average power output of 25 000 watt-minutes per day. This power charged 63 nickel-cadmium batteries, regulated in three groups to control distribution and to prevent overcharge damage.

Battery power is used directly, both regulated and unregulated, and may also be converted to alternating current, as in the case of the transport drive for the tape recorder. The average output power provided for Tiros operations was about 20 watts, with up to 50 watts available for a short, urgent demand.

As one result of a continuing power-supply improvement program at NASA's Goddard Space Flight Center, the radiation resistance of the basic solar cells has been improved considerably by an inversion to N/P cells. These cells, which have a 10- to 12-percent conversion efficiency, were included in Nimbus I and Tiros *I* (ref. 5).

Data Processing and Storage

Since the first Tiros, the requirements for storing meteorological data over a major portion of the Earth, combined with and for commanded readouts to ground stations over relatively short time periods, have led to sophisticated spaceborne tape recorders. These have reliable switching and can change from slow recording speeds to much faster readout speeds for transmission. The magnetic tape recorder can withstand the stresses of launch, and can record accurately and continuously over long periods of time in the face of spacecraft movements. Also, progress has been made on instrument bearing technology; dynamic tape-reel operation; wide-temperature magnetic tape; spacecraft-momentum compensation for recorder "on-off," reversal, and

running operation; and longer reels of tape, such as endless loops. New concepts were developed for miniaturizing recording and playback amplifier mechanisms, for electrically shielding vital components from magnetic fields, and for increasing the information packing density on the tape.

The satellite tape recorders store sensor, telemetry, and attitude data, both analog and digital. The information stored for one TV picture may approach 250 000 bits. For the next several years, such a tape recorder will provide the most practical means of satellite data storage, pending the development of other means, such as adequately sized memories. The main advantages of the latter will be elimination of moving parts and the choice of selecting specific data for readout without destroying it.

TECHNOLOGICAL ACHIEVEMENTS WITH NIMBUS

Spacecraft Configuration

The Nimbus satellite program, initiated by NASA in August 1959, required significant advances to improve on the Tiros system. The goals included the development of a spacecraft capable of the following:

(1) Complete global coverage, through the use of a quasi-polar orbit.
(2) Completeness and simplicity of observation, through use of an Earth-stabilized configuration.
(3) Accommodation of a number of relatively advanced sensors.
(4) Easy replacement of sensory subsystems.
(5) Collection of new operational and research data.

The attainment of these objectives led to a comparatively large and sophisticated spacecraft (fig. 12). As configured for its first flight, on August 28, 1964, Nimbus I was nearly 12 feet tall, 5 feet in diameter at the base, about 10 feet across with paddles extended, and weighed 830 pounds. The spacecraft consisted of three major elements (fig. 13): the sensory ring, the solar paddles, and the stabilization-and-control subsystem, connected to the sensory ring by a truss structure (ref. 12). In general, major improvement within each of the three basic elements has been achieved. The most significant of these accomplishments are described below.

Advanced packaging techniques were developed and used in the Nimbus sensory ring. It was designed and developed as an independent subsystem of the Nimbus spacecraft to cool and house the power-supply electronics and battery modules, the command clock, PCM (pulse-code modulation) telemetry, and the advanced sensors. To make this element mechanically and thermally independent, the design had to be sufficiently flexible to permit many tradeoffs in order to obtain optimum conditions for the entire spacecraft system. A design was desired that would permit the addition, elimination, or substitution of subsystems without redesign of the primary

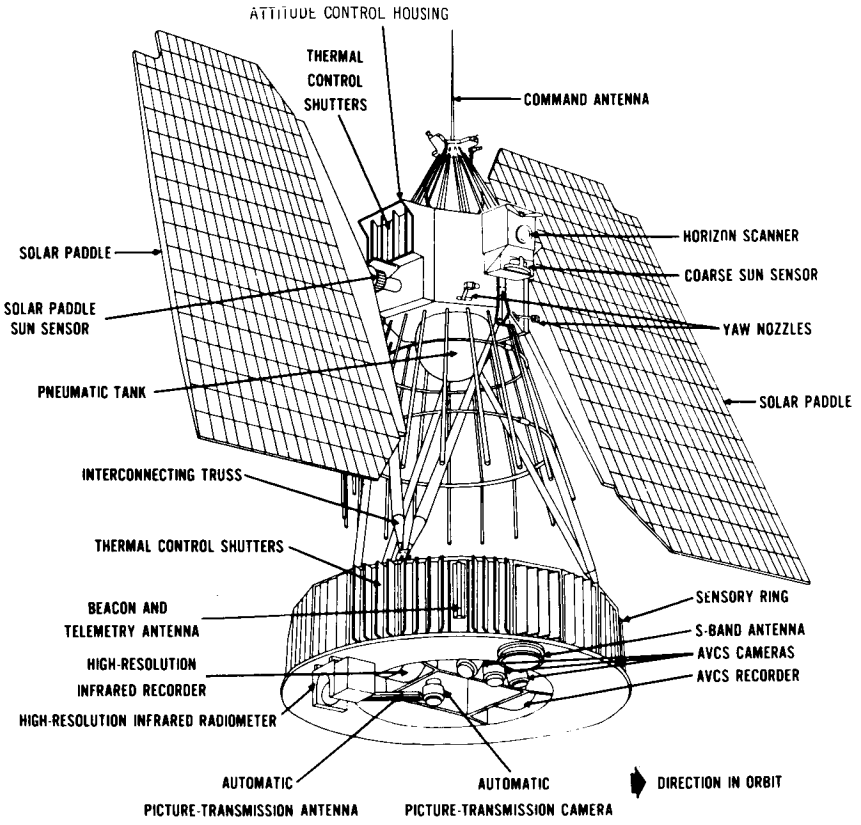

Figure 12.—**Nimbus I spacecraft and components.**

sensory ring. To achieve this feature, the following characteristics were sought:

(1) A high ratio of component packing density to weight, allowing size standardization of many subsystems.

(2) Ease in arranging modules to obtain optimum center-of-gravity location and thermal balance.

(3) An interface design that would insure reliable and clean separation.

These characteristics were achieved by using advanced modular techniques that allowed the sensory ring to be fabricated as 18 compartments (fig. 14). Each compartment consists of an upper and a lower section containing the solid-state modular subsystems (fig. 15). An active thermal-control system maintains isothermal conditions within the range of 25° C$\pm$10° C (ref. 13).

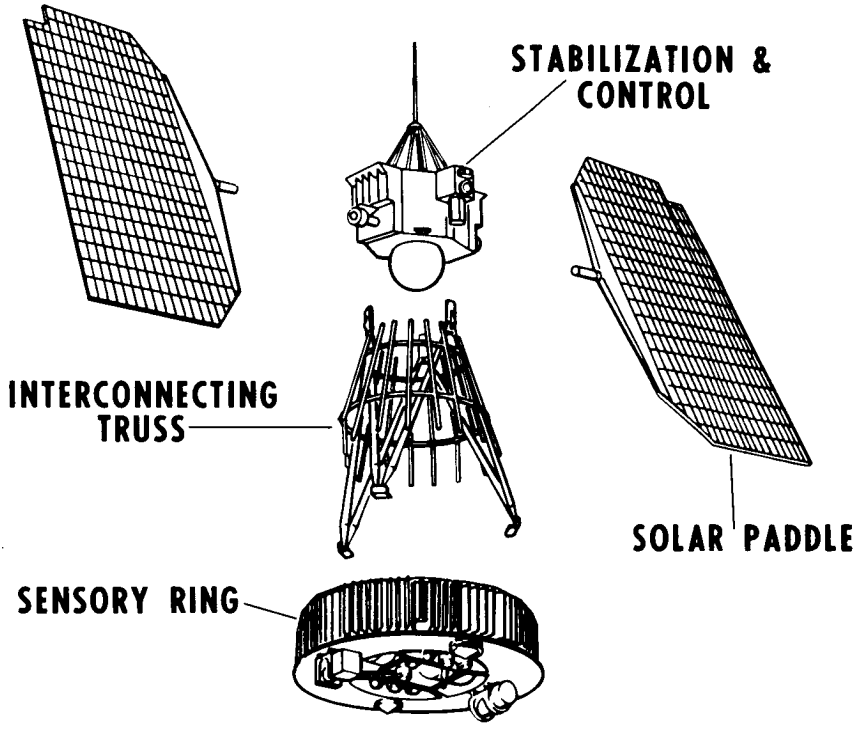

Figure 13.—Exploded view of major elements of Nimbus spacecraft.

Stabilization and Control

Another significant achievement in the Nimbus program is the development of a stabilization-and-control system that maintains constant Earth orientation of the base of the spacecraft sensory ring, for completeness and simplicity of global observations. To maintain operational flexibility of the satellite, a closed-loop control system was used for all three axes. This was one of the first attempts to use a three-axis control system for stabilization and attitude control of satellites. The first closed-loop control for a satellite was used on Discoverer II in April 1959. Controls in that case were established for one axis, with inertial methods serving to stabilize and control the two other axes. At the time the specifications for the Nimbus system were being developed, it was not even certain that a three-axis system was within the state of the art. Yet the vital role that this stabilization-and-control system was to play made such qualification essential to meet the mission objectives. The stabilization system was required to operate not

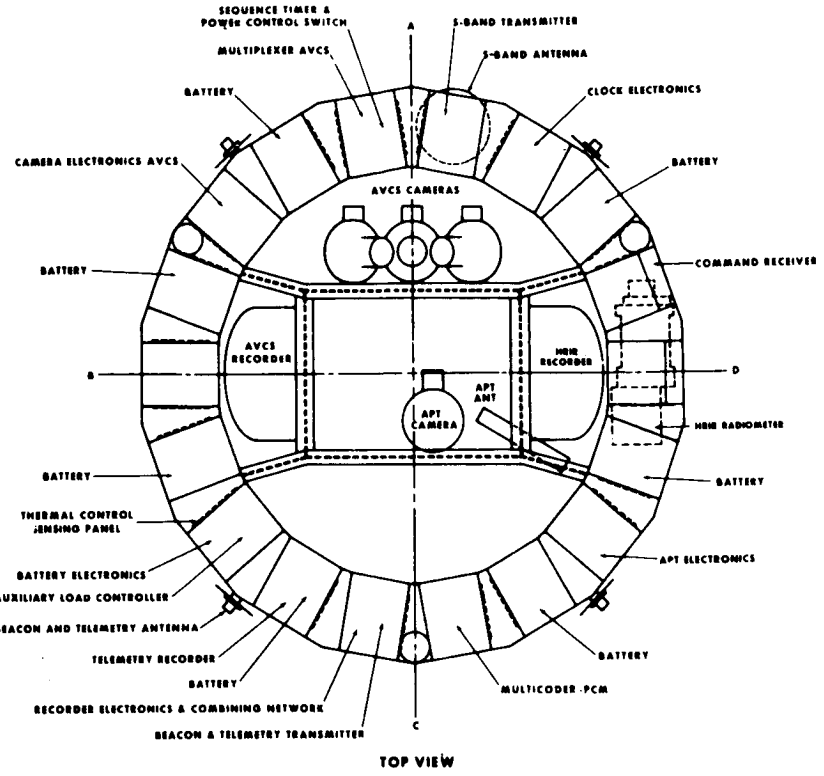

Figure 14.—Nimbus I sensory ring.

only close to its specification but to stay within it, or the useful life of the satellite would be jeopardized.

Essentially, the Nimbus stabilization-and-control system consists of a rate gyro and horizon scanners for attitude determination. Three flywheels and a pneumatic system are used as torque generators to provide attitude control of the spacecraft. A tank, located under the control housing, contains a store of Freon gas for the pneumatic system. Control of the spacecraft is defined by the spacecraft coordinate system shown in figure 16.

The design objectives were to achieve pointing accuracy in all three axes, which would make attitude corrections at a low-enough rate to permit global observations. The actual flight (Nimbus I) demonstrated that these objectives were attainable, although a malfunction in the solar paddle drive shortened the satellite's operational life. An impressive display of undistorted, high-resolution infrared and TV pictures was received while the stabilization-and-control system was operating.

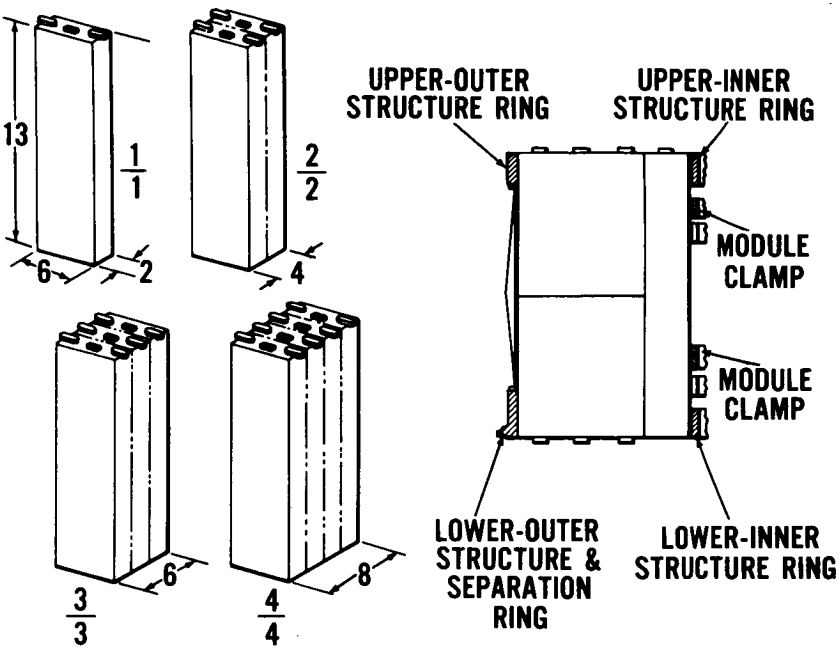

Figure 15.—Nimbus sensory-ring modules.

Power Supply

The power-supply system for the Nimbus spacecraft required a vast amount of research-and-development effort. Basically, the power supply consisted of an array of silicon solar cells, batteries, voltage regulators, and protective devices. Such components are readily available from the manufacturer; however, very few components were available that were suitable for the environment in which the Nimbus spacecraft was to be flown. Major breakthroughs were required, both in component development and in wiring techniques, before a power-supply system could be designed to meet the hazards of the Nimbus I space environment.

Temperature extremes of the Nimbus I orbit were expected to be −80° C to 60° C. Because no data were available on the operation of solar cells over this temperature range, especially with regard to life as a function of repeated cycling, tests were conducted to check the proposed design. The test, consisting of 1000 thermal cycles in a vacuum chamber, resulted in some fatigue failure of the interconnecting strips and also degradation of solar cells. Analysis of these results led to the conclusion that there was a deterioration of the cell contact. This resulted in the development of a better cell contact, which future Nimbus satellites will use (ref. 13).

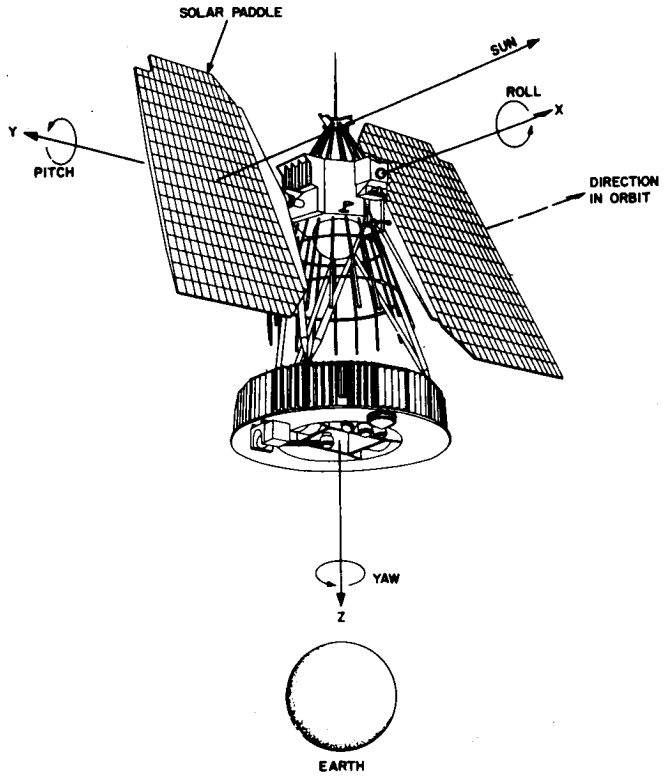

Figure 16.—Nimbus coordinate system.

Sensor Subsystems

Excellent pictures were obtained with the advanced sensors developed for the Nimbus I flight. This achievement would not have been possible if it were not for the advances made in sensors, magnetic-tape recorders, and in the adaptation of standard communication techniques to space operation during the early 1960's. Nimbus I has demonstrated the feasibility of using standard types of communication, at VHF and at UHF, to transmit a large amount of complex data in a short period. Over a quarter-billion bits of data were transmitted from the satellite and processed during each satellite orbit (refs. 14–15). The scope and size of the transmission and data-processing tasks presented a most formidable challenge to both the radio transmission and the computer engineers.

High-Resolution Infrared Radiometers (HRIR)

The excellent pictures taken by Nimbus I at night were obtained by means of the HRIR. In contrast to conventional, daytime satellite cloud

pictures, which must rely on sunlight scattered back into space by clouds, nighttime picture taking on Nimbus I was based on the principle that all surfaces on Earth emit infrared radiation according to their temperatures. The radiometer senses this radiation with a lead selenide photoconductive cell operating at 198° K (ref. 15). In addition, the HRIR system (fig. 17) consists of an optical subsystem, a mechanical drive, and a tape recorder. The radiometer measures the thermal radiation in the 3.4μ to 4.2μ region as it scans the Earth. It has a view angle of 27 minutes of arc, a 280-cps video bandwidth, and scans 560 elements at 0.83 rps over a 120° angle from horizon to horizon. The infrared radiation is modulated by a mechanical chopper, and its intensity is recorded on the tape recorder and transmitted from the satellite to the CDA stations via a UHF transmitter operating in the 1700-Mc/sec range. A facsimile system at the ground station reconstitutes the pictures with a resolution of 8 kilometers.

Advanced Vidicon Camera System (AVCS)

In addition to the HRIR, the AVCS was flown on Nimbus I. This permitted the entire daytime cloud cover of the Earth to be observed once a day at the specified resolution of 0.8 kilometer, a significant improvement over the Tiros cameras, which provided large area coverage. The AVCS

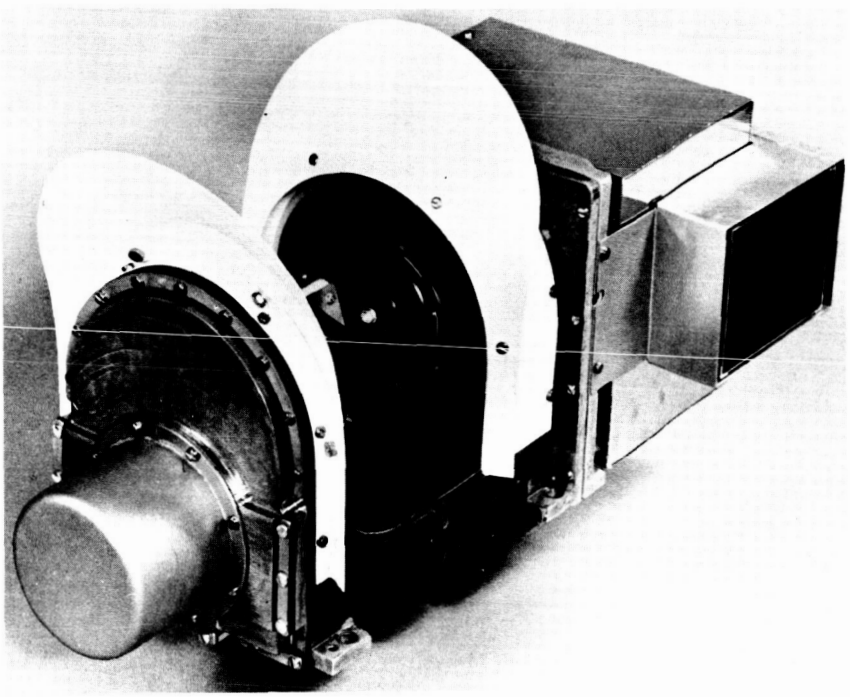

Figure 17.—Nimbus high-resolution infrared radiometer (HRIR).

is shown in figure 18 with its check-of-calibration collimators attached, and consists of three 800-line vidicon cameras and a tape recorder. Each camera has a 37° field of view and a variable speed of f/4 to f/16, with a dynamic range of 14 to 11 400 foot-lamberts. The 17-millimeter focal-length lens used with a 1-inch vidicon tube gives a ground resolution of one-half mile per line, as compared to the previous Tiros cameras, with a resolution of the order of 2 miles. The three TV cameras, arranged in a trimetrogon array, produce at an altitude of 800 kilometers a composite picture covering an area of 830 kilometers by 2700 kilometers. A total of 32 camera pictures were taken in each orbit and recorded on the tape recorder. This information was sent by a 1700-Mc/sec S-band transmitter to a ground station located at Fairbanks, Alaska.

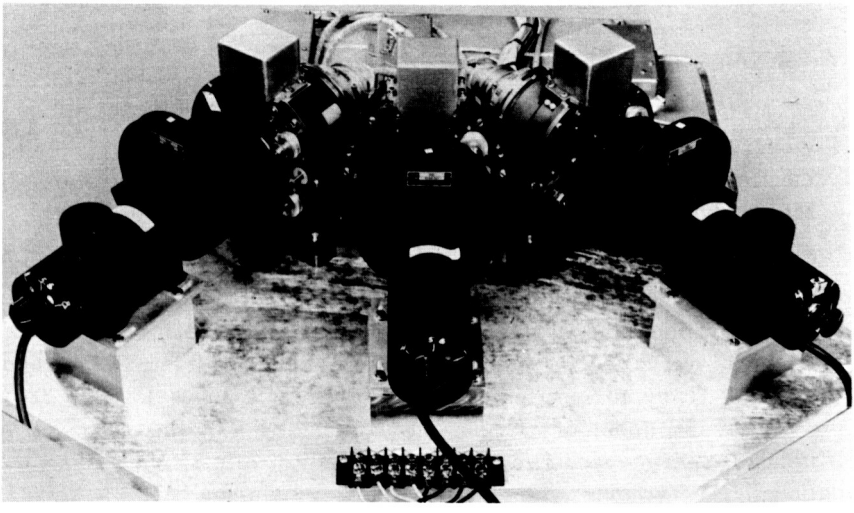

Figure 18.—**Advanced vidicon camera system (AVCS) with check-of-calibration collimators.**

Automatic Picture Transmission (APT) System

To provide real-time daylight cloud pictures for local weather analysis and prediction, the APT system was flown on Nimbus I. It was similar to that flown on Tiros VIII, which was discussed earlier. However, the APT system flown on Nimbus I (fig. 19) produced pictures of much higher quality than those from Tiros VIII. The pictures contained much more detail and exhibited none of the scalloping or banding common in Tiros VIII pictures. In addition, because of the characteristics of the Tiros system, particularly the fact that it was space oriented rather than Earth oriented,

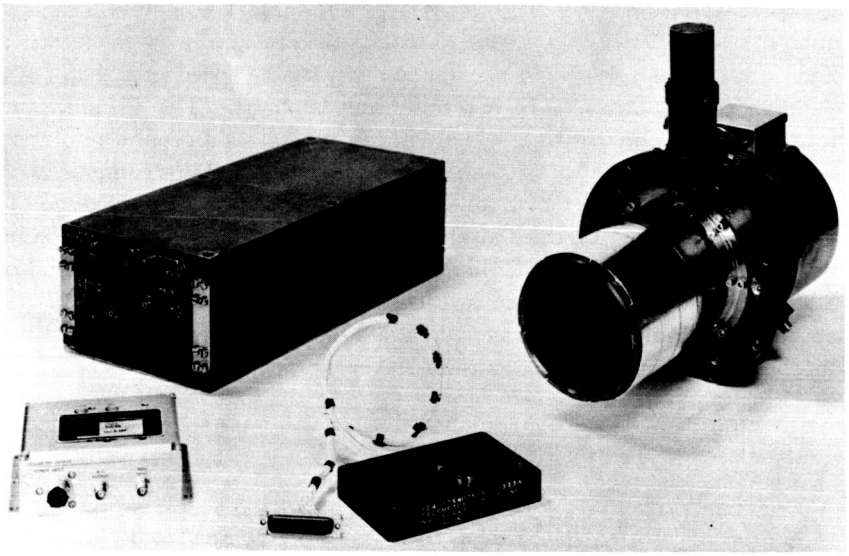

Figure 19.—**Nimbus APT-system components. From left to right: video electronics module, FM transmitter, telemetry-conditioning unit, and sensory housing.**

the coverage obtained by each APT ground station was limited, and the utilization of the data was more difficult than in the case of Nimbus I.

By 1964, over 60 APT ground stations were built and located throughout the world, ready to receive APT pictures from Nimbus I. The rapid growth in construction of APT stations worldwide during the last year or so is indicative of the general acceptance of this system nationally and internationally.

Nimbus I Performance

A measure of the success of any satellite is to compare its performance and that of its various subsystems with the design objectives. For Nimbus I, table III lists the design objectives and the performance of a number of items. From this listing one can recognize the success of the early period of the Nimbus development program. Nimbus I was launched on August 28, 1964. Although its achieved orbit was elliptical instead of circular, and although the spacecraft's life in orbit was rather short, the mission was considered to be highly successful. The orbit is a result of the short Agena second burn, so that the design objectives were not quite achieved.

The Nimbus I attitude controls, which represent a major advance in weather satellites, achieved initial stabilization and maintained satellite at-

Table III.—*Nimbus 1 Spacecraft Design Objectives and Performance*

Item	Design objectives	Performance
Orbit	Circular; 500 n. mi.; near-polar; Sun-synchronous; 99°.	Noncircular orbit: apogee, 518 n. mi.; perigee, 236 n. mi.; 98.7°; near-polar; Sun-synchronous
Attitude controls	Earth stabilized, 1° all axes.	Less than 1° in pitch and roll for 90 percent of the orbit. Less than 2° in yaw for 90 percent of the orbit
Lifetime	6 months	3½ weeks
Power	450-watts solar array	All achieved design objectives
Thermal controls	25° C ± 10° C	
Command system	128 coded commands	
Data transmission	400×10^6 bits/orbit	
AVCS	½-mile resolution, 8 gray scales.	
APT	1½-mile resolution, 6 gray scales.	
HRIR	Noise-equivalent temperature, 195° K; 5-mile resolution.	

titude within the design objectives in roll and pitch for 90 percent of the orbit. In yaw, the deviation was less than 2° for 90 percent of the orbit. It is evident that the control system was successfully coping with a significantly elliptical orbit. The other items all performed as required, including the power system, the thermal controls, the command system, the PCM telemetry system, the transmission system, and the advanced sensors (ref. 15).

SATELLITE TV PICTURES

Introduction

Water vapor, which comprises only about 0.2 percent of the total mass of the atmosphere, has a profound effect on the Earth's heat balance. Without water vapor the mean temperature of the Earth would drop by 40° C. Cloud patterns are the visible manifestations of this moisture, and of the dynamical mechanisms acting within the atmosphere. Clouds have been found to be highly organized, and reveal atmospheric phenomena on all scales. Before rockets and Earth-orbiting satellites, cloud data were limited mainly to surface observations and to aircraft observations made in the troposphere and lower stratosphere. Because of the spacing of these ob-

servations, a comprehensive picture of the cloud data over the entire globe, or even a major portion of a hemisphere, was lacking.

Cloud Observations

During the period from 1947 to 1960, meteorologists were privileged to study a few cloud photographs obtained from rockets (analysis of Project Hugo test firing, December 5, 1950.) These observations provided a view of the weather on a large scale, and even recorded cloud patterns associated with entire weather systems. Initially, most of the details of cloud structure and organization were of interest mainly to the research meteorologists. However, on one rocket-film sequence, significant multiple-circulation centers that could not be detected by the conventional weather-observing network were found associated with a storm system. The operational forecaster and research meteorologist began to realize the need for a weather observer in space (ref. 16).

Tiros I

On April 1, 1960, NASA launched the world's first weather satellite, Tiros I, using a Thor-Able booster. Tiros I demonstrated the practicality of TV space observations and provided system-design concepts. The cloud observations made by Tiros I confirmed and, in some cases, shed new light on the large-scale organization of clouds, and on mesoscale phenomena such as tornadoes and jetstreams.

Tiros I pictures showed that clouds were arranged in a highly organized pattern. The cloud vortex stood out as the most dramatic of these patterns (ref. 17). It was soon shown that these cloud vortices located accurately the atmospheric-storm regions. It has been shown that the arrangement of the cloud pictures follows closely the frontal pattern drawn by the meteorologists. This is clearly illustrated in figure 20.

Of the 23 000 cloud-cover pictures transmitted by Tiros I, more than 19 000 were usable for weather-analysis purposes. This opened a new era in weather observation by providing data, covering vast areas of the Earth, that had been unavailable to meteorologists.

Some storms were tracked for as long as 4 days, which demonstrated the feasibility of using TV satellite pictures for weather forecasting. A case history is that of the Tiros I observations of an extratropical storm near Bermuda on three occasions in early May 1960. A fortuitous set of circumstances provided three pictures of the same storm over a 4-day period, recording on film the degeneration of a vigorous cyclone (fig. 21). The weather maps drawn from conventional data correlated very closely with this series of pictures, thus affording a unique set of data on which to judge future pictures (ref. 18).

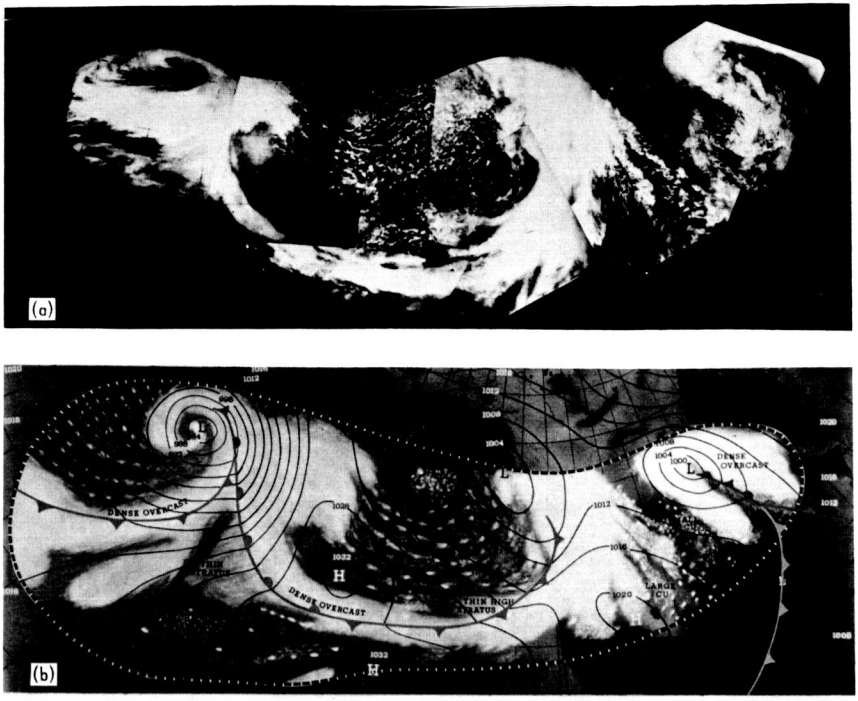

Figure 20.—**Storms and fronts—a family of weather systems. (a) A mosaic of Tiros photographs; (b) a weather map for May 20, 1960, with Tiros cloud data incorporated.**

Tiros II

Tiros II was the first of its series to use a Thor-Delta booster. The satellite was placed into orbit November 23, 1960, and provided more than 37 000 pictures of cloud cover. Weather-satellite longevity in space was clearly demonstrated when Tiros II far exceeded the expected life of 90 days; it performed for 10 months. The pictures' value was demonstrated by their use by the Weather Bureau, the Air Force, the Navy, and by foreign countries and international meteorological centers.

Between November 1960 and February 1961, conditions for taking pictures were favorable on 575 out of the 1046 orbits made by Tiros II. Nephanalyses were produced for 371, or 65 percent, of the 575 usable orbits, and relayed by the U.S. Weather Bureau's facsimile network to all Weather Bureau and military weather stations in the continental United States, plus commercial airlines, power companies, some TV and radio stations, and

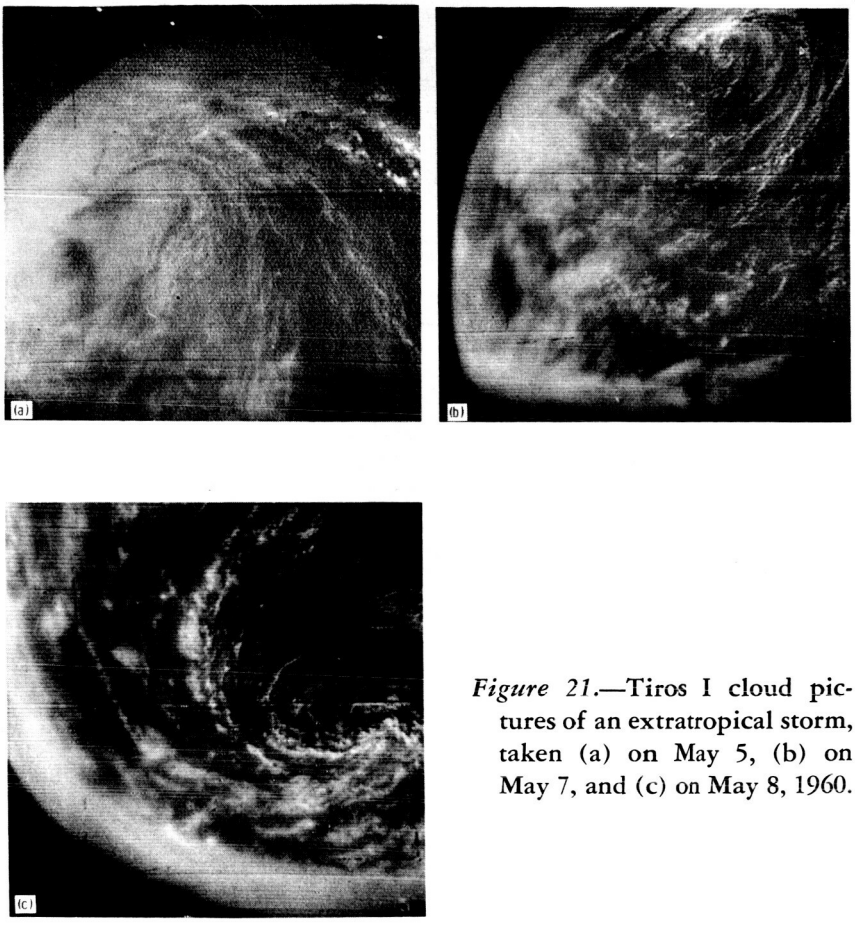

Figure 21.—Tiros I cloud pictures of an extratropical storm, taken (a) on May 5, (b) on May 7, and (c) on May 8, 1960.

many other organizations. The following examples show some of the operational uses of Tiros II.

(1) The International Aviation Forecast Center at Miami made use of Tiros II nephanalyses in preparing forecasts for air routes between New York and northern South America and between Miami and Panama City, Bogota, and Mexico City. General area forecasts for the Caribbean and Southern and Northern Atlantic areas were made from conventional meteorological analyses and corrobated by comparison with Tiros II nephanalyses.

(2) Tiros II data were used to establish, modify, and extend conventional nephanalyses and surface frontal analyses; and to brief pilots on en route weather. One series of charts covering approximately 30 days was used in

direct support of an exercise that involved deployment of aircraft over water and aerial refueling.

(3) Nephanalyses received via teletype were plotted on maps at the International Antarctic Analysis Center. The data were used to refine weather analyses in the region from Australia to Antarctica.

(4) The Australian Meteorological Service used the TV data in conjunction with their map analyses and in special research projects on storms over Australia.

A report, "Synoptic Applications of Nephanalyses From Artificial Satellites," by G. T. Rutherford, of the Australian Central Weather Office in Melbourne (ref. 19), summarizes experience in Australia with the nephanalysis transmissions of Tiros II.

> A large number of nephanalyses as interpreted from Tiros II photographs have been made available to the Bureau of Meteorology.
>
> Some of these have furnished general confirmation of our Southern Ocean analyses. Some have presented features which have called for reanalysis in a manner which has been verified by later history. Others have not lent themselves to ready interpretation of current or later analyses and a full appreciation of these will require closer study. Finally, a few nephanalyses have apparently been at variance with observations.
>
> Interpretation of nephanalyses or cloud photographs for use in analysis will involve not only a study of cloud patterns for models to be associated with various types of fronts and cyclonic vortex-spiral systems, but also an attempt to identify the types of cloud represented and the nature of the cloud-producing mechanism; i.e., weather fronts, convergence turbulence or convection.
>
> The utility of satellite photographs when their interpretation is more thoroughly understood is likely to have far-reaching and scarcely foreseeable effects on extended range and day-to-day forecasting. In Australia, the opportunity of participating in the Tiros II experiments has laid the groundwork to this end.

During the lifetime of Tiros II, research meteorologists were actively engaged in the analysis and interpretation of the data. Pictures of icepack conditions in the St. Lawrence proved that weather satellites could locate ice boundaries in relation to open seas. Also, Tiros II observations were used in selecting the proper weather conditions for the suborbital flight of Alan B. Shepard, Jr., in May 1961, and the launching of Ranger I, 3 months later.

Tiros III

Tiros III, which was placed into operation July 12, 1961, was particularly credited with the detection of tropical storms. All six of the major hurricanes of the 1961 season were observed by Tiros III. Hurricane Esther was detected by the satellite 2 days before it was observed by con-

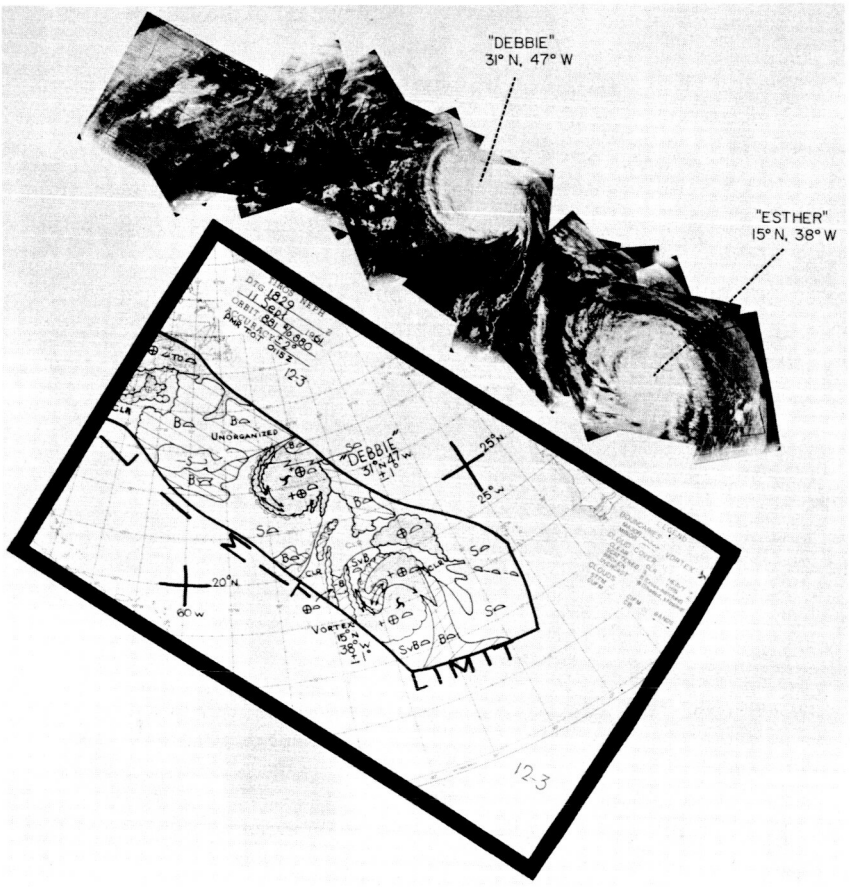

Figure 22.—**Nephanalysis and mosaic of Tiros III pictures taken during Orbit 881, on September 11, 1961, showing Hurricanes Debbie and Esther.**

ventional methods. Hurricane Debbie was spotted on some of the same passes. This is shown in figure 22, with the resulting nephanalysis.

Information that resulted in 70 storm advisories was sent to weathermen throughout the world.

Tiros III TV photographs were used in the support of launches involving Project Mercury, Ranger, the Air Force's Discoverer series; the Navy's 1961 Antarctic resupply mission; and the firing of Long Tom meteorological rockets in Australia. During Tiros III's lifetime, more than 24 000 usable cloud-cover pictures were received and evaluated out of a total of 36 000 pictures transmitted.

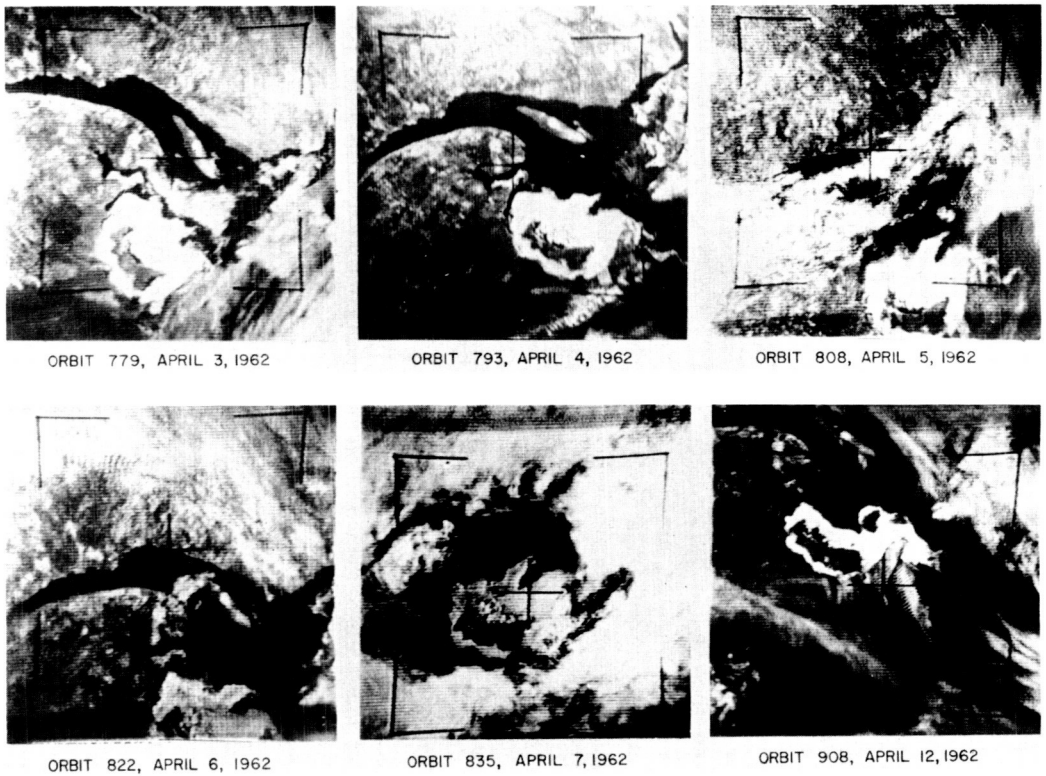

Figure 23.—Tiros IV pictures of ice, taken in early April 1962, proved superior photographs from aircraft for ice reconnaissance.

Tiros IV and V

During 1962, the fourth and fifth Tiros satellites were successfully launched. TV pictures from Tiros III and those from Tiros IV and V provided large amounts of data for meteorological research. Research with the TV pictures included preliminary investigations of the formative stages of hurricanes, the determination of atmospheric motion, investigations of tropical circulations and the Pacific Ocean dry zone, studies of ice and snow, and exploration of the use of cloud pictures for direct input to numerical weather-prediction models (ref. 20).

Tiros pictures were also used to confirm the capability of a weather satellite for ice reconnaissance. Under Project Tirec (Tiros Ice Reconnaissance), a joint NASA-U.S. Weather Bureau-U.S. Navy-Canadian Goverment project, aircraft took photographs on successive days while flying the predicted path covered by Tiros IV. The aircraft pictures were compared with those taken by Tiros IV (fig. 23), with the conclusion that weather-satellite pictures provide a better means of ice study over large areas than does conventional aircraft reconnaissance.

In addition, Tiros IV photos were used in Project Bright Cloud, a joint NASA–USAF venture to develop a cloud-identification system based on the shape and brightness of cloud cover.

Tiros VI and VII

In 1963, three Tiros satellites (Tiros V, VI, and VII) were in overlapping operation, and provided for the first time TV pictures of the cloud cover of various parts of the world on an almost continuous basis. TV pictures from these satellites were the basis for continued effort on adapting satellite data to current forecasting methods (i.e., to numerical prediction models); and on investigations of the relation between large-scale cloud features and the field of atmospheric motion. Under Project Equalant, an oceanographic survey of the tropical Atlantic, and with data from the International Indian Ocean Expedition, cloud photographs and radiation data over the tropical oceans were studied for clues to the origin and development of tropical cyclones. There were continued studies of Tiros pictures of the bright, sharply delineated clouds that appear to be associated with severe hail- and tornado-producing thunderstorms. One researcher noted a remarkable agreement between the radiometer-measured intensities of reflected insolation and the brightness of clouds and terrain in pictures taken by satellites. Cloud-producing severe local storms were found to be correlated with areas of negative relative vorticity. Some unique pictures showed cloud spirals and cycloids, never before observed, downwind from the Madeira and Canary Islands (ref. 21).

Tiros V had set a record of 320 days when its last camera failed in May 1963. It provided 48 547 meteorologically useful pictures, which furnished the basis for over 1800 operational nephanalyses. Tiros VI ceased operating on October 11, 1963, after a useful lifetime of 388 days. During its lifetime, Tiros VI detected a sandstorm in Saudi Arabia, and it furnished data used as the basis for many storm advisories to foreign countries, to the Air Force, and to Navy installations throughout the world. Throughout the period since its launch, Tiros VII continued to provide satellite coverage of large areas of the world and was backed up by a sister satellite, Tiros VIII, launched in December 1963.

Tiros VIII

Tiros VIII provided an innovation in satellite TV picture taking. From the more advanced Nimbus spacecraft, the APT system provided meteorologists in all parts of the world with cloud-cover pictures by direct readout from the satellite. Unlike the standard TV system carried on the early Tiros satellites, APT transmits pictures on a slow-scan principle, similar to that used to send radio photographs. Each APT ground station can receive, depending on the satellite's elevation angle above the horizon, up to three pictures during each pass. This concept is illustrated in figure 24.

Direct applications of APT pictures included support of the International Indian Ocean Expedition, the Galapagos Expedition, and the Ranger, Relay and Echo launches.

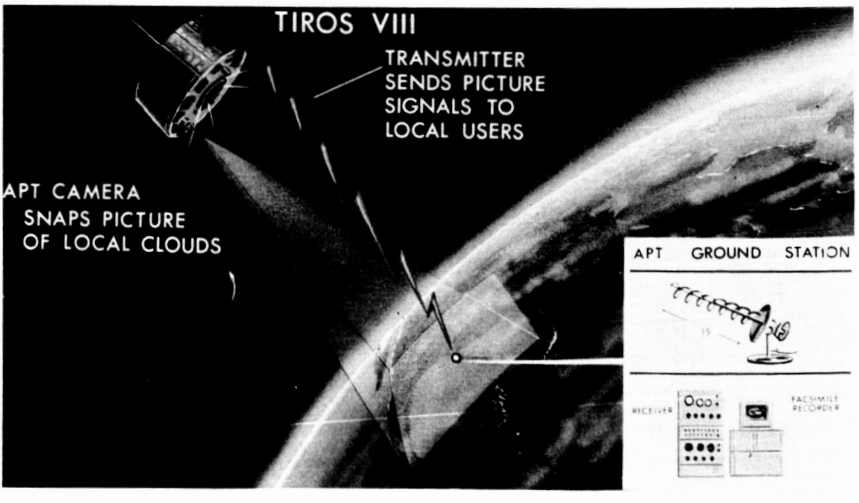

Figure 24.—Tiros test of automatic picture transmission (APT) system.

Nimbus I

The Tiros launches demonstrated the utility of weather satellites in research and operations. However, it was not until the launch of the first Nimbus satellite in August 1964 that weather satellites achieved a major breakthrough in TV pictures taken.

During its 3½ weeks of life, Nimbus I took 12 137 individual frames of AVCS pictures and an estimated 1930 APT cycles. It recorded Hurricanes Cleo, Dora, and Ethel, and tropical storm Florence; and spotted Typhoons Ruby and Sally in the Pacific.

Just about 9 hours after Nimbus I was launched into orbit from the Western Test Range, the full potential of the APT system was graphically illustrated by the pictures received. The first three pictures, as can be seen in figure 25, were quite remarkable. They show Texas to the left in the lower picture and the circulation around Hurricane Cleo to the right. In the center, down the middle of the United States in both pictures, there is a well-defined cold frontal system (ref. 22). The correlation between the frontal system shown on the weather map and pictures by the APT system is unusually good. The Weather Bureau stations in Boston, New York, Suitland, Md., and San Francisco received this first transmission and were quick to convey their enthusiasm for the high quality and usefulness of these pictures. During the operating lifetime of Nimbus I, numerous acknowledgments were received from APT users, many of them foreign, who have either procured U.S.-made ground sets or built sets on their own.

Figure 26 is an AVCS picture taken when Nimbus I was over the border area of Afghanistan and the Soviet Union. Tributary watercourses of the Amu-Dar'ya River are shown to the upper left. When compared with pictures made with the Tiros system, the improvement in clarity is quite noticeable. Of greater interest is the fact that the Nimbus I pictures, as first seen at Goddard Space Flight Center, were already gridded with latitude and longitude lines by the ground equipment. This information was provided by a computer using the orbital and attitude data points for the satellite when the picture was taken. The consecutive black and white dots mark the latitude and longitude. In the light areas of cloudiness in the lower part of the picture, the black dots stand out, whereas in areas of no cloudiness, where the picture is dark, the white dots show up, so that the lines are always quite distinct. The computer also prints out in numbers the latitude and longitude of a specific intersection on the picture, which is indicated by the arrowhead in the center. In this case, the arrow indicates the intersection of 38° north latitude and 66° east longitude. All longitudes are measured east of Greenwich, and hence the three-digit number is used.

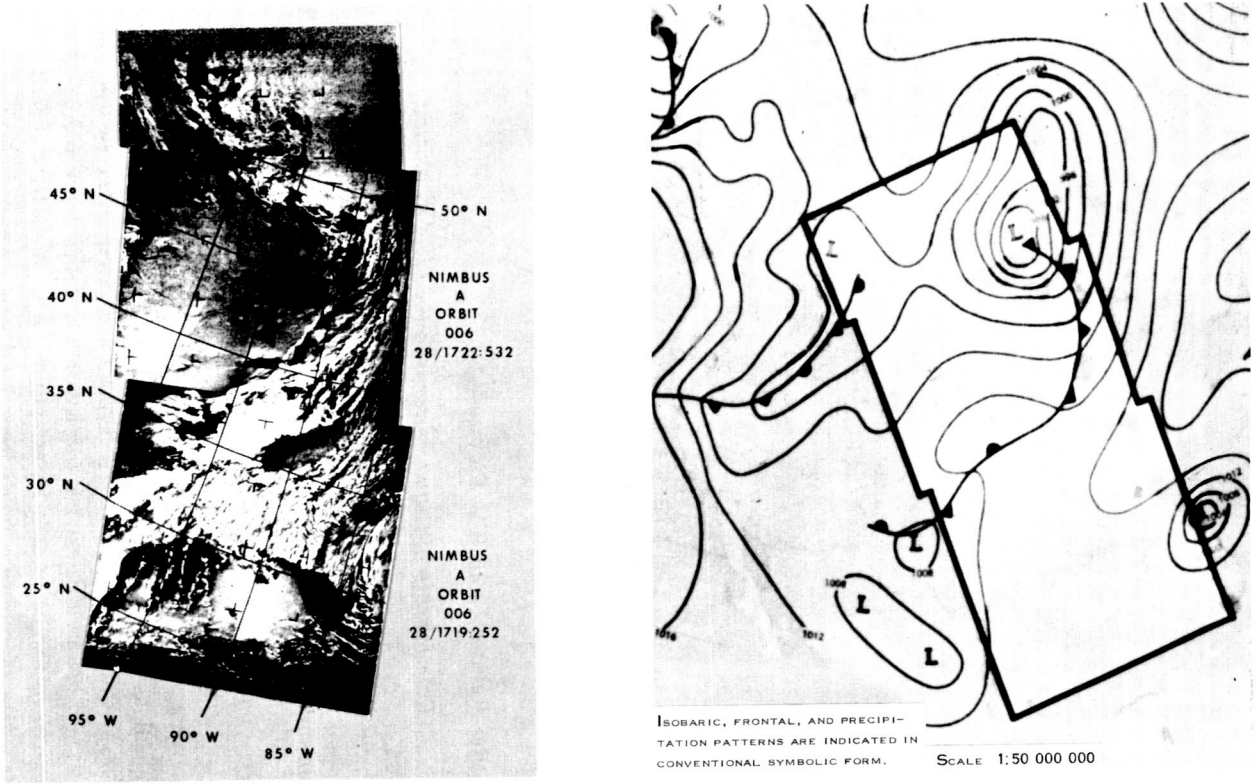

Figure 25.—**First three APT pictures from Nimbus I, August 28, 1964, and corresponding weather map.**

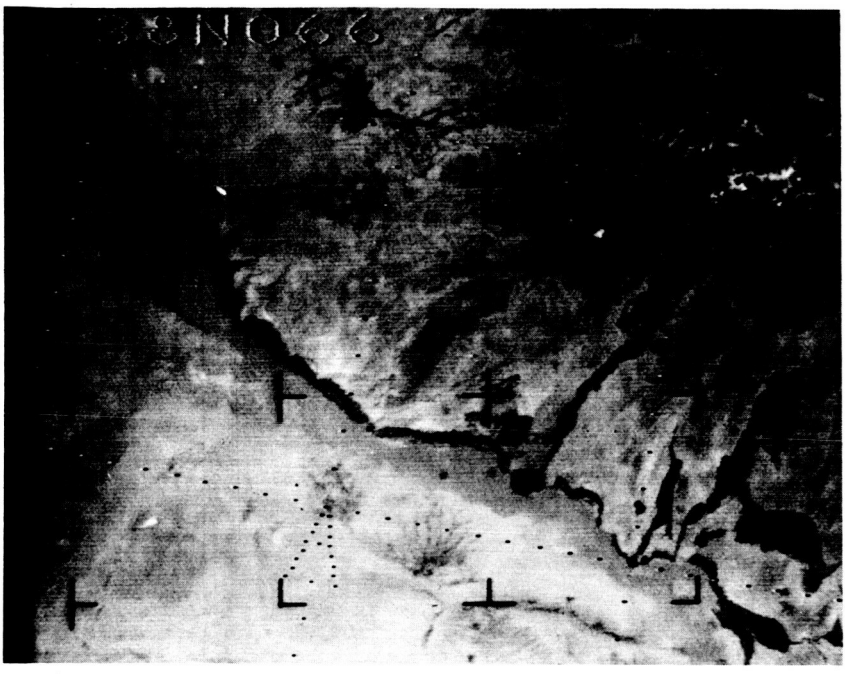

Figure 26.—**Nimbus I AVCS picture of border between Afghanistan and the Soviet Union at 38° north latitude, 66° east longitude.**

Scientific Results From TV Pictures

Relationship of Cloud Patterns to the Field of Motion

Among the most striking cloud patterns seen in satellite pictures are the large-scale cyclone vortices, whose spiral bands (fig. 27) are sometimes over a thousand miles in diameter. These vortices, in both the temperate and the tropical regions, have many common characteristics, yet they are all different. During the past few years, the focus of investigation has been upon classification. As an initial approach, a series of atlases has been developed. Tiros III, IV, V, and VI pictures alone yielded over 200 cases of tropical, as well as extratropical vortices from which cloud-vortex patterns have been categorized (ref. 23). From these cases, it has been possible to illustrate 16 histories of extratropical-vortex cloud patterns and 12 histories of tropical-vortex patterns. Investigations of such patterns have revealed the structure of moisture fields, the cloud structure of frontal zones, the relationship of spiral bands to the wind field, and cloud patterns associated with jetstreams (ref. 24).

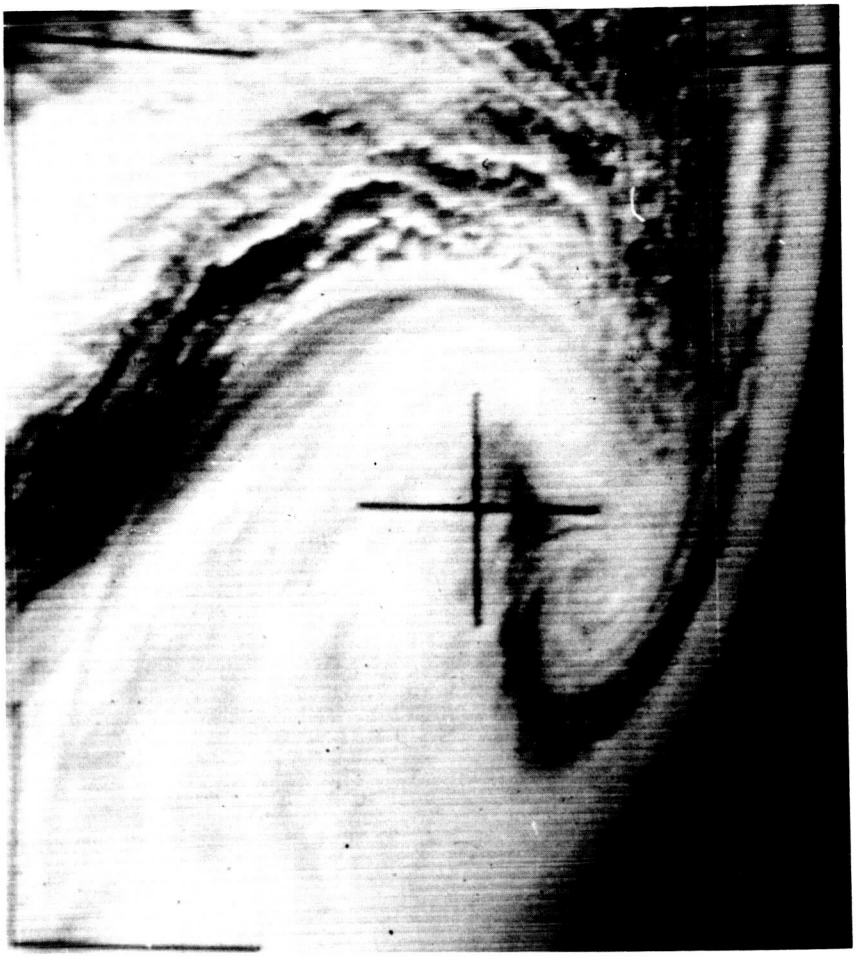

Figure 27.—**Tiros VI picture of a vortex near Australia on October 14, 1962.**

Such atlases have been useful to the research meteorologists in their rather detailed studies of the cloud forms; tabulation of average cloud dimensions, areas, and times of occurrences; and empirical and theoretical conclusions as to the physical and synoptic causes of their formation. These atlases, when correlated with synoptic data, have in the past revealed some interesting information. When pictures from Tiros, such as those cataloged in the atlases, were subjected to cursory analyses, it was found, not surprisingly, that the satellite cloud patterns fitted very closely the synoptic pattern. Exhaustive analyses, however, particularly for cyclonic disturbances, revealed

some discrepancies between the synoptic computed motions of the atmosphere and the cloud patterns seen in the satellite pictures. These discrepancies, as yet informal, made modifications of past theoretical cyclone models necessary. For example, the positive and negative vertical motions associated with cyclones are generally depicted as rather broad areas by computer methods, using general upper-air and surface weather observations. When these computed motions are compared with the prevailing clouds shown in satellite pictures, it becomes evident that the actual vertical motion field in the atmosphere is finer in structure than the computed field, particularly in areas of sparse data. This has suggested the use of cloud pictures as a check against computed parameters, or their direct use as initial data input. As a result of these findings, research projects are currently in progress to determine the feasibility of deriving sufficient information from cloud pictures for use as initial moisture, vertical-motion, and divergence input to numerical prediction models. In addition, the empirical and theoretical correlation of satellite pictures of cloud patterns with frontal systems and pressure patterns, both surface and upper air, will provide a method for the derivation of the synoptic patterns over those areas that do not have dense meteorological-observation networks (ref. 25).

Cellular Cloud Patterns

The so-called cellular cloud pattern frequently found in satellite pictures is shown in figure 28 (ref. 26). Especially in the lower right quarter, the pattern suggests semicircular arcs of clouds with clear areas in the center, a pattern similar to that found in the laboratory by Graham (ref. 27). The clouds in figure 28 were embedded in an atmospheric layer in which the temperature decrease with height was close to the adiabatic lapse rate. This relatively unstable layer was capped by a marked inversion, at levels varying from 1000 to 3000 meters over the area.

In the laboratory, these patterns are deformed from hexagonal Bénard cells by the superposition of vertical shear of the horizontal wind on the hexagonal patterns. But there are important differences between the laboratory results and the results revealed by Tiros pictures; among the most intriguing is scale. In the laboratory, the characteristic ratio of width of cells to height is $w/h=3$. By contrast, for the cells in the Tiros picture $w/h=30$, or about a factor of 10 larger. This value is computed from the fact that the cellular diameters in the picture range from 32 to 80 kilometers. If we take the height of the inversion as the depth of the fluid, then h varied from 0.95 to 2.4 kilometers.

Several studies have been conducted to explain the flatter cells observed by Tiros. Insertion of variable values of the horizontal "eddy" coefficients, K_x and K_y, which are larger than the vertical "eddy" coefficient, K_z, into

Figure 28.—**Cellular cloud pattern appears in this Tiros I picture taken northeast of Bermuda at 1612 GMT, April 4, 1960.**

a modified classical theory can produce significantly flattened cells. Baroclinic instability, introduced by horizontal temperature gradients, can apparently also produce flat cells independent of K (refs. 28 and 31).

Mesoscale Eddies Produced by Islands

Another class of interesting phenomena is that of the mesoscale spiral and cycloid patterns produced in the lee of elevated islands under suitable atmospheric conditions. Several examples of these were discussed by Hubert and Krueger in reference 29, and two of their figures are reproduced here (figs. 29 and 30). Figure 29 shows a general field of cellular clouds, probably under a strong low inversion, with very little vertical shear of the horizontal wind. But starting in the vicinity of Madeira Island and extending downwind for about 240 kilometers is a long cloud pattern arranged like a series of arcs in a cycloid. Hubert and Krueger point out that

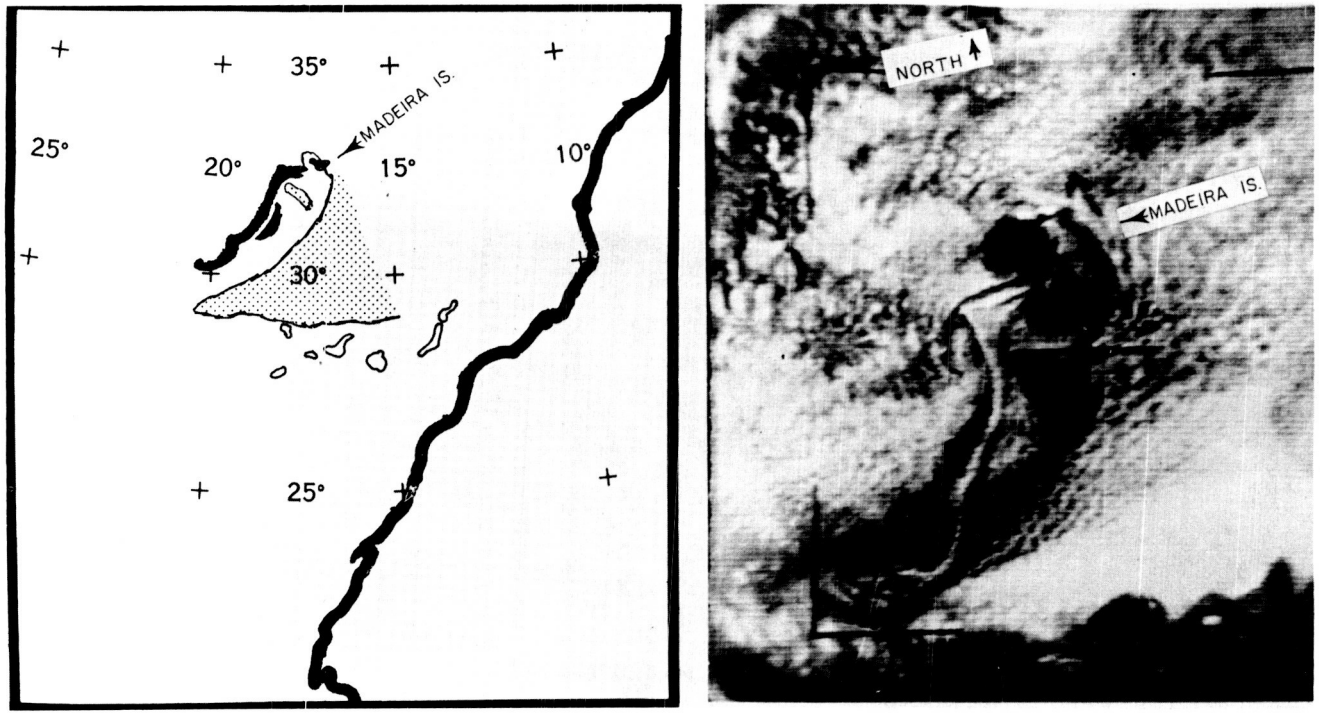

Figure 29.—Cycloidal pattern downstream from Madeira Island, off northwest Africa, photographed by Tiros V during pass 031 at 1650 GMT, June 21, 1962.

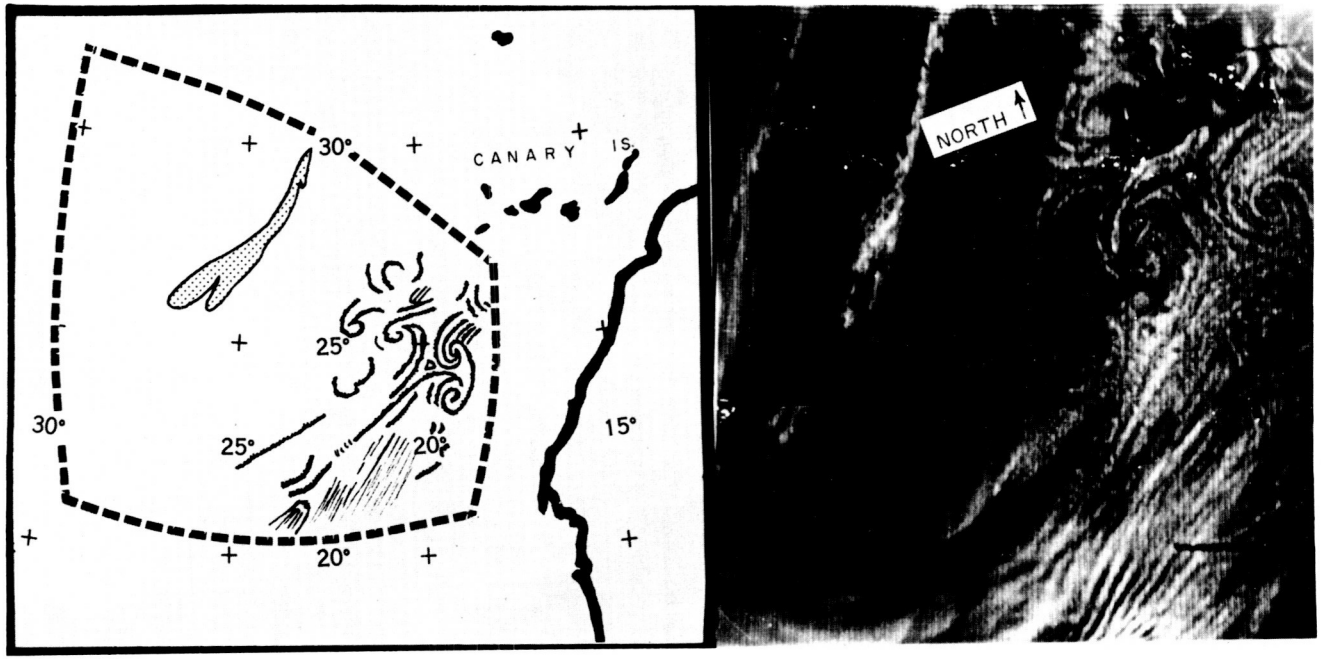

Figure 30.—Complex eddy pattern downstream from Canary Islands, photographed by Tiros V during pass 187 at 1400 GMT, July 2, 1962.

the presence of the inversion favors the production of inertial oscillations in the air. The presence of the islands modifies the balance of forces that existed in the airflow upwind from the islands. This imbalance of forces produces inertial oscillations, which take the form of cycloids if the oscillations are stable. It was shown that some of the cloud patterns were the result of purely mechanical eddies produced by obstacles to the flow, others may be the result of inertial oscillation, and others may be produced by inertial instability.

Tropical Vortices

Because of the lack of data over the tropical oceans, it has not been possible to study weather disturbances in these areas as extensively as in the middle latitudes. Now satellite pictures of the tropical areas are available for investigation. The genesis and life history of tropical storms are under intensive study. A study on Hurricane Anna (refs. 30 and 31), and another on the formation of Hurricanes Debbie and Esther (ref. 32), showed that there is a strong probability that these hurricanes originated in low-pressure areas in Africa.

Hurricanes often begin as small cold-core disturbances in the easterly wind zones of the Tropics (ref. 33). In a cold-core disturbance, the air is coldest near the center, where the air is rising. Such conditions cannot persist without a forcing mechanism in the environment. Additional mechanisms must therefore act to produce the warm-core, self-sustaining convection of a hurricane. The heat released by condensation in the clouds can gradually change the cold core into a warm core. A stage may then be reached when the air is withdrawn vertically from the system rapidly enough to make the associated low-level inflow unstable. This is analogous to an experiment by Faller (ref. 34), using a rotating water tank from which water was withdrawn at the center. The water was pumped back into the tank along its perimeter. Under the proper conditions of speed of rotation and fluid velocity, instability developed in the Ekman boundary layer. This instability produced convective-type bands spiraled toward the center of the tank.

The spiral bands observed in the Tiros III pictures of Hurricane Anna (fig. 31) are consistent with laboratory results and suggest the onset of instability in the friction layer during the early, formative stages of a tropical cyclone.

Wave Patterns in Clouds

Rather regular wave patterns are observed fairly frequently in clouds. One such wave pattern is produced by the flow of wind at right angles to a mountain range. When the wind direction is almost at right angles to a mountain range, such as the Andes, and when the temperature and wind

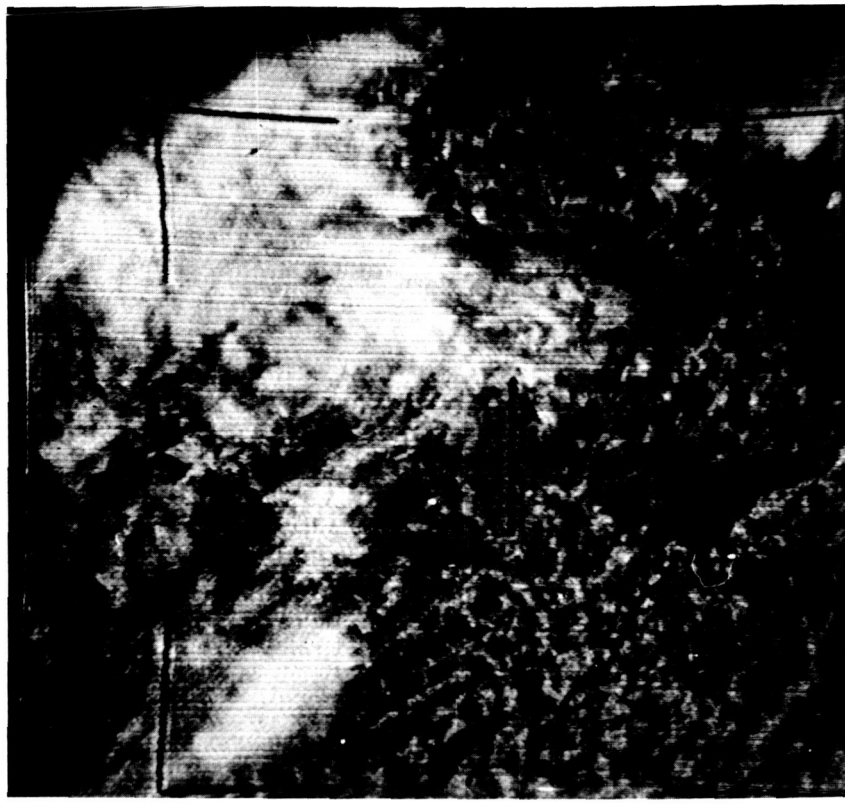

(a) July 16, 1961.

***Figure 31.*—Cloud mass from precursor Hurricane Anna shown in mosaic of photos taken by Tiros III.**

vary in a certain way with height, waves will form. These waves become visible when clouds form in the upward-moving part of the wave.

Döös (ref. 35) has considered such a case, based on figure 32. In the lee of the Andes Mountains, a remarkably regular and uniform wave pattern appeared in the clouds. The wave pattern extended about 320 kilometers downwind from the mountains and at least 400 kilometers in a north-south direction. The measured wavelength of the clouds, although not exactly the same everywhere, was about 11 kilometers. Döös, using available radiosonde data, found that the theoretical wavelength was also about 11 kilometers—in close agreement with observation.

There is another, less well-defined wave, with a wavelength of about 48 kilometers, in this cloud picture. This does not agree with a theoretical

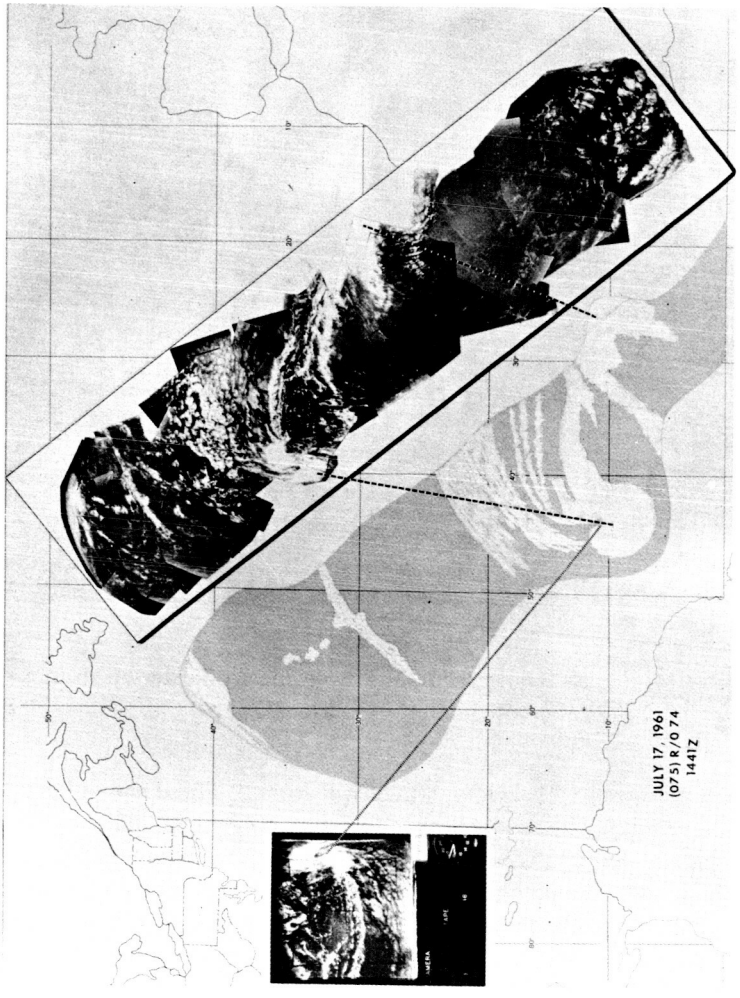

(b) July 17, 1961.

Figure 31.—Concluded.

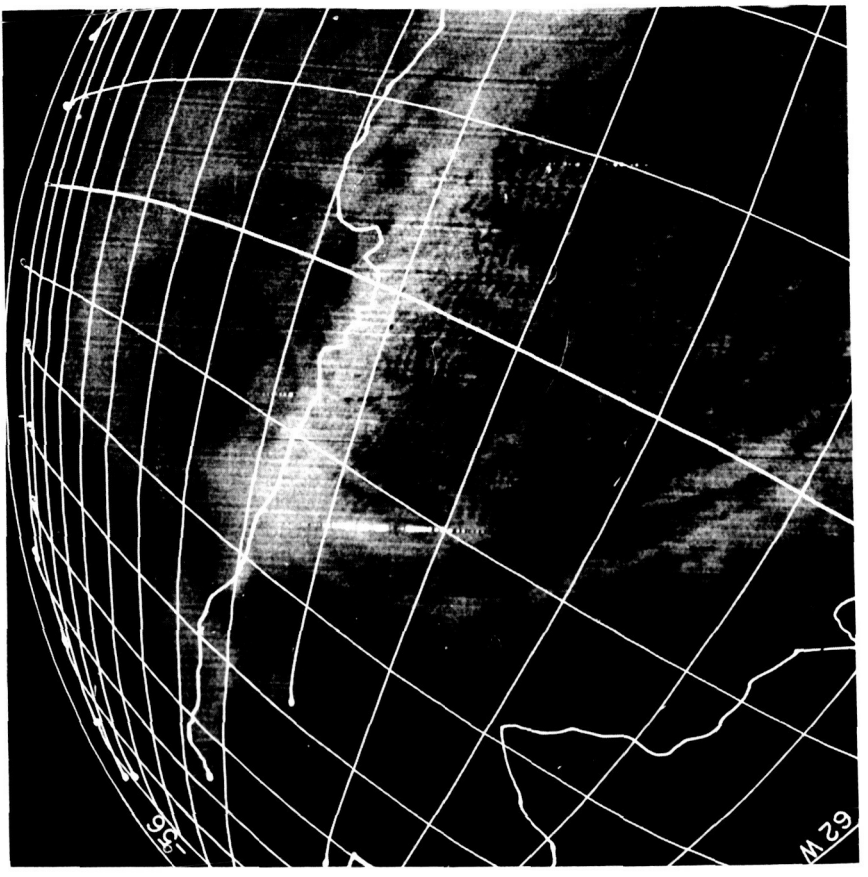

Figure 32.—**Wave-cloud pattern in lee of Andes Mountains, photographed by Tiros I on April 1, 1960.**

value of about 70 kilometers. Thus, there may be other causes for this poorly defined pattern, such as irregularities in terrain downwind from the main mountain range.

Cloudiness Associated With Jetstreams

Tiros pictures of cloud patterns in the vicinity of jetstreams were examined and compared with surface, upper-air, and pilot-report data (ref. 36). The cases studied revealed that the northern edge of the middle and high cloud shield associated with the jet was detectable when there were no low clouds to confuse the pattern. In Tiros pictures, this sharp, distinct edge on the cold side of the cloud shield can be distinguished from other cloud boundaries by its straight smooth appearance and its great length. The

edge of this high cloud shield could also be identified where it overlay a lower cloud deck. One case examined covers an area over northeastern United States which was observed by Tiros VI on November 20, 1962 (fig. 33). Superimposed on the nephanalysis are the jetstreams and the maximum wind analysis prepared by the National Meteorological Center.

The configuration of the jetstreams is quite similar to Kadlec's Type C jetstream-and-cirrus model (fig. 34). According to Kadlec, when a polar jet with anticyclonic curvature forms a converging pattern, an area of extensive cirrus occurs both upstream and downstream from the area of confluence. Upstream, the cirrus shield lies along and to the south of the subtropical jet and extends to the area where the two jetstreams converge. This point of convergence is usually where the maximum wind speeds in the two jets converge.

Figure 35, a mosaic of Tiros pictures, covers the area from Mississippi to Labrador. The interesting feature in the mosaic is the dark streak that extends from central Kentucky to near Baltimore and then east-northeastward toward Sable Island. Arrows A and B point out two portions of it in the mosaic. In the nephanalysis as originally prepared (fig. 33), this dark streak was shown as a narrow clear area. Ground stations' observations showed overcast low clouds, and this fact supports the proposition that this streak is a shadow cast by the higher cloud deck on lower clouds.

This and subsequent analyses indicate that with certain conditions of lighting and satellite altitude, the northern edge of the cirrus cloud shield, which lies immediately south of the jet, can be easily identified by a shadow cast by the higher cloud deck on the underlying surface. This suggests that satellite cloud pictures, when properly interpreted, can become a powerful tool in identifying the jetstream in data-sparse areas.

Convective Clouds and Their Relation to the Vertical Wind Shear

Several investigations (refs. 37–40) have shown an apparent relationship between the structure of cumuliform clouds and the vertical shear of the wind field in which they are embedded. Small cumulus clouds were observed to move with the wind and to lean in the direction of the vertical shear. Larger cloud towers lean in the direction of the wind shear, but usually to a lesser degree than the shear alone would indicate.

Several Tiros pictures of cumulonimbus clouds and thunderstorms over the Florida area were compared with synoptic surface and upper-level wind data (ref. 41). It was evident that cumulonimbus anvils are at least partially shaped by the environmental winds. The direction of the vertical wind shear between the lower troposphere and the cirrus level is the parameter generally most clearly indicated by the anvil-cloud orientation.

207-342 O-66—5

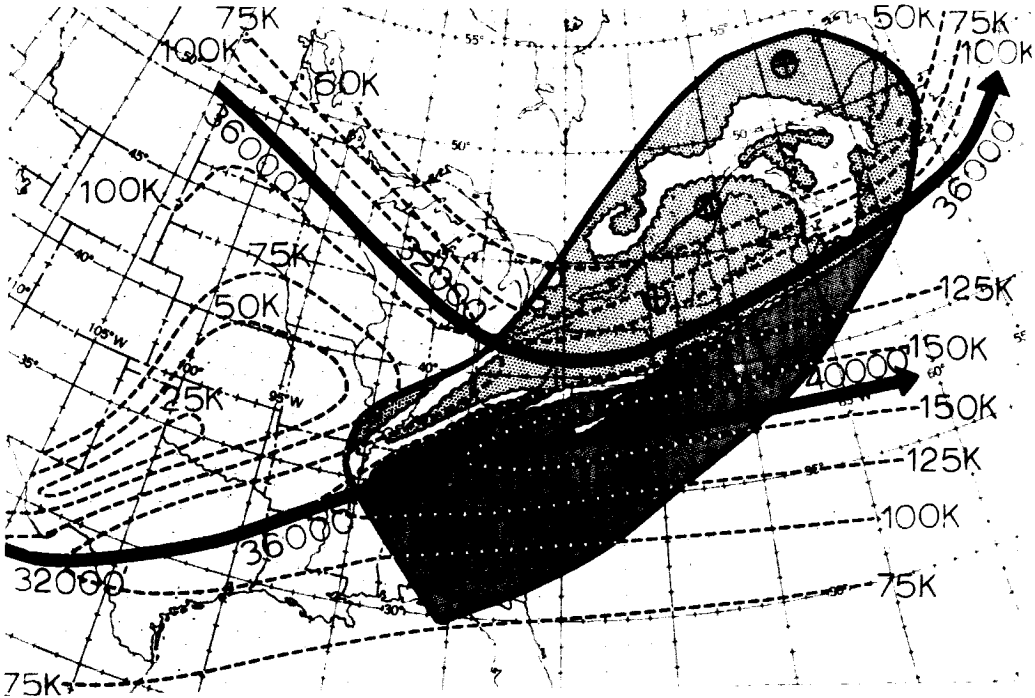

Figure 33.—Nephanalysis of Tiros VI's 922d orbit, 1355 GMT, November 20, 1962. The 200-millibar isotach analysis for 1200 GMT and the positions of the jet at that level are superimposed. The height of the maximum wind is entered along the jetstream positions. The darker shading denotes the high cloud shield, and the lighter shading denotes lower cloud shield.

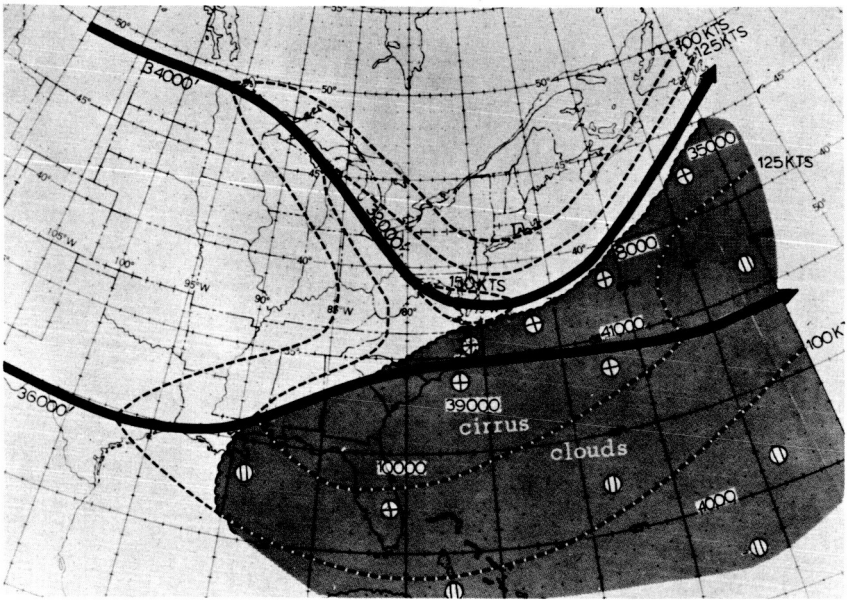

Figure 34.—**Kadlec's model (Type C) of the cirrus cloud pattern associated with two converging jetstreams. Darker shading, high cloud shield; lighter shading, lower cloud shield.**

In this study, good general agreement was found between anvil orientations and the vertical shear, but because of small differences between shear and upper-level winds, there was often good agreement with the upper-level winds themselves. Therefore, a preference for shear, while believed to exist generally, was not well established in these particular cases. Local topographic influences, such as islands, coasts, and mountain peaks, may exist that cause the movement of cumulonimbus clouds to deviate from the mean flow. Another general conclusion was that cumulonimbus and thunderstorm clouds not embedded in dense stratiform layers appear as relatively small- or medium-sized, irregular, bright masses in Tiros pictures.

Hurricane-Model Considerations

Satellite pictures of hurricanes show the complete storm in relationship to its environment. In the hurricanes studied (ref. 42), "outer convective bands" or "pre-hurricane squall lines" appear to partially ring the storm. These bands are usually separated from the rim of the high cloud shield by a relatively clear channel, distinctly visible for long distances along the circumference. It was hypothesized that this clear channel may be formed through the action of a major subsiding branch of the hurricane's circula-

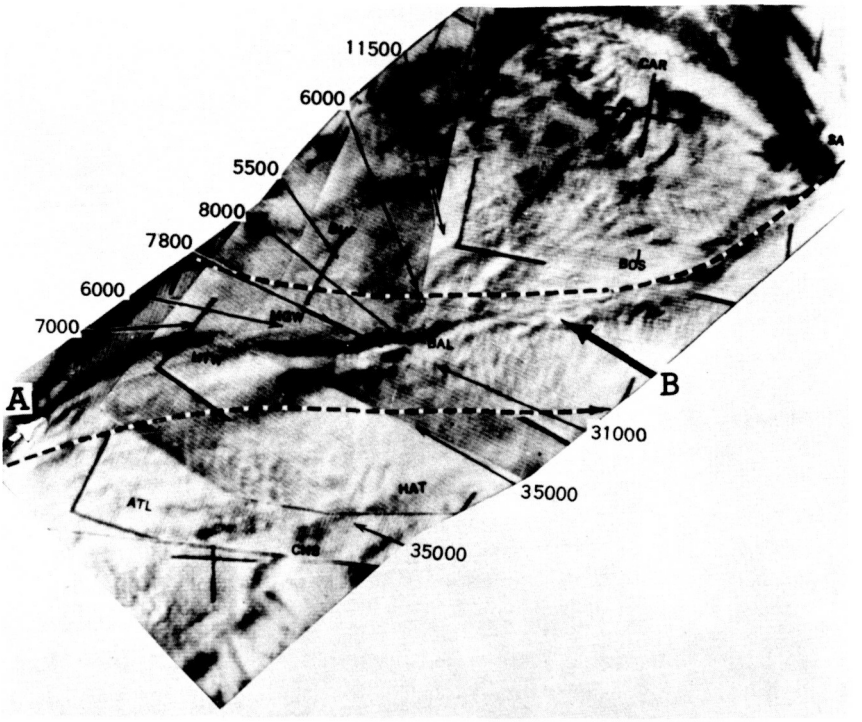

Figure 35.—**Mosaic of Tiros pictures taken over northeastern United States and Canada, with height of cloud tops in thousands of feet as reported by pilots within an hour of picture time. The dashed lines are the position of the jetstream at 200 millibars as analyzed by National Meteorological Center. A and B point out a long, narrow dark streak which was concluded to be shadow cast by higher cloud deck on lower clouds.**

tion. The pictures also reveal extensive areas of convective, cirrus-producing cloudiness in the wake of the storm. This cloudiness appears to be intimately associated with that of the hurricane, and strongly influenced by outflow effects. Time cross-section analyses of Hurricanes Carla (1961) and Anna (1961), using conventional data, also suggest peripheral subsidence. The area of possible subsidence, in both instances, occurred under an upper shear line, where air diverging in the outflow layer from the hurricane converged with air emanating from a subtropical high-pressure cell. A jetstream in the case of Hurricane Carla appeared in the region of the annular zone (subsidence) at the edge of the high cloud shield. This high-speed current curved anticyclonically along the northern quadrant of the

storm. Then, on being directed southward, it split into two main branches. The eastern branch curved cyclonically into a trailing vortex, apparent as a cold low at 200 millibars. The western branch continued southward in alinement with the curvature of cloud streaks forming the cirrus "tail" of Hurricane Carla. These features appear to be typical of many hurricanes in certain stages of development.

Remarks

From the few examples presented, it may be seen that satellite cloud pictures present challenging research problems. Research is required to deduce the nature of the processes involved in cloud formation and the state of the atmosphere, in as much quantitative detail as possible.

It is quite clear from the foregoing that the advent of satellite pictures has had a strong influence on operational and research meteorology throughout the world. Operational aspects especially are affected as can be deduced from the impressive list of storms viewed by meteorological satellites from July 1961 to December 1964 shown in table IV. The influence will grow stronger as improvements are made in TV picture-taking technology, and research continues with pictures already taken by both the Tiros and Nimbus types of satellites.

SATELLITE RADIOMETRIC MEASUREMENTS

Introduction

The Earth's atmosphere is generally considered to operate as an enormous heat engine, energy in the form of heat from the Sun is applied mainly to the equatorial zones and the resulting temperature gradients cause the large-scale motions of the atmosphere, and thus convert heat energy into kinetic energy. Some idea of the distribution of the net radiant energy absorbed by the Earth and its atmosphere at different latitudes can be gained from figure 36. In this figure, the shaded area represents the range of various *estimates* of the net absorbed radiation in gram-calories/cm^2/min as a function of latitude for the Northern Hemisphere (ref. 43). Although considerable variation exists in the estimates of radiation absorbed at any latitude, there is general agreement on a net heating south of about 35° N and net cooling at more northerly latitudes. Measurements are needed of the global distribution of the radiant energy absorbed and emitted by the Earth-atmosphere system. Since "weather" results from winds attempting to equalize the nonuniform distribution of the net radiant energy received from the Sun, it is important to measure accurately the radiant energy that drives the atmospheric heat engine.

Table IV.—*Tropical Storms Observed by Meteorological Satellites July 1961 Through December 1964*

[* Indicates storm discovered by satellite observation]

Atlantic Ocean

Hurricane Anna, 7/61
Hurricane Betsy, 9/61
Hurricane Carla, 9/61
Hurricane Debbie, 9/61
Hurricane Esther, 9/61*
Hurricane Frances, 9/61*
T/S unnamed, 9/61*
Hurricane Alma 8/62
Hurricane Becky, 8/62*
Hurricane Daisy, 10/62
Hurricane Arlene, 8/63*
Hurricane Beulah, 8/63*
Hurricane Cindy, 9/63
Hurricane Debra, 9/63*
Hurricane Edith, 9/63*
Hurricane Flora, 9/63*
Hurricane Ginny, 10/63
T/S Helena, 10/63*
T/S Brenda, 8/64
Hurricane Cleo, 8/64
Hurricane Dora, 9/64*
Hurricane Ethel, 9/64*
T/S Florence, 9/64*
Hurricane Gladys, 9/64
Hurricane Hilda, 9/64
Hurricane Isbell, 10/64

Eastern Pacific Ocean

T/S Liza, 7/61
Hurricane Madelaine, 7/61*
T/S Orla, 9/61
T/S Pauline, 9/61
T/S Willa, 7/62
T/S Ava, 8/62
T/S Claudia, 9/62
T/S Emily, 6/63
T/S Jennifer, 9/63*
T/S Irah, 9/63
Hurricane Mona, 10/63
T/S Natalie, 7/64
Hurricane Odessa, 7/64
T/S Prudence, 7/64
T/S Sylvia, 8/64
T/S Tillie, 9/64*

Indian Ocean

Unnamed, 9/63
Tropical Low Amanda, 12/63
Tropical Low Betty, 12/63
Tropical Cyclone Hazel, 3/64*
Tropical Cyclone Katie, 3/64
Tropical Cyclone Jessie, 4/64
Tropical cyclone unnamed, 12/64*

Western Pacific Ocean

Typhoon Kathy, 8/61
Typhoon Lorna, 8/61
Typhoon Marie, 8/61*
Typhoon unnamed, no date*
Typhoon Nancy, 9/61
Typhoon Pamela, 9/61
T/S Ruby, 9/61
Typhoon Sally, 9/61
Typhoon Tilda, 9/61
Typhoon Joan, 7/62
Typhoon Opal, 8/62
Typhoon Ruth, 8/62
Typhoon Sarah, 8/62*
Typhoon Thelma, 8/62
Typhoon Vera, 8/62*
Typhoon Wanda, 8/62*
Typhoon Amy, 8/62*
T/S Bernice, 9/62
T/S Celia, 9/62
Typhoon Dinah, 9/62
Typhoon Emma, 10/62
Typhoon Freda, 10/62
Typhoon Gilda, 10/62
Typhoon Jean, 11/62*
Typhoon Karen, 11/62*
Typhoon Lucy, 11/62
Typhoon Olive, 4/63
Typhoon Wanda, 7/63
Typhoon Bess, 7/63
Typhoon Carmen, 8/63
Typhoon Della, 8/63
Typhoon Ella, 8/63
Typhoon Faye, 9/63
Typhoon Gloria, 9/63
T/S Hester, 9/63*

Table IV.—*Tropical Storms Observed by Meteorological Satellites July 1961 Through December 1964*—Continued

[* Indicates storm discovered by satellite observation]

Western Pacific Ocean	*Western Pacific Ocean*
T/S Irma, 9/63	T/S Pamela, 8/64*
Typhoon Lola, 10/63	Typhoon Ruby, 9/64*
Typhoon Ora, 10/63	Typhoon Sally, 9/64
Typhoon Susan, 12/63	Typhoon Tilda, 9/64
Typhoon Tess, 5/64	Typhoon Wilda, 9/64
Typhoon Winnie, 7/64	T/S Anita, 9/64
Typhoon Betty, 7/64	T/S Billie, 9/64
Typhoon Cora, 7/64	Typhoon Clara, 10/64
Typhoon Doris, 7/64	T/S Dot, 10/64
T/S Elsie, 7/64	T/S Ellen, 10/64
Typhoon Flossie, 7/64	T/S Fran, 10/64*
T/S Grace, 7/64*	T/S Georgia, 10/64*
Typhoon Helen, 7/64*	Typhoon Hope, 10/64
T/S June, 8/64	T/S Iris, 11/64*
Typhoon Kathy, 8/64	Typhoon Kate, 11/64*
Typhoon Marie, 8/64	Typhoon Louise, 11/64*
T/S Nancy, 8/64*	Typhoon Opal, 12/64

	Observed	Discovered
Atlantic Ocean	26	13
Eastern Pacific Ocean	16	3
Western Pacific Ocean	69	19
Indian Ocean	7	2
TOTAL	118	37

Before the development of rockets and Earth-orbiting satellites, actinometric measurements were restricted mainly to determinations of the solar constant with a highly specialized pyrheliometer at a few observatories, the total solar radiation at the Earth's surface measured with a pyrheliometer at some first-order weather stations, and the hours of sunshine obtained with a sunshine recorder or recording black-bulb thermometers at first-order weather stations. A few measurements of the outgoing "effective" radiation have been obtained for research purposes by the use of special radiometers that were mounted at the surface or carried aloft by balloons and aircraft. However, it was impractical to use these techniques in a global synoptic network (ref. 44). Satellites carrying infrared radiometers provided the first capability for obtaining radiation data on a global synoptic basis.

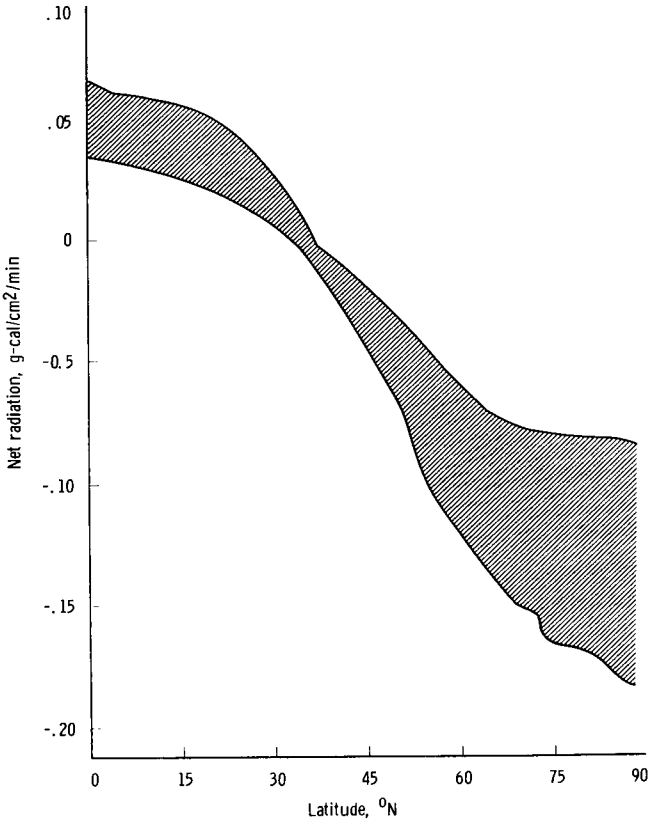

Figure 36.—**Annual average absorbed radiation for different latitudes of Northern Hemisphere.**

Table V lists the meteorological radiometric experiments that have been flown on U.S. scientific satellites. The type of equipment and the main purpose are shown in adjacent columns. In addition, the overall accuracy of the measurements, spectral and spatial resolutions, and the geographic coverage are shown. The months of useful life for Tiros I–VI are: 2½, 10, 4½, 4½, 10½, and 13, respectively. Tiros VII and VIII are still operating (as of January 1, 1965).

Explorer VII

The first successful radiation experiment on a satellite was by Explorer VII (launched on October 13, 1959) which measured the integrated radiation over broad areas. Despite the low resolution, the data show macroscale weather patterns (ref. 45). Figures 37, 38, and 39 are composite charts

Table V.—*Meteorological Satellite Radiometric Experiments*

Satellite	Equipment	Mission	Accuracy	Resolution		Coverage	Calibrated in flight
				Spectral	Spatial [a]		
Explorer VII	Black and white balls.	Heat balance	Medium	Low	Low	Good	Indirect checks possible.
Tiros II, III, IV	MRIR 5-channel radiometer.	Multipurpose	Medium	Medium; 5 filters.	40 miles per scan line.	Good	Zero balance only.
	Low-resolution radiometer.	Heat balance	Medium	Low	Low	Restricted by spin.	No.
Tiros VII	MRIR 5-channel radiometer.	Multipurpose	Medium	Medium; 5 filters.	40 miles per scan line.	Good	Zero balance.
	Low-resolution radiometer.	Heat balance	Medium	Low	Low	Restricted by spin.	No.
Nimbus I	High-resolution IR radiometer.	Cloud cover (night).	Good	Good; 3.5μ–4.2μ.	Good	Good; night only.	Yes; zero and blackbody.

[a] The resolutions quoted refer to the subsatellite point.

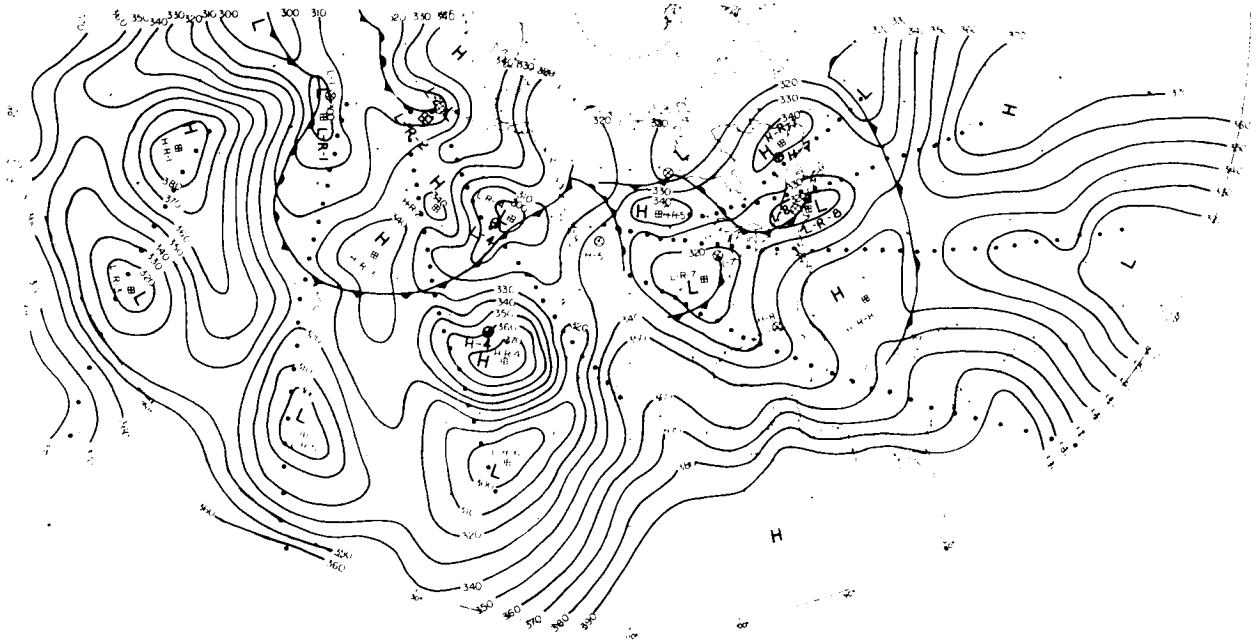

Figure 37.—Map of long-wave radiation loss, December 1, 1959. Lines are isolangleys, connecting equal long-wave radiation loss values in langleys per minute $\times 10^{-3}$. Surface pressure centers and fronts are composite to the satellite passage time. Surface pressure centers, marked by circles, are designated "L" for Low and "H" for High, plus an Arabic number (thus L–1). Radiation centers, marked by squares, are distinguished from surface centers by the inclusion of R (thus L–R–1 is radiation Low No. 1, which is associated with surface Low L–1). Satellite observation points and orbit path are shown by dots.

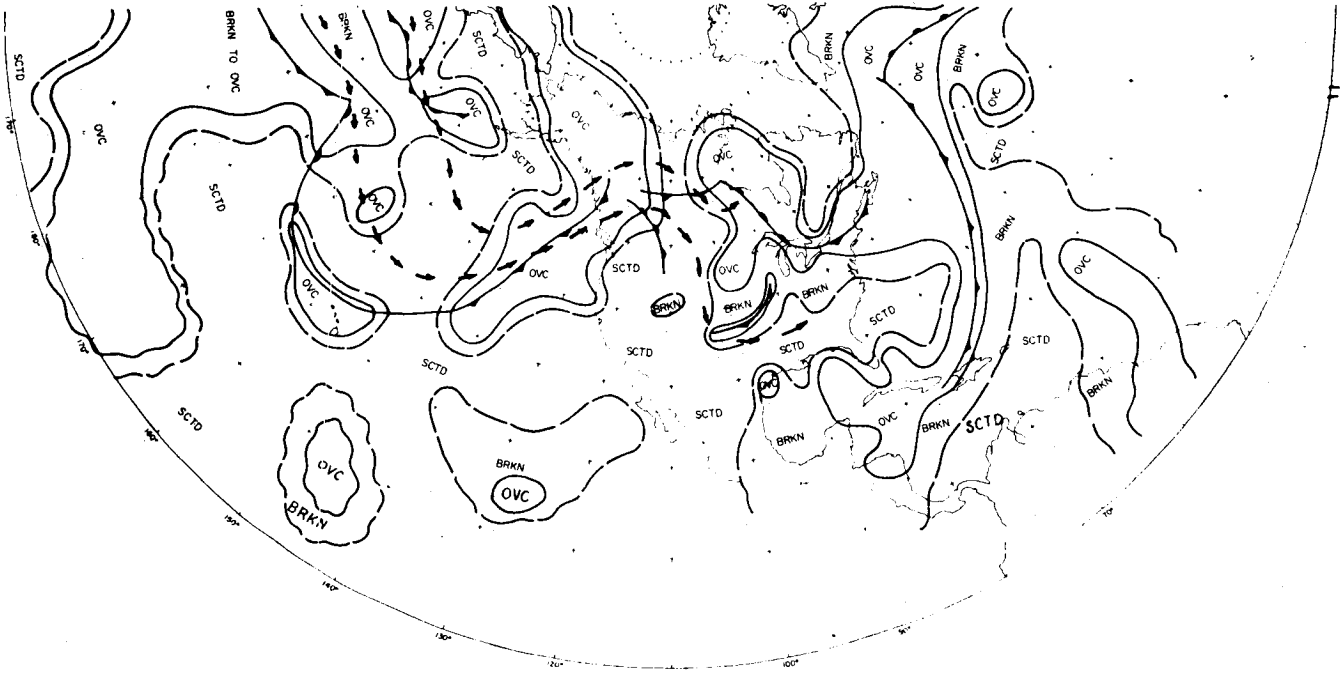

Figure 38.—Composite nephanalysis, December 1, 1959, based on 0000, 0600, and 1200 GMT surface maps. Overcast (OVC) areas are enclosed within solid lines. Broken lines separate the clear-to-scattered (SCTD) areas from the broken, 5/8 to 7/8 (BRKN). Wavy lines indicate that the actual cloud area edge is unknown because of lack of data. Arrows show regions of maximum winds, from the 0000 GMT, 300-millibar chart.

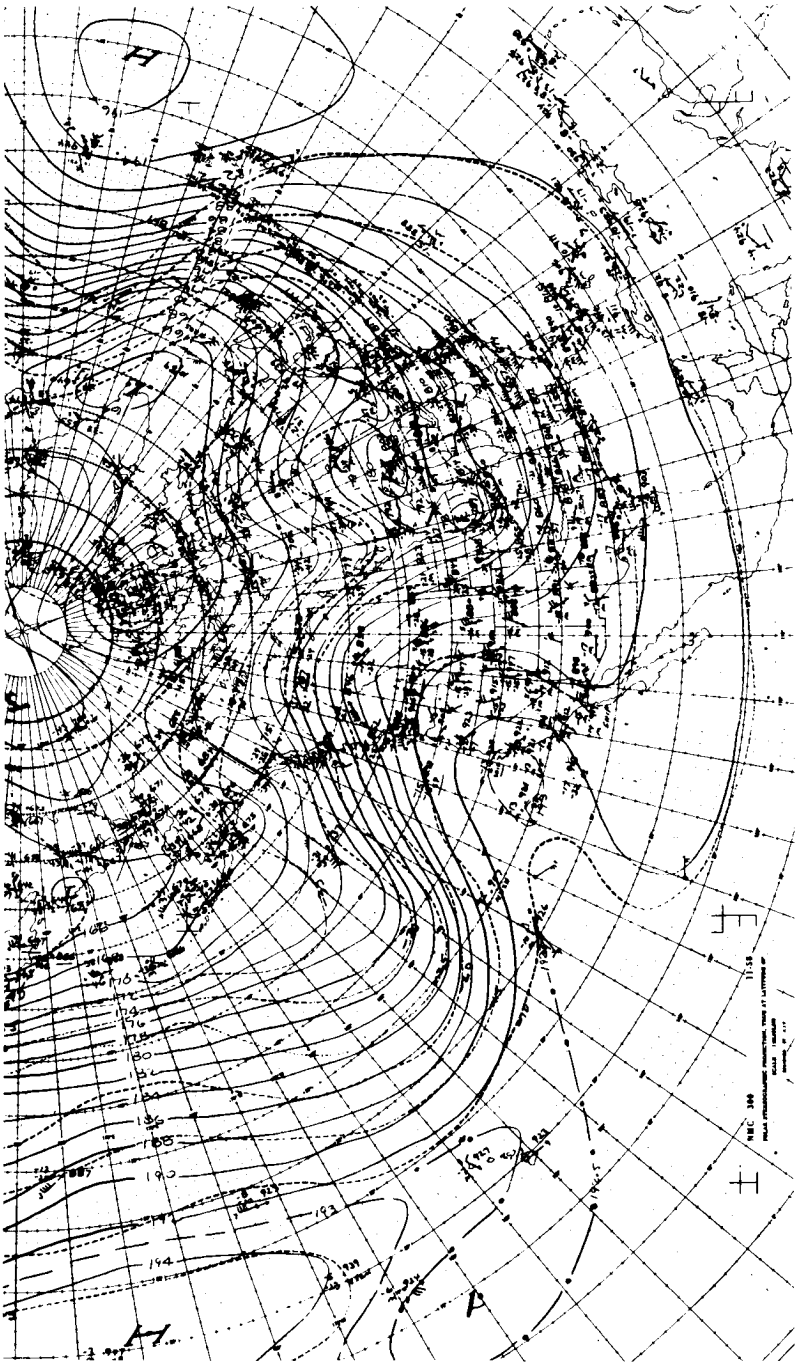

Figure 39.—500-millibar map, 1200 GMT, December 1, 1959.

of radiation loss, cloud cover, and the 500-millibar contours for December 1, 1959. The results indicate a definite relationship between the radiation centers and their corresponding surface low- and high-pressure centers, surface pressure center locations, 24-hour intensifications and movements, and the conformity of the movements to the 500-millibar geostrophic flow. The data obtained by this sensor indicated a close inverse correlation between energy loss by thermal radiation and cloud cover. Clouds are opaque to wavelengths greater than 3 μ, and trap the far-infrared radiation, so that the emission to space occurs only from the tops of clouds, where the temperatures are generally lower than at the surface. Consequently, the outgoing radiation is greater over clear areas than over cloud regions.

Tiros MRIR Measurements

Tiros II, III, IV, and VII have carried five-channel radiometers with ground resolution of about 50 x 50 kilometers. The details of each channel are listed below (ref. 25).

Channel	Approximate bandwidth, μ	Short description
1	6–6.5	Water-vapor absorption
2	8–12	Atmospheric window
3	0.25–6	Mainly reflected solar radiation
4	7–30	Emitted terrestrial radiation
5	0.55–0.75	Reflected solar radiation in the same visible regions as the television cameras

On Tiros VII, a 15-μ channel, in place of channel 1, was inserted to take radiation measurements in the 15-μ CO_2 band, which may be interpreted as a measure of the average temperature of the atmosphere within the 15–35-kilometer region (ref. 46).

The five-channel-radiometer composite signal and data from other instruments are recorded on magnetic tape at the ground station. The data tapes in original analog form are then sent to the NASA Goddard Space Flight Center for demodulation and conversion into digital form for computer processing. Acceptable data are further processed to produce a binary tape, which combines orbital and radiation-calibration data with the digitized raw radiation data to produce the final meteorological radiation (FMR) tape. The FMR tape is in the form in which radiation data are stored in the archives. This binary tape, which locates each radiation datum point by latitude and longitude, by nadir and azimuth angle, and

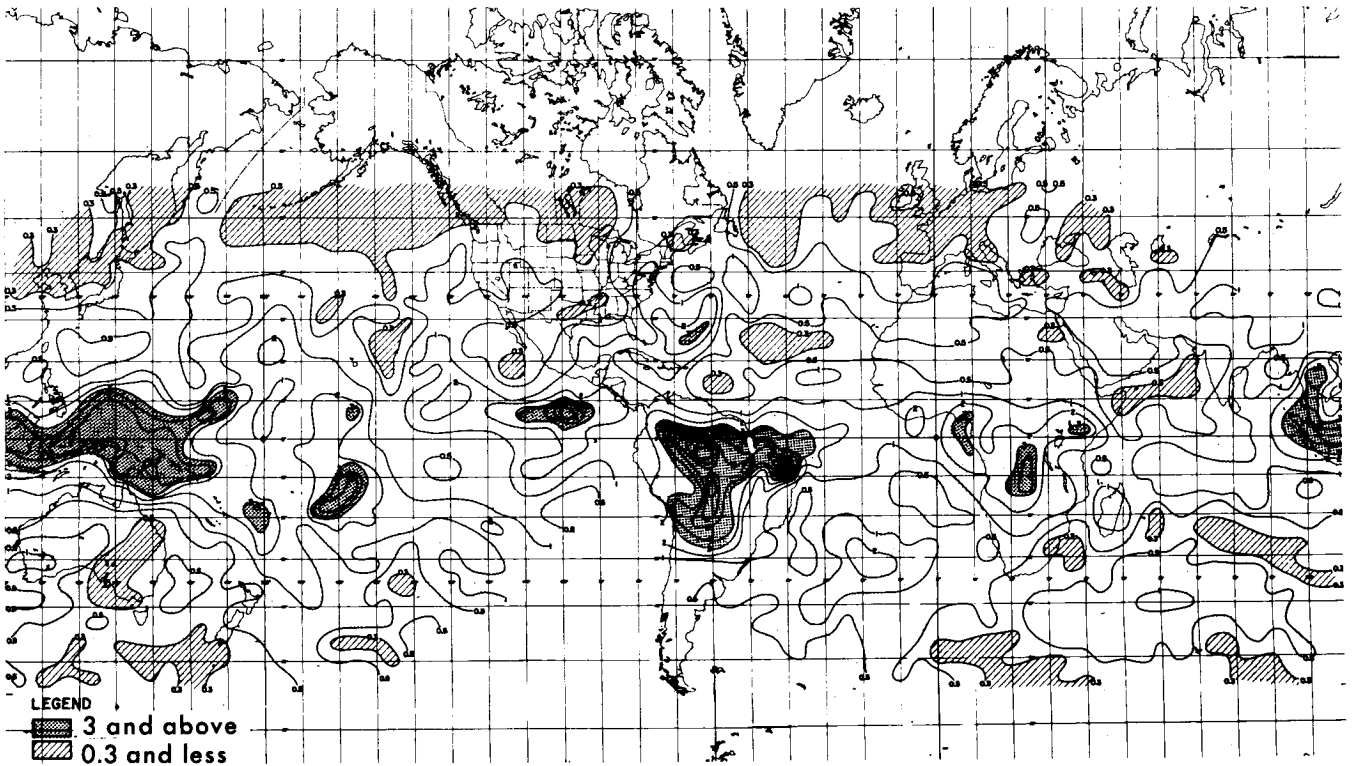

Figure 40.—Map based on Tiros IV data showing average water-vapor content (decigrams/cm^2) above 500 millibars, April 11–18, 1961.

in time, and which gives the intensity of radiation in watts per square meter, is used in the computers for analysis of the data. Selected data from all five channels of the scanning radiometer on the Tiros satellites have been mapped by computers and published by NASA and the U.S. Weather Bureau (ref. 47 has a bibliography).

Spectral Channels

Channel 1.—The data from channel 1 (6μ to 6.5μ) have been used to measure radiation emanating from the water-vapor layers in the upper troposphere on almost a global basis. Channel 1 maps (fig. 40) present a gross picture of the upper-tropospheric moisture patterns. This is based on a preliminary analysis, and further work is required in view of the problem of instrumental degradation and the assumption of constant relative humidity. Methods are being developed to estimate the mean vertical relative humidity of the troposphere based on the channel 1 measurements for the upper portion of the troposphere and channel 2 data in the lower half of the troposphere (ref. 48).

Channel 2.—Studies have been made of channel 2 measurements through the 8- to 12-μ window. Figures 41 and 42 show a computer-drawn, high-resolution radiation map and an analysis using these data (ref. 49). These measurements show the "effective" temperatures of the radiating surfaces below the satellite. The radiating surfaces are the tops of clouds in overcast areas, and the Earth's surface in cloud-free areas. In areas of scattered or broken clouds, the data are difficult to interpret in terms of cloud-top or ground temperature. In the middle and low latitudes, contours separate the cold tops of middle and high clouds from the usually warmer tops of low clouds or the Earth's surface. These maps indicate the gross pattern of cloudiness on the night side of the Earth, where television pictures are not available. In addition, an approximate determination of the height of the top of overcast clouds can be made by correlating the effective temperature with actual or climatological lapse rates.

Channel 3.—Channel 3 (0.25μ to 6.0μ) indicates mainly reflected solar radiation. The average value shown by this channel should give a more accurate estimate of the Earth's albedo. Preliminary analyses indicate values somewhat lower than those currently accepted (ref. 50). The albedo estimates from channel 3 data will be very useful for studies of the Earth's heat balance, since the net solar radiation absorbed by the Earth-atmosphere system can readily be derived from them. Combination of these short-wave values with the long-wave information derived from channel 4 will yield the value for the net radiation received (or lost) by the Earth-atmosphere system.

Figure 41.—Computer-plotted radiation map for 8- to 12-micron "window."

Channel 4.—Infrared flux, mapped from the channel 4 (7μ to 30μ) data, have also been examined. There is, of course, substantial correspondence between maps of channel 2 and channel 4 data, since radiation sensed by channel 4 includes a very substantial contribution by the 8- to 12-μ region. The emission over the remainder of the 7- to 30-μ region is primarily from the carbon dioxide and water vapor absorption bands, which absorb radiation emitted by the Earth's surface and the lower atmosphere. Emission from the top of the atmosphere in these bands originates mostly higher in the atmosphere, and they represent lower temperatures than those detected in the 8- to 12-μ region. The relatively uniform horizontal distribution

of these atmospheric constituents probably helps to account for the relatively uniform differences between the radiation maps derived from measurements in channel 2 and channel 4.

Channel 4 data have been used to prepare daily composite radiation charts for the Northern Hemisphere. Average values for each 5° latitude circle between 20° N and 55° N, and the average value for all latitudes were obtained for each data-day from these charts. Time variations of these averaged values of radiation show that the large-scale variations in long-wave radiation are related to time variations in hemispheric energy parameters (ref. 51).

Channel 5.—Maps of channel 5 (0.55- to 0.75-μ) measurements have been closely investigated by Fujita (ref. 52), who found a remarkable agreement between the intensities of this reflected solar radiation and the brightness of clouds and terrain seen in the TV pictures from the satellites. It was also noted that visual reflections from the top of cirrus varied with the size of the ice crystal, scattering, solar zenith, etc., suggesting that radiation measurements would show a decrease in channel 5 response and an increase in channel 2 response as radiation from lower cloud layers penetrates upward.

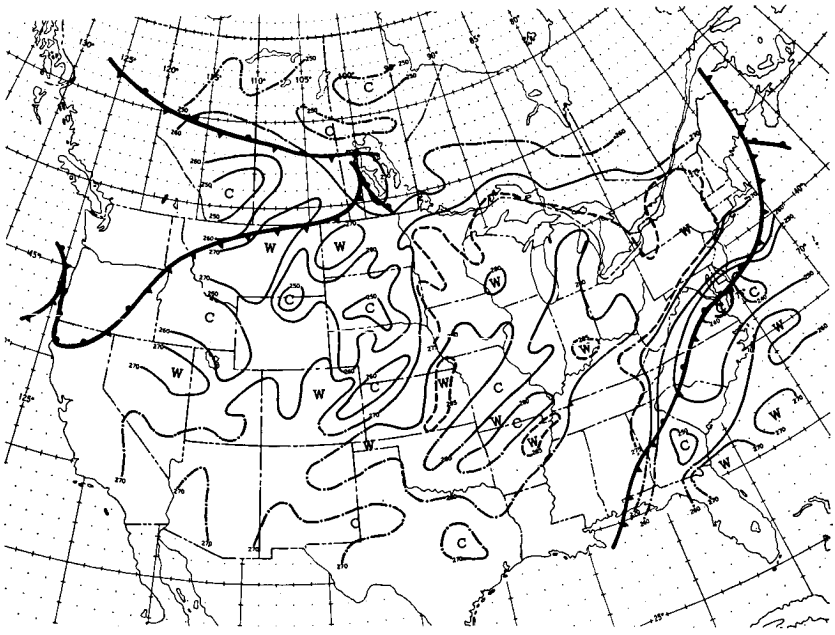

Figure 42.—Analyzed radiation map, 8- to 12-μ "window."

207-342 O-66—6

Analysis of Radiation Data

The Tiros radiation data have provided meteorological information concerning:

(1) The distribution of meso- and macroscale cloud patterns, both daytime and nighttime, and estimates of overall cloud-top heights.
(2) A preliminary estimate of the global distribution of energy sources and sinks in the Earth-atmosphere system; namely, the difference between the solar energy absorbed, and the infrared energy emitted, by the Earth and the atmosphere.
(3) The global distribution of mean temperature in the stratosphere.
(4) The distribution of water vapor in the upper troposphere (fig. 40).

Cloud-Cover Analysis

The cloud-cover analysis using the MRIR data ranges from mesoscale to almost global scale.

The capability of using the radiation data for detailed cloud analysis has been demonstrated many times (refs. 30, 48, 53, 54).

In one case, discussed in reference 48, cloud systems over the Caribbean, associated with Hurricane Anna, were plotted from Tiros III radiation measurements in the 8- to 12-μ channel. The storm could be tracked on the basis of its radiation pattern alone over a distance of more than 4000 kilometers. A mesoscale analysis of the cloud-top temperatures was made, and from these temperatures the height contour of the cloud-top surface was estimated. The height of the cloud tops in the center of Hurricane Anna was found to be approximately 15 kilometers, in contrast to other cloud systems in the vicinity at much lower altitudes. Such cloud-height differences could not be detected by TV cloud observations. Furthermore, the measurements in the 8- to 12-μ channel on Tiros have become an excellent tool to map cloud cover and height on a global scale, since this method is independent of illumination by sunlight.

Besides the detailed structure of the mesoscale cloud system, the general distribution of cloudiness in the macroscale is of interest to the meteorologist. The high inverse correlation between the outgoing radiation in the water-vapor window (8μ to 12μ) and cloudiness (refs. 49, 55, 56) represents a most useful application of the radiation data.

As an example, a cloud-cover map of almost the entire globe was produced from seven orbits of Tiros III for July 18, 1961, in both daytime and nighttime (fig. 43). This map disclosed a wealth of global features, such as the extensive cloud cover over high southern latitudes, where a number of typical winter storms were in progress; over the North Pacific, where a series of frontal systems ranged from Japan to the Gulf of Alaska; and over the intertropical convergence zone, north of the Equator. A major tropical

Figure 43.—Global cloud-cover map for July 18, 1961, from Tiros III observations of the infrared radiation between 8 and 12 microns.

storm, Flossie, was located over the Philippines. Also, high radiation intensities were seen over clear skies, particularly over the North African and Arabian deserts, where radiation is received from the very hot Earth's surface. Nimbus I, with its HRIR, has produced similar global analyses of cloud cover and height but with resolutions greater by one order of magnitude and covering the entire globe from pole to pole.

Heat-Budget Analysis

Global heat-budget estimates have been made using radiation data obtained by meteorological satellites. These estimates confirm previous theoretical estimates on the global distribution of total radiation emission (refs. 47, 57, 58). The Tiros results clearly show a minimum of outgoing radiation just north of the "meteorological" equator, and a maximum in 20° to 30° latitudinal belts. The minimum is due to the extensive cloud cover in the equatorial zone, while in the regions of maximum outgoing radiation (the two subtropical belts), the total outgoing radiation decreases with increasing latitudes, especially toward the winter pole.

The important parameter in the study of the dynamics of the atmosphere is, however, the net atmospheric energy balance and not the outgoing radiation alone. The net energy balance is made up of the difference between the incoming solar radiation, mostly in the visible, and the outgoing terrestrial radiation, in the infrared. It is well known that the energy balance shows an excess near the Equator and a deficiency at the poles. Using the satellite data on the energy balance of the entire Earth-atmosphere system, it is possible to derive the time variations in latitudinal averages of the net energy balance.

Estimates of the incoming energy from the Sun can be made from satellite measurements of the reflected solar energy. The amount of energy absorbed in the Earth-atmosphere system is derived from these data by subtracting the reflected energy from the known value of the solar constant. Tiros IV and VII have given estimates of the albedo of the Earth for all parts of the globe between 60° N and 60° S for periods of over 2 years. Preliminary results indicate that the albedo shows a relative maximum at the Equator, minima in the two subtropical belts, and an increase with latitude from these minima up to the value of about 50 percent at 60° latitude. The latitudinal gradient is found to be steeper than previous theoretical estimates (ref. 47). There is some uncertainty concerning the Tiros data because of the instrument degradation; therefore, these are tentative conclusions, and additional measurements are required for verification.

From the Tiros VII radiational data, estimates of the seasonal values of long-wave radiation and albedo (figs. 44 to 47) and the annual values (figs. 48 and 49) were derived. Data from London (ref. 58) are shown for

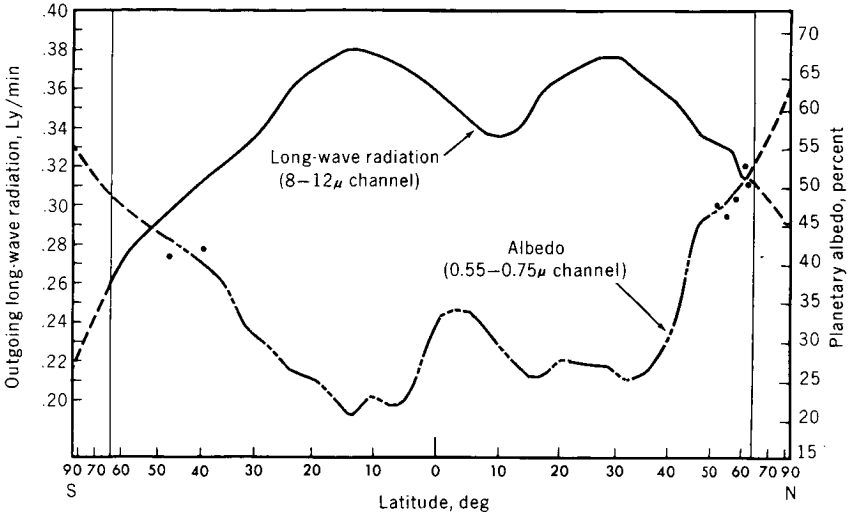

Figure 44.—Outgoing long-wave radiation and albedo for June to August 1963 (Tiros VII). The abscissa is scaled in proportion to zonal areas (sine of the latitude).

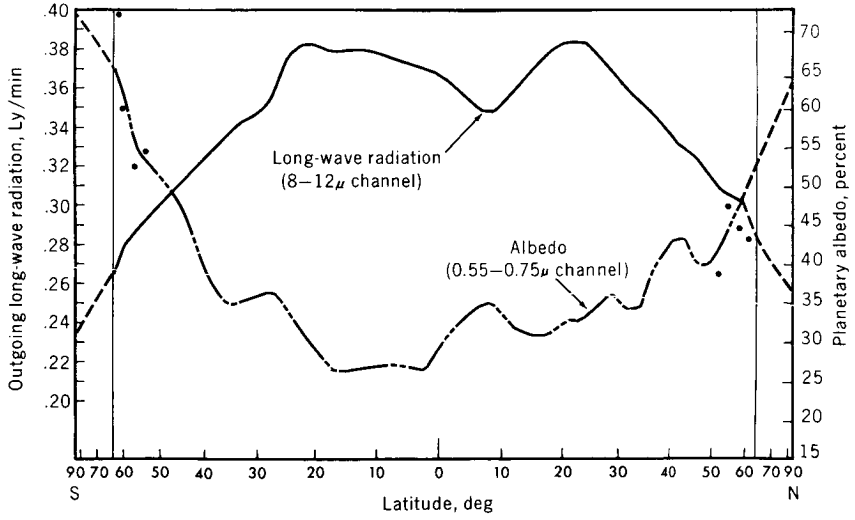

Figure 45.—Outgoing long-wave radiation and albedo for September to November 1963 (Tiros VII). The abscissa is scaled in proportion to zonal areas (sine of the latitude).

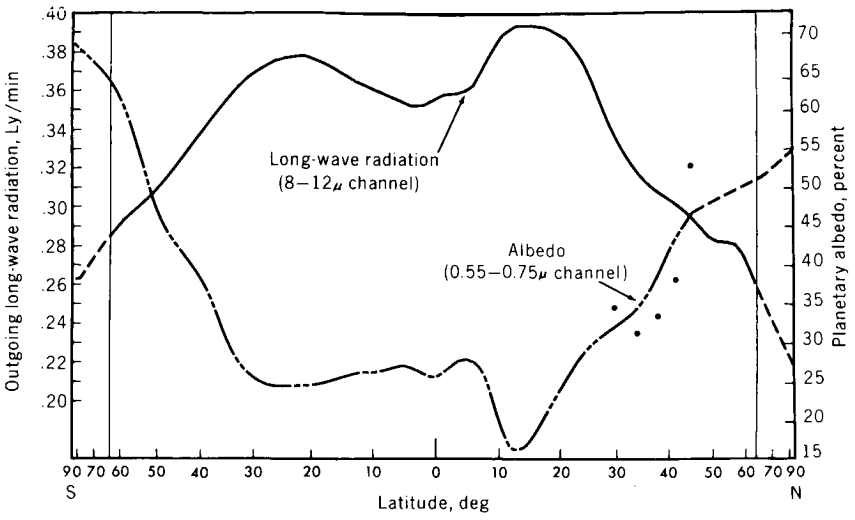

Figure 46.—Outgoing long-wave radiation and albedo for December 1963 to February 1964 (Tiros VII). The abscissa is scaled in proportion to zonal areas (sine of the latitude).

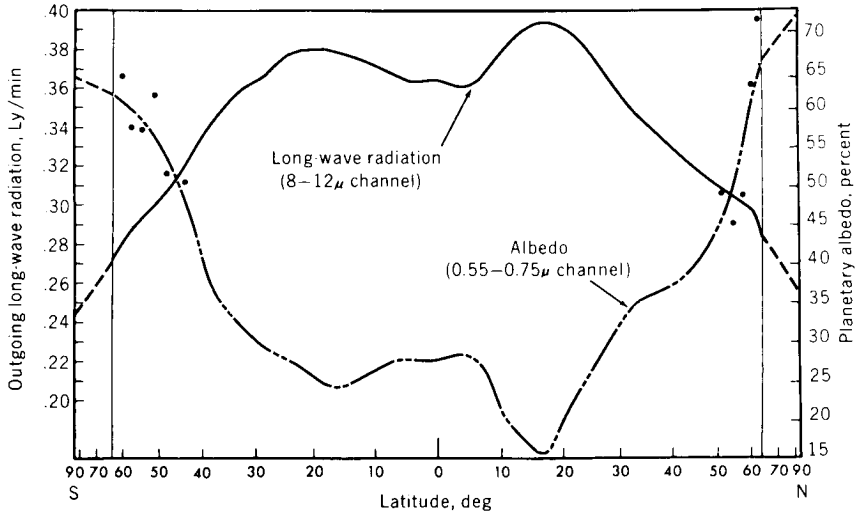

Figure 47.—Outgoing long-wave radiation and albedo for March to May 1964 (Tiros VII). The abscissa is scaled in proportion to zonal areas (sine of the latitude).

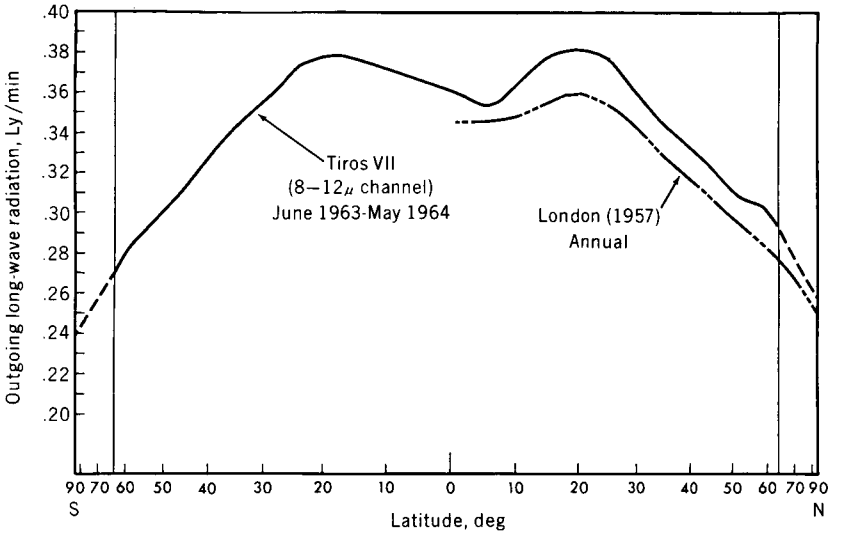

Figure 48.—Annual mean outgoing long-wave radiation. The corresponding values of London (1957) for the Northern Hemisphere are shown for comparison. The abscissa is scaled in proportion to zonal areas (sine of the latitude).

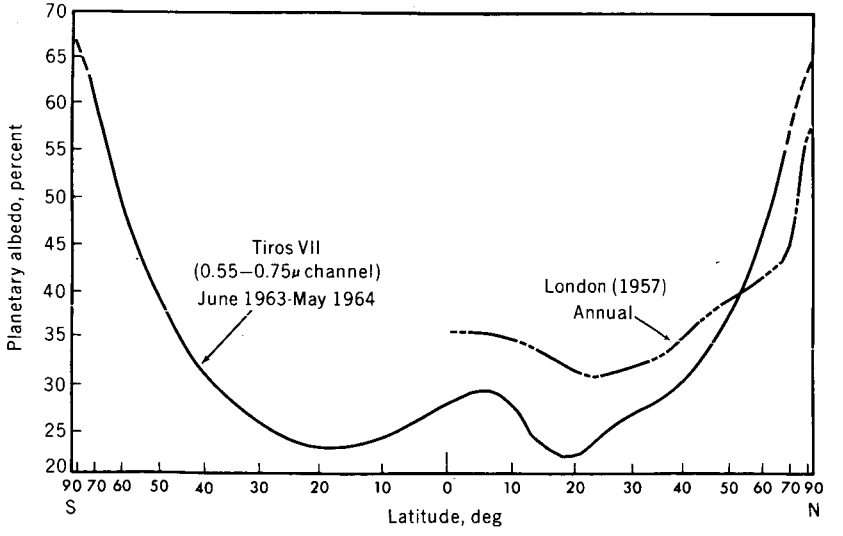

Figure 49.—Annual mean planetary albedo. The corresponding values of London (1957) for the Northern Hemisphere are shown for comparison. The abscissa is scaled in proportion to the annual zonal insolation (top of the atmosphere).

comparison in figures 48 and 49. Two maxima in the long-wave radiation, associated with the subtropical high-pressure regions, show up clearly in all figures, as does a tropical minimum, caused by the cloudiness of the intertropical convergence zone (ITC). The long-wave tropical minimum remains in the Northern Hemisphere in all seasons except December, January, and February, clearly pointing up the asymmetry between the hemispheres. Similarly, the long-wave maximum occurs over the subtropical high of the Northern Hemisphere in all seasons except June, July, and August, when the long-wave radiation over the subtropical high in the southern latitude becomes only slightly larger. Generally, more long-wave radiation is emitted from the extratropical latitudes of the Northern Hemisphere than from the same latitudes of the Southern Hemisphere in corresponding seasons. However, for tropical latitudes, the situation is reversed, less radiation being emitted from the Northern Hemisphere than from the Southern Hemisphere in corresponding seasons. This characteristic tends to equalize the total radiation emitted from the two hemispheres annually. The albedo minima occur in the tropics of the winter and spring hemispheres, but are lowest when they occur in the Northern Hemisphere.

The tropical annual minimum in the long-wave radiation is located at latitude 5° N, whereas the maximum long-wave radiation is located at latitude 20° N (fig. 49). The emission is smaller in the Northern Hemisphere between the Equator and latitude 15°, but larger between 15° and the pole, than in the Southern Hemisphere. The overall long-wave emission is slightly larger than London's (ref. 58), as would be expected from a comparison of the Tiros-inferred albedo of 32.2 percent with London's 35.2 percent.

Stratospheric Temperatures

As described earlier, Tiros VII was equipped with a sensor to map the emitted terrestrial radiation in the 15-μ CO_2 band. Because of the absorptive properties of CO_2, atmospheric layers at altitudes between 10 and 40 kilometers contribute most to the observed radiation in this wavelength interval. The radiation measurements acquired by Tiros VII in this channel can, therefore, be interpreted in terms of the average temperature of the lower stratosphere. The results, on a global scale, show patterns of stratospheric temperatures, corresponding approximately to average temperatures in the 15- to 35-kilometer region, which bear a strong relationship to stratospheric circulation. In general, the temperatures near the summer pole (65° latitude) were of the order of 240° K, decreasing toward the winter pole, where the stratospheric temperatures were found to be about 200° K. The equatorial regions (20° N to 20° S) were isothermal at 230° K.

An analysis of the stratospheric temperatures on a regional basis has already shown several interesting features. An intense warm area over the North Pacific, related to the well-known Aleutian anticyclone, has been clearly identified. Sudden stratospheric warmings were observed by the satellite. These stratospheric warmings have attracted considerable attention since they were first noticed over Berlin in 1950. In figure 50, there are two stratospheric temperature charts, taken roughly a week apart from Tiros VII data, that show the possibility that these radiometric measurements identify the sudden stratospheric warmings that sometimes occur during the winter season. During the winter of 1964, there was not the sharp, intense sudden warming that had been identified in other years, but the moderate warming that did occur over the Eurasian continent is clear, and may be seen in the upper-right corner of the map on the right.

The significance of the sudden warming phenomena and their correlation with tropospheric events is not fully understood. The availability of continuous global measurements of stratospheric temperatures by satellites will certainly resolve many questions about these phenomena and their relation to the sudden changes in the stratospheric circulation.

Distribution of Water Vapor

Using Tiros radiation data, a method was developed for determining the mean relative humidity of the upper troposphere and the surface temperature of the clouds or the ground (refs. 59, 60). The application (ref. 47) of this method, using the 6- to 6.5-μ and the 8- to 12-μ data from Tiros IV for the period April 11–18, 1962, produced estimates of the water-vapor content of the atmosphere for the area between 55° North and South latitudes (fig. 40).

The chart shows three major concentrations of water vapor over Indonesia, South America, and Africa. Two additional moist regions are at 6° N 100° W, and 15° S 160° W, which are near the April position of the ITC zone and were found to persist 2 weeks later. There was a marked dry area over the Sahara Desert, extending westward to the Caribbean Sea, and relative dryness everywhere near latitude 20° N. While many approximations were used in this analysis, the patterns are encouraging for additional work. The satellite measurements are of particular interest, since they enable detailed study and comparison of these phenomena in both hemispheres.

Nimbus HRIR Measurements

The Nimbus HRIR was designed to perform two major functions: first, to map the Earth's cloud cover at night to complement the TV pictures

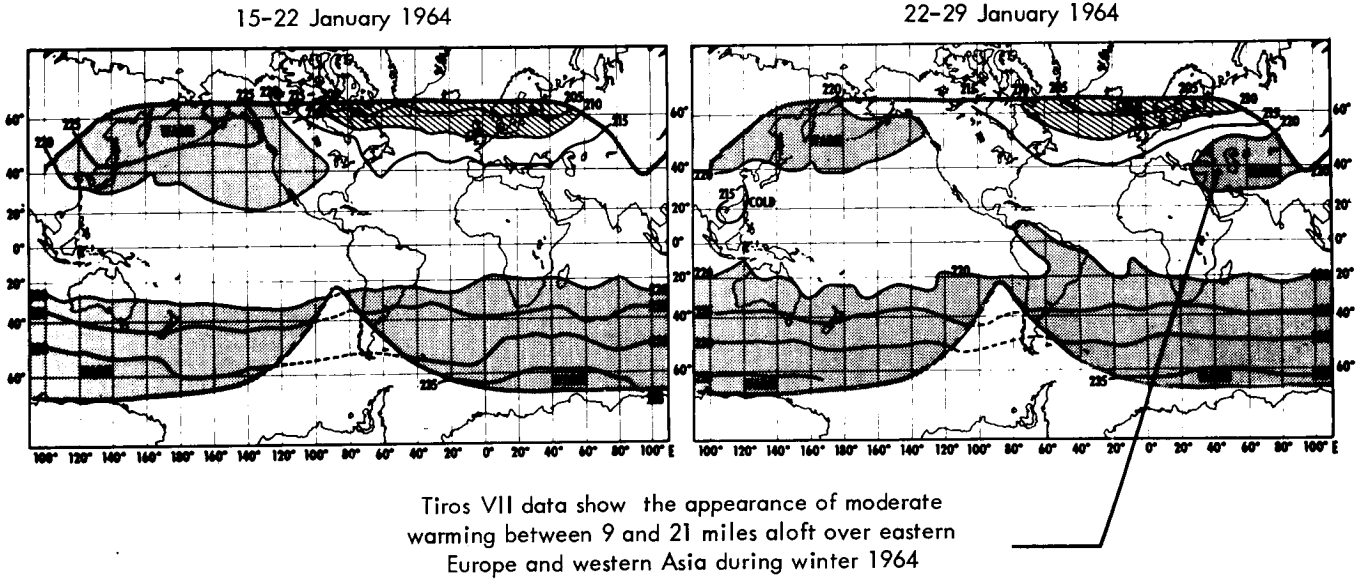

Figure 50.—Maps of global stratospheric temperatures based on Tiros VII data.

during the day; second, to measure the cloud-top and surface temperatures. During the 26 days of Nimbus I operation, data were obtained for about 50 percent of all nighttime orbits. Each orbit covered a strip from horizon to horizon (about 2,000 kilometers) and ranging from North Pole to South Pole. Because the radiometer operates in the 3.4- to 4.2-μ region, measurements taken during the day include reflected solar radiation and therefore do not reveal the true surface temperatures. However, reflected sunlight in this spectral region does not saturate the radiometer, and usable pictures can be made, although of poorer quality. Radiation intensities corresponding to equivalent blackbody temperatures ranging from 210° to 330° K were resolved with an accuracy of 2° K or better.

The Nimbus I control system has a demonstrated accuracy of about 1°. A pointing error of 1° corresponds to a subsatellite error of 14 kilometers at an altitude of 800 kilometers. This is an acceptable error for meteorological analysis on a global basis (ref. 61).

Cloud-Cover Pictures

The photofacsimile recorder gives a visual readout of the HRIR data for real-time use. The data are presented on 70-millimeter filmstrips, some of which are shown in figures 51 to 54. Although these figures are considerably degraded by the photographic reproduction, it is possible to recognize high-, medium-, and low-level clouds and the boundaries between land and water. In general, terrain features, such as mountain ranges and large rivers and lakes, can be distinguished. The blackness of each picture element varies directly with the intensity of the radiation sensed by the radiometer. Thus, the lower-altitude clouds appear darker than the higher ones. Because of film limitation, the intensity resolution is an order of magnitude less than that contained in the recorded analog data.

Figure 51 shows most of Europe and the northern tip of Africa, viewed by the HRIR near midnight on September 12, 1964. High clouds cover the Alps, but much of Europe is clear.

Figure 52 is a comparison of Hurricane Dora pictures taken by the HRIR and by the APT camera, 12 hours earlier. At the time the HRIR picture was taken (near midnight on September 9, 1964), the storm center was located off the coast of Florida. The eye of Hurricane Dora is clearly visible in the infrared, but is difficult to spot in the APT picture because it is obscured by low-altitude clouds.

Figure 53 shows part of an orbital strip covered by the Nimbus I HRIR near midnight on September 2, 1964, ranging from about the Equator at the bottom to southern Canada at the top. The warm waters off the Gulf of California are in the very dark area near right center, in contrast to the

Figure 51.—**Nimbus I high-resolution infrared-radiometer map of Europe, September 12, 1964.**

somewhat cooler temperatures of the Pacific Ocean, shown by the dark gray in the left center. A large, spiral-cloud system at the bottom indicates a tropical storm. Between this high spiral-cloud system and California is a medium gray area, which is a large mass of very-low-altitude clouds. The line along the right edge of the picture indicates the horizon seen by the radiometer. There is a clear indication of fluctuation in that line near the tropical storm at the bottom. This indicates the disturbances that the high-altitude clouds of the storm presented to the Nimbus I horizon scanner control systems, causing the spacecraft to roll slightly as it passed.

Figure 54 shows a portion of an HRIR strip map taken near midnight on September 1, 1964, ranging from Antarctica, near the bottom, to about 30° S latitude at the top. The bright area at the bottom is Antarctica, with the Ross Ice Shelf clearly visible. Small dark spots on the bottom left indicate isolated areas 10° C to 15° C warmer than the surrounding ice.

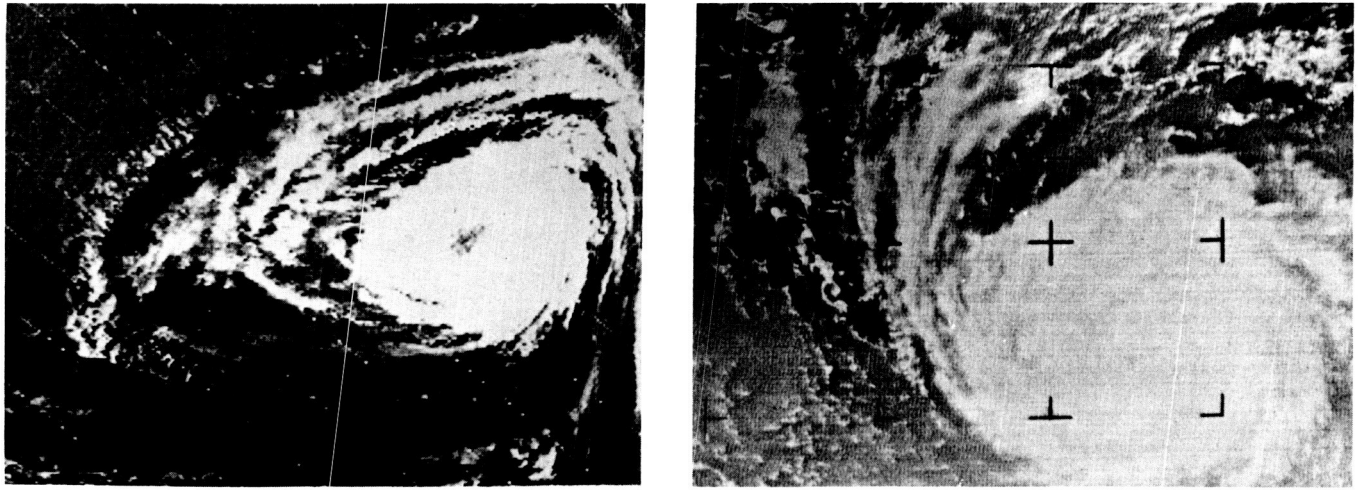

Figure 52.—Hurricane Dora as seen by Nimbus I on September 9, 1964. Left, by its HRIR; right, by its APT system.

Figure 53.—Nimbus I HRIR orbital strip showing parts of California and Baja California on September 2, 1964.

Figure 54.—Nimbus I HRIR orbital strip map showing Antarctica on September 1, 1964.

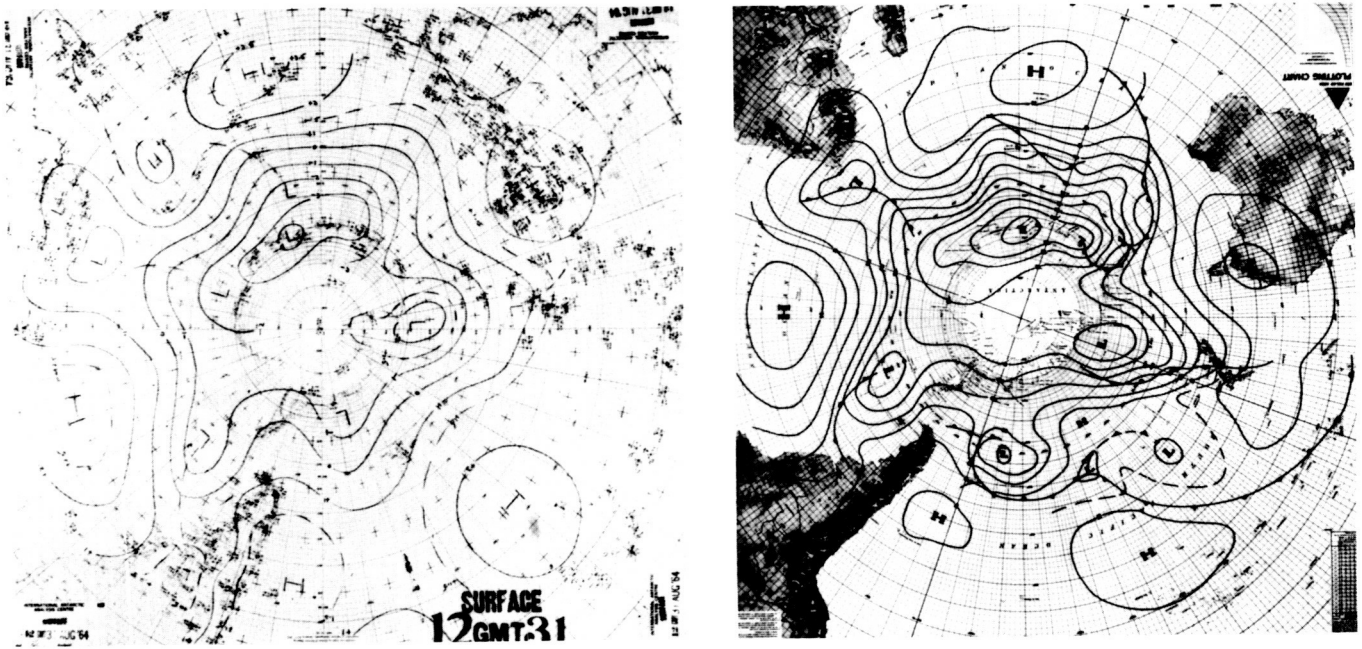

Figure 55.—Maps of Antarctic surface analysis for 1200Z, August 31, 1964. The map at left is based on conventional data alone; the one at right is based on both conventional and Nimbus HRIR data.

These spots may be related to volcanic regions in Antarctica. The cloud spiral in the upper left indicates a small storm over the otherwise generally clear South Pacific Ocean, and the diffuse light gray mass over Antarctica probably indicates low-altitude clouds whose tops are warmer than the surface.

Storm Identification and Analysis

As an illustration of how HRIR data may aid in the analysis of weather data over sparsely settled areas, figure 55 compares the surface analysis drawn by the International Antarctic Analysis Center, using only conventional data, with the analysis drawn using both conventional and Nimbus I HRIR data. The HRIR data are at least equal to the conventional data in locating low-pressure cells and frontal systems, and inferring their relative intensity (ref. 62).

Weather satellites have probably yielded their greatest benefit to mankind thus far by their storm-surveillance of remote areas. Figure 56 illus-

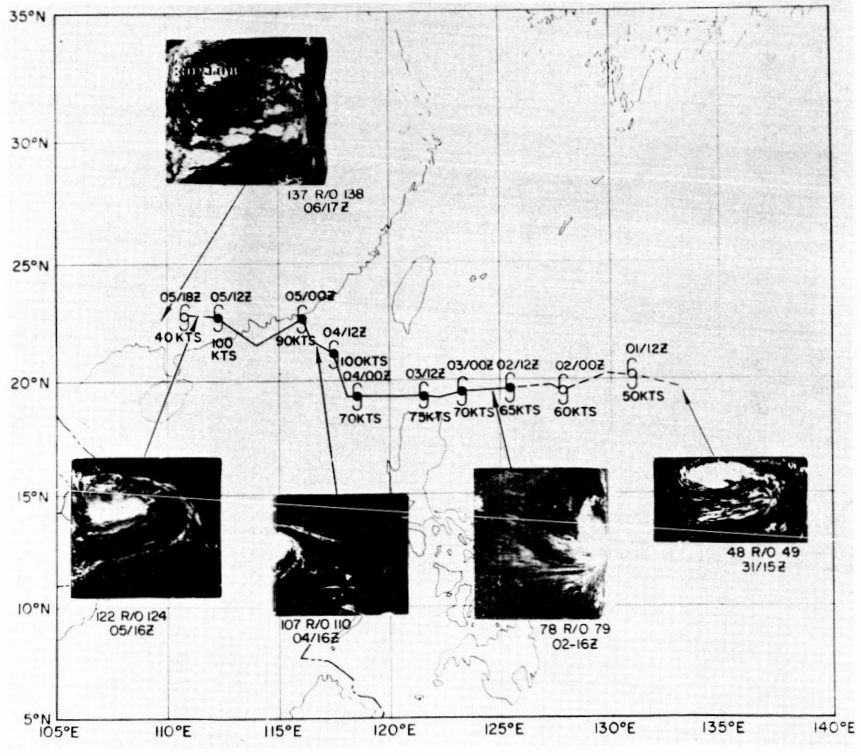

Figure 56.—Nimbus I HRIR glimpses of the track of Typhoon Ruby, with corresponding map positions, in the period August 31 to September 6, 1964.

207-342 O-66—7

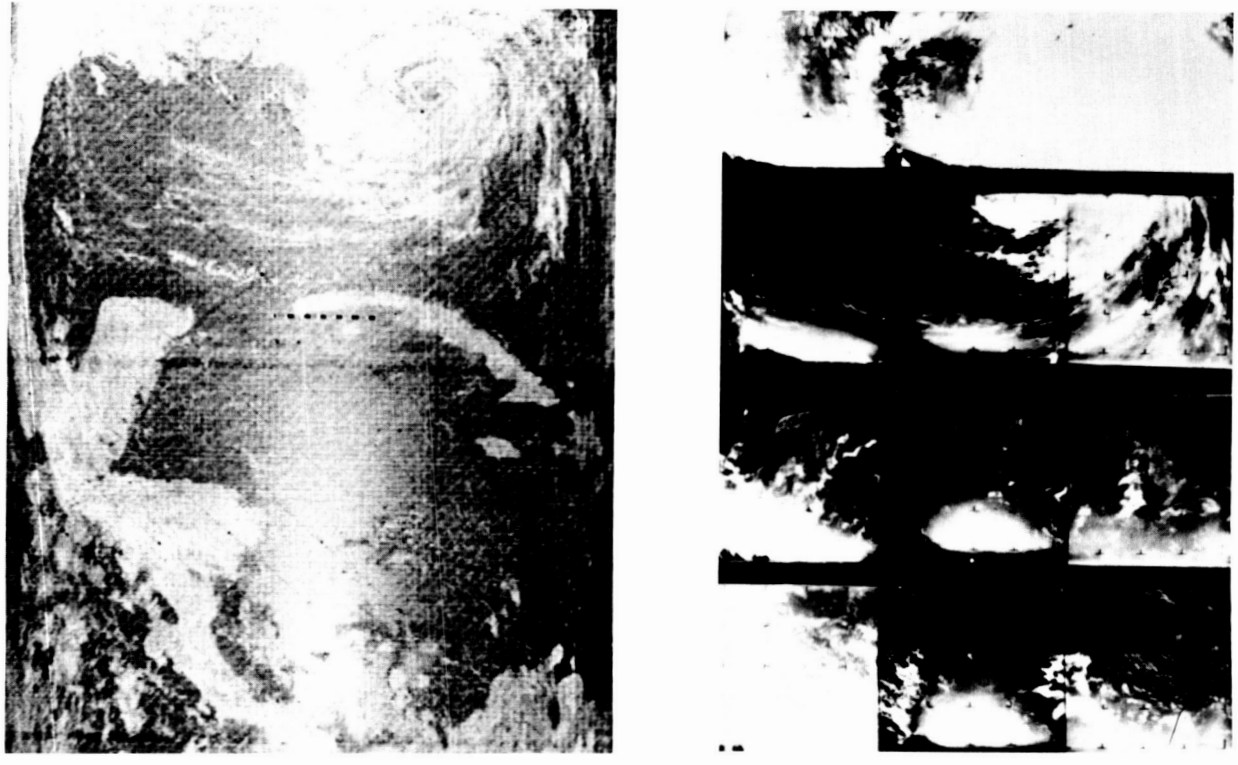

Figure 57.—Comparative, concurrent observations of Hurricane Dora at 1700 U.T. on September 10, 1964, by Nimbus I. Left, HRIR; right, AVCS.

trates the ability of the Nimbus I HRIR to detect and track major storm systems. The first picture in the sequence, taken on August 31, 1964, shows Typhoon Ruby a day before it was detected by aerial reconnaissance. The next two pictures of Ruby are at the edge of the filmstrip, where there is a great deal of distortion, but the characteristic shapes are easily recognizable. There is sufficient overlap between two adjacent orbits that a weather system the size of a tropical storm will not go undetected if readout is achieved. In the fourth picture of the sequence, on September 5, 1964, Typhoon Ruby has become a very large storm, and 150-knot winds were reported (by newspaper) in Hong Kong. In the last picture of the series, Typhoon Ruby has entered the mainland of China and started to dissipate. Much cloudiness remains, but the clouds are disorganized. One tropical storm in the Pacific was detected by the Nimbus I HRIR 6 days before it was located by aircraft reconnaissance.

Figure 57 shows a daylight Nimbus I HRIR observation compared with simultaneous AVCS pictures. As with the TV system, objects with the highest reflectivity, rather than those with the highest infrared emission, appear lightest. Hurricane Dora, near the top of the picture, shows that cloud patterns can be defined fairly well when they occur over water. Over land, the energy from both clouds and the land surface tends to saturate the HRIR, detail diminishes, and clouds are not readily distinguishable. It appears that the HRIR is better able to delineate shorelines through thin, wispy clouds than the TV system, at least in this instance, as may be seen by the shoreline of Cuba. It is also apparent that land reflects much more isotropically than water. It should be noted that no equivalent blackbody temperatures can be derived from daylight observations with HRIR.

Figure 58 shows that the Nimbus I HRIR is capable also of detecting small-scale features, such as the Sierra Lee Wave. An examination of the weather charts showed the classical prerequisites to be present. The wind direction was nearly constant with height, and normal to the mountain range; upstream from the mountain range, there was a temperature inversion at 5000 feet; and a moderate vertical wind shear with the windspeed reaching a maximum of 84 knots at 37 000 feet was present, as shown by the Oakland, California, radiosonde.

Summary

Meteorological satellites have demonstrated the capability to measure, over a wide portion of the electromagnetic spectrum, the radiation from the Earth-atmosphere system. These data have been used to map the Earth's cloud cover at night, to measure the temperature of cloud tops and of the Earth's surface, to compute the Earth's heat budget, to measure radiation from the upper portion of the water vapor and CO_2 layers in the atmosphere,

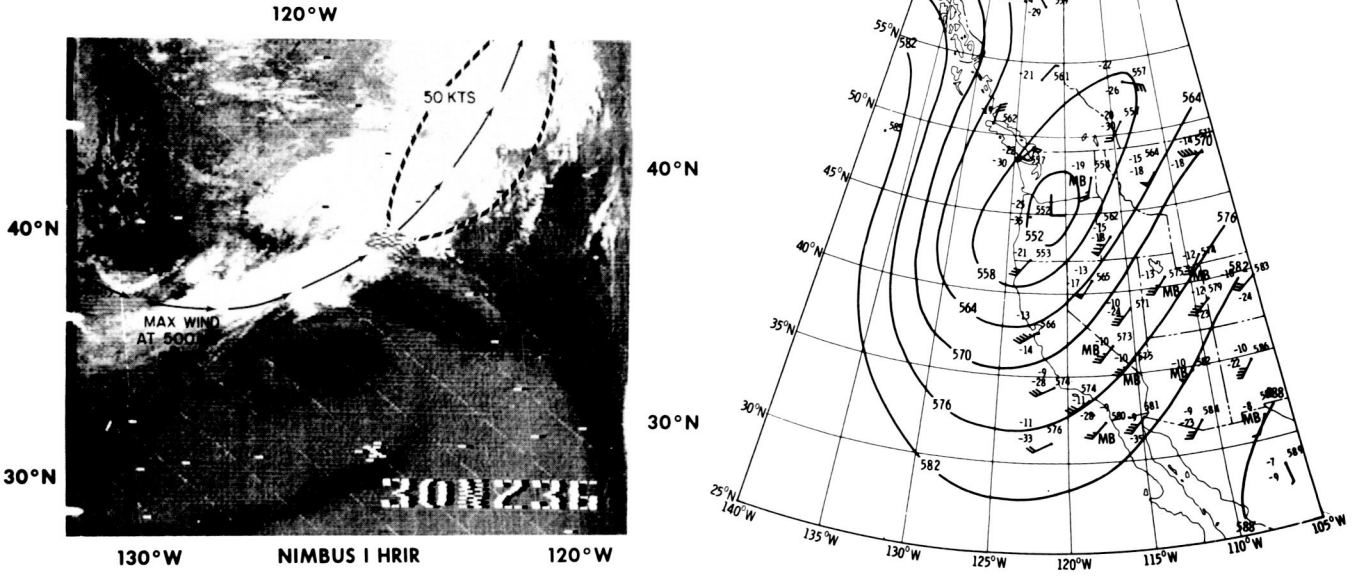

Figure 58.—Sierra Lee Wave, as observed by the Nimbus I HRIR (left) at 0759 U.T. on August 31, 1964, and as depicted (right) on a 500-millibar chart at 1200Z the same day.

and to compute the Earth's albedo. They have also been used to demonstrate the applicability of radiometric measurements in weather analysis over sparsely settled areas; in detecting and tracking major storms; in observing mesoscale weather disturbances; in determining the global distribution of mean temperatures in the stratosphere during a full seasonal cycle; and in measuring the distribution of water vapor in the upper troposphere; and in determining the global distribution of energy sources and sinks in the Earth-atmosphere system.

The major limitation of the Tiros MRIR data, to date, is the uncertainty in the absolute values of the measurements, resulting from the postlaunch degradation of the instrumental response. Degradation correction methods have been devised that can be used as a guide for interpreting the data in terms of absolute value. However, because they were derived from large-scale averages, caution should be exercised in applying them to individual measurements. The data are of value for relative measurements over a short period of time, such as the contrast mapping of cloud systems. Also, there are theoretical difficulties in the interpretation of these measurements. For example, the Earth's surface and cloud layers do not emit exactly as a blackbody, and absorption and reemission, by gases, and aerosols, can change markedly the characteristics of outgoing radiation from the surface. The radiometer calibration, as well as data-conversion procedures, introduces some uncertainties into the data. To solve these problems, there is intensive research in detector development and calibration, radiative-transfer theory, and the emissivities of solids and gases (ref. 47).

Operational Applications

Tiros I was the first satellite launched to test the feasibility of meteorological measurements by means of a satellite. However, in anticipation of the possible operational use of the data, teams of meteorologists were stationed at the data-acquisition stations to study the incoming data as it came in. Within 60 hours after Tiros I was launched, pictures less than 6 hours old were being interpreted and the analyses forwarded by facsimile transmission to the National Meteorological Center of the U.S. Weather Bureau, at Suitland, Md. (ref. 16). These analyses were incorporated into the regular analyses and forecasts of the Weather Bureau. Copies were also relayed to the U.S. Navy and Air Force, in the United States and overseas, where they proved to be very useful (ref. 63). The agreement between the cloud patterns observed by Tiros I and the frontal and isobaric patterns drawn by the meteorologist is illustrated in figure 20. The data from subsequent research meteorological satellites have continued to be used operationally.

Storm Tracking and Identification

Cloud pictures obtained from satellites have proved to be a valuable tool for the forecaster. While these pictures have contributed significant information regardless of the conventional data coverage, their contribution is particularly valuable in data-sparse areas. Many features, for example, cloud vortices, synoptic-size crescent-shaped cloud patterns related to upper-level troughs, and cloud bands, have been analyzed using available conventional data supplemented with satellite data. In data-sparse areas, such as the central Pacific Ocean, synoptic features, e.g., closed circulation centers in the midtroposphere, often must be located on the basis of very few conventional data points, which may be a thousand miles or more apart. In some instances, a pressure center may be more than a thousand miles from the nearest conventional observation point. Obviously, the location and central pressure of such a system cannot be determined accurately using conventional data, nor can the area within the last closed isohypse be determined except roughly. Yet accurate locations, day-to-day movements, and variations in size and intensity of these centers are among the basic parameters needed by the forecaster (refs. 16, 63).

The optimum use of satellite data has varied with the availability of other types of data. Where conventional data are relatively plentiful, the satellite data will serve primarily to modify or aid in the interpretation of a conventional analysis. In data-sparse areas, the satellite data have usually been used on at least an equal basis with other observations. On occasion, it has been necessary to use the satellite data as the primary basis for the analysis, but with the attempt to achieve an analysis compatible with data from all sources. For example, in the absence of conventional data, analysts and forecasters have often inferred large-scale streamline patterns from the streaky appearance of middle and high cloudiness associated with cloud vortices and bands such as those visible in figures 51 and 52. These inferred streamline patterns, supplemented with climatology, have permitted reasonable estimates to be made of 500-millibar macroscale patterns; e.g., major troughs and ridges.

Another manner in which satellite data have been of considerable value arises from the accepted practice of relying heavily on continuity when locating pressure systems and forecasting in data-sparse areas. Often data from a single station will be disregarded because the wind direction or speed does not fit the pattern expected from continuity. Checks of available satellite pictures or nephanalyses have often revealed a significant cloud pattern that suggested vortex development. Thus, the data from a single observation point, used in conjunction with satellite cloud information, have often led to a revised analysis considerably more accurate than one based solely on continuity (refs. 64 and 65).

The most vivid extratropical cloud patterns noted have been cloud vortices. The principal features of these patterns are sufficiently recurrent to enable the experienced analyst often to deduce the approximate stage of cyclonic development. From these cloud pictures, it has been possible to infer pressure-center positions, unusual pressures, future system development, airmass conditions, frontal positions, precipitation patterns, and surface and upper-level winds.

Experience has shown that when cyclogenesis begins as, or in association with, a frontal wave, it can sometimes be detected as a broadening or bulging of the frontal cloud band. Even in an area of fairly dense observations, the development may not be apparent in the synoptic data until 12 hours after it can be recognized in the satellite pictures. In the later stages of the development of the frontal wave, its degree of maturity can be inferred from the satellite picture; for example, from the increasing concentricity of the spiral bands of clouds and the narrowing of the clear-air corridors between the bands. Satellite data have confirmed the classical polar-wave model first hypothesized by Bjerknes and Solberg more than 40 years ago. Figure 59 presents satellite pictures of cyclones in various stages of their life cycles for comparison with the life cycle developed by Bjerknes and Solberg, shown at the left.

Satellite data clearly depict the locations, shapes, and extents of mesoscale cloud features. Such precision of identification is rarely available from conventional data, other than radar observations of precipitation. Operational experience with satellite pictures has shown that mesoscale interpretation is greatly aided by available conventional information.

Clouds and precipitation are greatly influenced by the mesoscale circulations and structures embedded in synoptic patterns and that may not be directly detectable from synoptic observations. It has been observed that a mesoscale cell may dominate the weather within a limited portion of one occluded cyclone, but have no counterpart in another and otherwise very similar cyclone. Circulations either too young or too old and diffuse to be detectable in a synoptic-scale analysis can often dominate the cloud and precipitation fields in their area. The satellite has often provided otherwise unavailable information on these mesoscale patterns.

It is now known that jetstreams, tropopause discontinuities, and shear lines are of major importance in the identification of areas likely to contain clear-air turbulence. Over data-sparse areas, the general location and configuration of jetstreams can often be inferred from satellite cloud pictures (ref. 35).

One important application of satellite cloud data has been in the analysis of cloud and circulation patterns over areas of sparse conventional data.

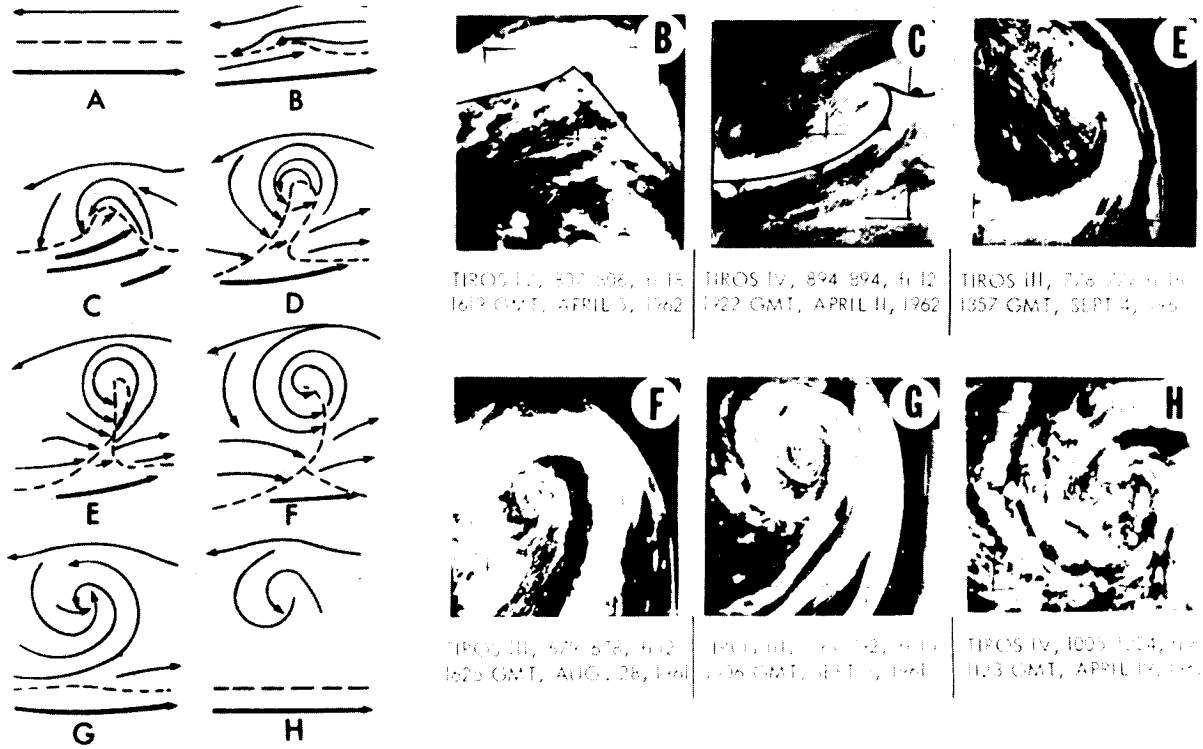

Figure 59.—Life cycle of a cyclone, as hypothesized by Bjerknes and Solberg in 1922 (sketches at left) and observed by Tiros III and Tiros IV cameras in 1961 and 1962.

The tropics are the largest area of insufficient data. As a result, tropical forecasters have benefited the most from satellite pictures. The best example of this was during the 1961 hurricane season, when Tiros III gave the first indications of Hurricane Esther and also provided important data on the first four hurricanes of that season. Another example was the Nimbus I detection of Typhoon Ruby a day before it was detected by aerial reconnaissance.

Tropical Analysis

Although the midlatitude meteorologist obtains from satellite pictures a new look at familiar atmospheric circulations, his tropical counterpart is obtaining, in many areas, the first look at unknown circulation regimes. Since a synoptic climatology of the tropical regions is not yet well established, new concepts must be formulated and erroneous concepts corrected. Satellite data have permitted, for the first time, studies of tropical areas where previously time sections provided the only means of deducing the horizontal distribution of meteorological parameters. Significant weather-producing systems are often revealed only by a small change in wind direction and pressure and an increase in cloudiness and precipitation—forecasting clues that are often obscured by local and diurnal effects.

Investigations based on satellite data tend to confirm that the Easterly Waves do exist, but are smaller and less frequent than had been believed. At the transition from tropical disturbance to weak tropical storm, the satellite pictures usually indicate whether further intensification is likely. Asymmetrical distributions of surface winds have been found to be frequently correlated with asymmetrical cirriform canopies. Experience has shown that the most intense winds are contained in an area only a short distance outside the ring of maximum convective activity associated with wall clouds, and in the more active regions of the spiral bands. If these areas can be identified in satellite pictures, a useful inference can be made as to the extent of the destructive winds (refs. 64–66).

Special Storm Advisories

The meteorological satellites, particularly Tiros, have provided significant support to the operational users. Over 1000 special storm advisories have been issued by the U.S. Weather Bureau on the basis of these satellite data, and over 50 exceptionally severe storms—hurricanes in the Atlantic Ocean and Caribbean Sea, and typhoons in the Pacific Ocean—have been observed and tracked. Radiation data from meteorological satellites are not being used operationally, but the correlations between the various radiation temperatures and weather patterns indicate potential operational usefulness.

NONMETEOROLOGICAL APPLICATIONS

In the design, development, and flight of meteorological satellites, the primary scientific concern has been with the identification of cloud features and their interpretation in terms of atmospheric processes. For this reason, the design of satellite camera systems has been directed toward satisfying meteorological requirements for these specific types of cloud-cover observations.

However, the application of meteorological-satellite pictures to the mapping of other geophysical distributions is very promising. It is reasonable to consider the possibility of following in detail the variations of many geographical features, including the following: location and movement of sea ice; freezeup and breakup of ice in major rivers and lakes; extent of snow cover; height of snowline in mountains; variations in the extent of swamps and flooded areas; leafing of trees and leaf fall; changes in the extent of forests due to lumbering, clearing, or burning; and extent of ocean-silt deposition (ref. 67).

Thus, while NASA's meteorological-research satellite program has been aimed toward obtaining meteorological information, there have already been many indications of how a meteorological-satellite system could very well fulfill both research and operational needs in other scientific fields.

With some difficulty, one can distinguish between the interest of the meteorologist in ice, snow, and forest fires and that of the oceanographer, hydrologist, and forester. Since ice is generally considered to be of more immediate economic interest to the oceanographer than to the meteorologist, satellite ice studies are considered nonmeteorological. The same reasoning applies to satellite observations of forest fires and snow cover. The relationship between satellite observations of clouds and the migration of locust swarms is somewhat more direct, but locust studies also share this somewhat dubious distinction (ref. 67).

Ice

The first satellite picture of sea ice was obtained within hours after Tiros I was launched on April 1, 1960. Since then, each Tiros satellite has observed ice in such areas as Hudson Bay, the Gulf of St. Lawrence (fig. 60), Sakhalin Island, and the Antarctic (ref. 68).

With Nimbus I, the problem of cloud-snow-ice identification was extended to the Arctic and Antarctic regions. The technique of identifying surface features is being applied to both the AVCS and HRIR pictures. The combination of high-resolution AVCS pictures, variable satellite altitude, low Sun angle, and nighttime IR observations, resulted in the acquisition of a number of striking examples of oceanographic, geologic, and geographic features in polar regions. Nimbus I ice pictures included ex-

Figure 60.—Comparative picture strips taken by Tiros II of ice in the Gulf of St. Lawrence on March 23 and March 29, 1961.

amples of ice beginning to form in the Foxe Basin region of Canada, the Barnes Ice Cap on Baffin Island, the snow-covered peninsula in Greenland, and were used to compute the elevation of Petermann Glacier from the pattern of sunlight and shadows from the low Sun elevation. In the Antarctic, the Filchner Ice Shelf and the extension of small glaciers along the coast were pictured. It appears possible to map almost the entire ice shelf surrounding the Antarctic using Nimbus pictures. Also, the first satellite picture of an iceberg was obtained by Nimbus I. This iceberg had apparently calved off the Filchner Ice Shelf near the southeastern end of the Antarctic peninsula. This iceberg was also visible in the HRIR picture taken about 12 hours later.

The capability to conduct routine ice reconnaissance from satellites is important, since ice constitutes a major hazard to navigation, and has a direct bearing on the wintertime economy of many countries, especially in the Northern Hemisphere. Aircraft and icebreakers provide almost all of the ice observations used by forecasters to predict ice conditions for commercial or military vessels in such areas as the Gulf of St. Lawrence or the Antarctic icepack. As early as a few weeks after the launch of Tiros I in 1960, it could be concluded that ice reconnaissance from satellites was feasible. Two years later, with the launch of Tiros IV, civilian and military aircraft, ships, and weather stations participated in a joint Canadian-United States program to evaluate the use of satellites for ice reconnaissance and surveillance.

Snow

Snow is the primary source of water for many cities in North America. For this reason, a knowledge of the amount of snow accumulation and rate of snowmelt is essential to those concerned with water conservation, flood control, and navigation on inland lakes and rivers. The long-range weather forecaster is interested in the extent of snow cover because of its effect on air-mass modification. Of less direct economic importance, a knowledge of snow boundaries is useful in predicting the migration of large game, such as deer and elk.

At present, reports of snow depth and extent are obtained from fixed ground stations, snow survey parties, and aircraft. There are still major gaps in the observation network, however, that could be filled, at least in part, by the use of satellites.

In a test to determine how accurately snow boundaries could be mapped from satellite pictures, the boundary of a forest fire in eastern Canada was mapped from Tiros pictures of snow covering the burned area; measurements obtained agreed very favorably with fire boundaries shown in aerial photographs and mapped by the Consolidated Paper Corp., Ltd., of Canada (fig. 61). Today, apparent snow and tree lines, when observed in satellite

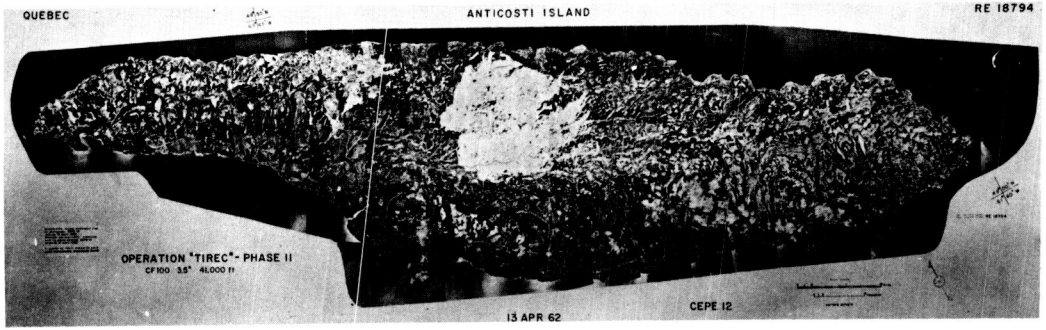

(a) Mosaic of aircraft pictures obtained from 41000 feet on April 13, 1962.

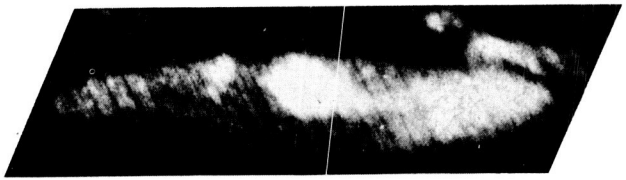

(b) Enlargement of Tiros IV wide-angle (78°) photograph obtained on Orbit 0793, April 4, 1962.

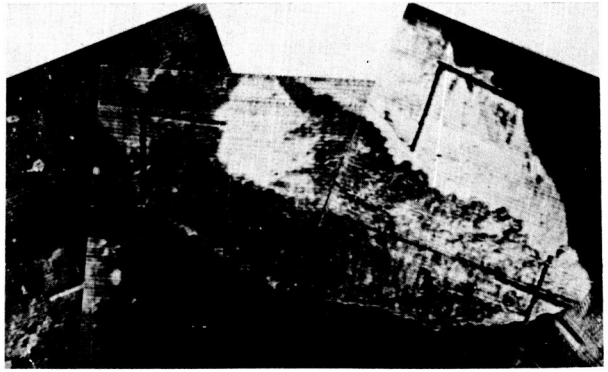

(c) Enlarged portion of a mosaic of Tiros II narrow-angle (12.7°) photographs obtained on Orbit 1850, March 29, 1961.

Figure 61.—**Comparative samples of snow-cover mapping in eastern Canada, as done by aircraft-borne camera (a) and Tiros II and Tiros IV cameras (b) and (c).**

pictures, are indicated on the nephanalyses along with cloud information, and plans are presently taking shape to determine the extent to which observations from satellites could be applied directly to river and flood forecast programs and watershed measurements.

Forest Fires

Satellite applications to forest-fire operations fall in three categories: (1) an investigation of prefire weather conditions, (2) fire detection, and (3) postfire surveillance. A proposed program to investigate prefire weather conditions using satellite data envisions a detailed study of the presence or absence of clouds over a specific area, and thus the likelihood of precipitation. Forest-fire detection, especially early enough for effective fire control, appears out of the question with present systems, although smoke has been recognized in a few of the Tiros photographs. HRIR scanners and passive microwave sensors planned for future satellites may prove best for early detection of fires (ref. 69). The feasibility of postfire mapping of burned areas through use of satellite pictures of snow cover has already been discussed in the preceding section. While not especially applicable to the contiguous United States, where a relatively dense fire-control network already exists, postfire surveillance would be most valuable in less well observed areas such as Alaska and Canada.

Insect-Pest Control

The synoptic weather pattern depicted on Tiros nephanalyses, as well as the satellite pictures themselves, has been used on several occasions in conjunction with surface meteorological observations to forecast the migration of swarms of the desert locust—a highly mobile, prolific insect that breeds largely in arid regions, such as the Sudan.

The 60 nations subject to attack by this insect spend approximately $15 million annually on its control, under the direction of the Food and Agriculture Organization, supported by the United Nations Special Fund. Through a cooperative arrangement among the member nations, supplies of insecticides are stockpiled in areas likely to be invaded. When swarms are located, they are sprayed from aircraft.

The effectiveness of this method of control depends largely on the ability to predict the invasion area. Meteorological factors are important in predicting the breeding areas of the locust swarms, their time of emergence, and their migration. The significance of atmospheric convergence, on both a microscale and a macroscale, in the concentration and migration of swarms has long been noted. The immediate application of satellites in this field will be confined largely to locating frontal systems and other areas of convergence by analyzing satellite television or infrared observations (ref. 67).

Sea-Surface Temperatures

Since the oceans cover nearly three-quarters of the Earth's surface, their surface temperature is a most significant geophysical quantity. This is true in operational meteorology and oceanography, and in basic research. Meteorological investigations have been conducted in both the Tropics and middle latitudes on the effect of sea-surface temperature on migratory storm systems. Tropical meteorological studies have shown that hurricanes rarely form when the sea-surface temperature is less than 79° F, and it has been hypothesized that, prior to recurvature, hurricanes move along the band where the sea surface is the warmest. In the synoptic analysis of midlatitude weather situations, sea-surface temperatures are used extensively, when available, in airmass determinations as an aid to the proper placement of fronts. Studies of east coast cyclonic development relating to dynamic weather prediction have revealed evidence that the temperature of the sea surface is significant in the development process.

In oceanography, the need for accurate daily sea-surface temperatures for large areas of the world is even more acute, for basic studies and also to support both military and commercial activities.

All these applications are severely hampered by the lack of adequate sea-surface temperature information, although in a gross climatological sense (seasonal means and variability), sea-surface temperatures are rather well known over many of the oceans of the world. The synoptic and mesoscale temperature distributions and variations are far less well determined. Along the routes frequently followed by ocean vessels, measurements do approach an adequate synoptic density, but such routes traverse only a small fraction of the some 140 million square miles of ocean. Closer and more frequent observations have been confined to a few extremely limited areas, such as parts of the Gulf Stream, over short periods of time. Even in these few instances of intense sampling, the areas to be traversed and the very few oceanographic ships and aircraft available have necessarily resulted in comparatively widely spaced observations.

The satellite has provided a worldwide observing tool that, it appears highly probable, can do much to fill present deficiencies in sea-surface temperature measurements. For example, in the absence of clouds, and sometimes even in broken cloud cover, the 8- to 10-μ data from the Tiros radiometer provide a useful measure of the instantaneous sea-surface temperature gradients, perhaps of the day-to-day temperature variations, and possibly of the temperatures themselves.

The Nimbus I HRIR has demonstrated the capability of measuring sea-surface temperatures over cloud-free areas.

chapter 3

Upper-Atmosphere (Above 30 Kilometers) Meteorological Sounding Rockets

BACKGROUND

EARLY ROUTINE OBSERVATIONS of the upper air were made with instruments carried by kites, airplanes, and balloons. In 1936, the first daily 500-millibar maps were published, and it was soon evident that they offered an excellent tool for forecasting the movement of low- and high-pressure systems as well as frontal systems. At present, there is probably no forecaster who does not use these maps.

The kites and airplanes were displaced by balloons and radiosondes, since they reached higher altitudes. An important atmospheric feature was thus discovered—the westerly jetstream. This is a relatively narrow current of very fast-moving air with very strong vertical wind gradients sometimes causing strong turbulence.

With better balloons and instrumentation, higher layers of the atmosphere were explored and new discoveries were made. It was found that while the westerly jet occurs at higher latitudes at about 8- to 10-kilometer altitude, an easterly jet occurs at around 10° to 20° N latitude and altitudes of 30 to 35 kilometers.

Another remarkable discovery from the high-altitude network was the so-called explosive or sudden warming phenomena. These were, in most cases, strongest at the top of the balloon ascents and occurred mostly during the winter (January and February). In 1957, this phenomenon was observed, and the temperature at high elevations within a few days rose very sharply by about 45° to 65° K. Figure 62 shows the temperature change observed at four locations (ref. 70). Such large and rapid temperature changes as these do not occur at any point on the surface of the Earth, except perhaps on the Greenland icecap. Associated with the sudden warming phenomenon is a complete change in the entire upper-air circulation pattern. These circulation changes have been well analyzed for the 1958 explosive warming (refs. 71–73). The normal pressure pattern during the winter shows a low-pressure center near the poles, with more or less concentric isobars from the pole to the subtropics. During a disturbance such as this, the simple pattern is replaced by alternating high- and

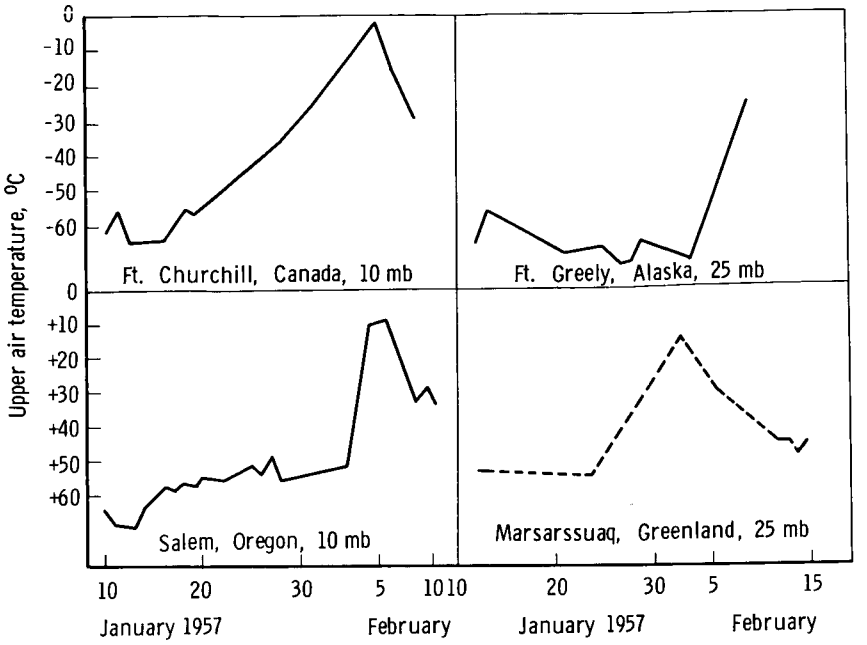

***Figure 62.*—Stratospheric temperature curves at different stations in January and February 1957.**

low-pressure systems and high pressure over the pole. After the disturbance, the winter pattern is gradually restored.

The most surprising fact, however, is that this pattern did not drift with the stratospheric winter westerlies, as expected, but from east to west. Two questions immediately arose:

What was the temperature structure above the balloon ascents? Are there higher steering levels affecting the airmasses around 30 kilometers, or even higher?

Another phenomenon was also observed about this time. In the equatorial latitudes, a pronounced oscillation in the zonal wind with a period of approximately 26 months was noted at pressure surfaces of 25 and 50 millibars. The oscillation decreases in amplitude downward and becomes almost undetectable at 100 millibars (refs. 74–76). There is evidence that this oscillation increases in amplitude with increasing altitude above balloon heights, and there is the suggestion that this approximately biennial oscillation can be traced through the temperate latitudes. The study of this phenomenon raises the question: What is the origin of this oscillation, its dynamics, and its extent?

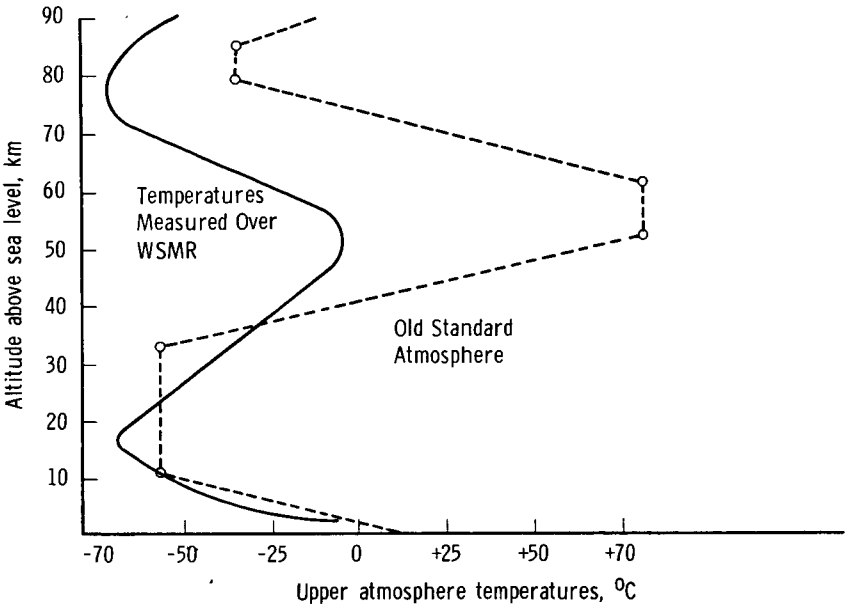

Figure 63.—**Comparison between an early NACA Standard Atmosphere and rocket data obtained by rocket-grenade experiment at White Sands Missile Range, N. Mex., prior to 1952.**

The first attempts to measure the physical properties of the upper atmosphere with rockets were carried out with the V–2 rockets. A research rocket, the Aerobee, was specifically designed for upper-air research and used to measure, among other things, the wind, temperature, density, and pressure. The first experiments were flown at the White Sands Proving Ground in the late 1940's and early 1950's. Some results were published in 1952 (ref. 77), and there were surprisingly great differences between these rocket measurements and the NACA Standard Atmosphere, which was used by airplane and rocket designers. Figure 63 is based on data obtained at one spot, at about 30° N latitude, and one can see that at about 50 kilometers the new results indicated a temperature approximately 70° C cooler than the Standard Atmosphere. The next question was whether the same results could be obtained in more northerly areas.

The International Geophysical Year (1957/1958) offered an opportunity to answer this question, and series of Aerobee launches were carried out at Fort Churchill, Canada. There were four successful rocket launches in the winter and five in the summer, using an acoustic-grenade technique that uses the time of arrival and the angle of sound-wave fronts at the ground to

determine the atmospheric structure (ref. 78). The summer-temperature data looked similar to the year-round data at White Sands Proving Ground, indicating that during the summer there is apparently not much variation in the temperature structure beween 30° and 60° N latitude, although the temperatures at 50 kilometers and below at Fort Churchill were somewhat

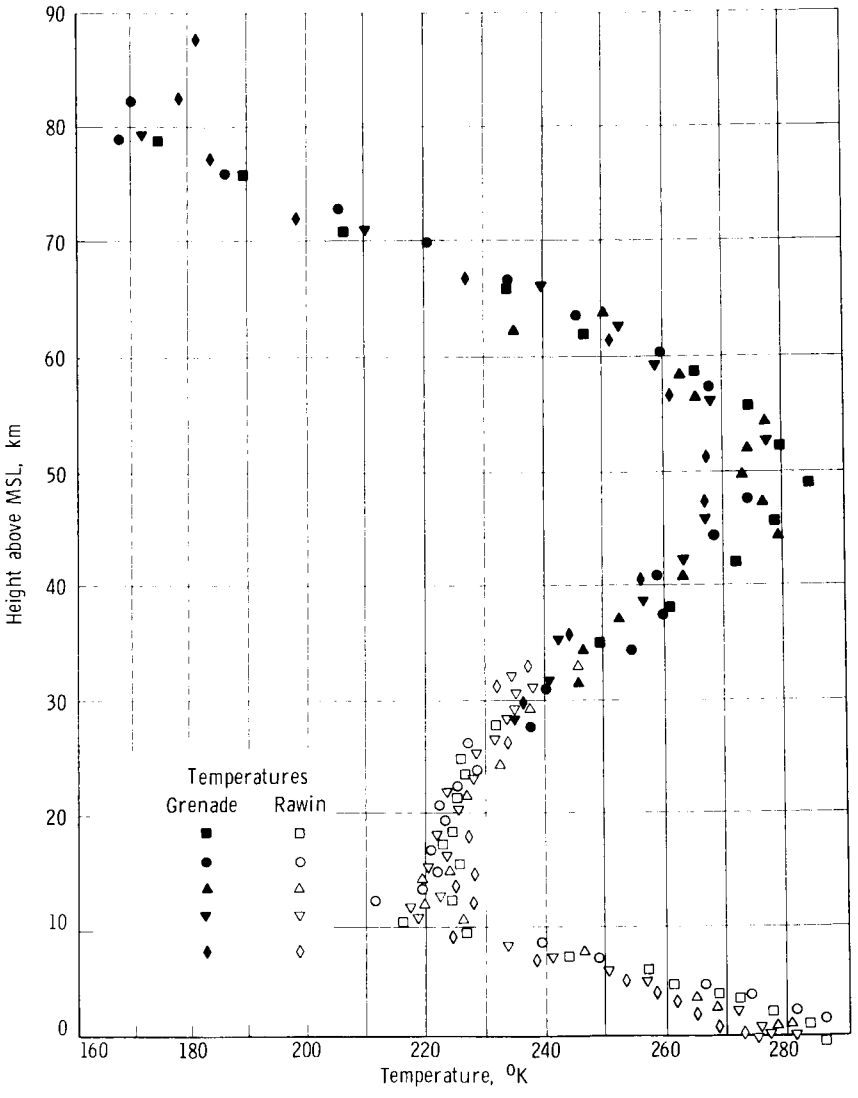

Figure 64.—Summer (1957) temperatures over Fort Churchill, Canada 59° N), as determined by the rocket-grenade experiment.

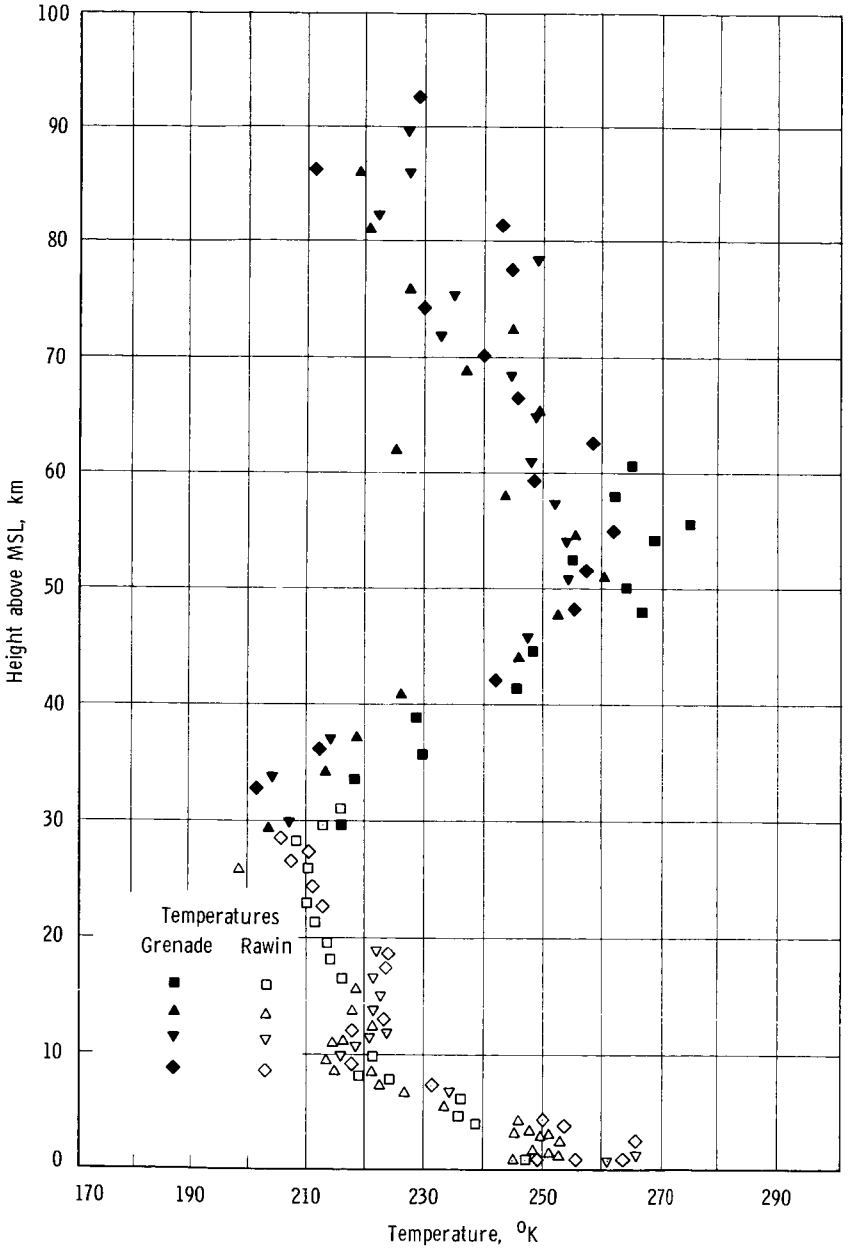

Figure 65.—Winter (1957–58) temperatures over Fort Churchill, Canada (59° N), as determined by rocket-grenade experiments.

higher than at White Sands, and above 65 kilometers the temperatures at Fort Churchill were lower. Figure 64 shows the summer soundings at Fort Churchill.

The winter data, however, are quite different (fig. 65). The most remarkable fact is that at around 80 kilometers there is a temperature difference between winter and summer of about 60° to 70° K, with the winter being warmer. Because of this difference in temperature structure, the density during the winter between 30 and 80 kilometers is much lower than during summer.

Several rocket experiments at Fort Churchill using the atmospheric drag on a falling sphere (ref. 79) and several pitot-static-tube experiments (ref. 80) produced results similar to those of the grenade experiments. A series of nine grenade experiments at Guam during November 1958 yielded results that agreed with measurements at White Sands (ref. 81).

Some of the rocket launches at Fort Churchill in the winter occurred at the time of the 1958 sudden-warming phenomenon. Before the sudden warming was observed at the top level of the balloon ascents, the wind pattern observed by the rocket experiments changed completely, and the temperature at 45 kilometers rose 50° K over a 3-day period; that is, a few days earlier than at balloon level. The mechanism causing the large temperature increases to start at high levels and progress to lower levels is not known.

METEOROLOGICAL OBSERVATIONAL PROGRAM ABOVE 30 KILOMETERS

In order to conduct synoptic sounding-rocket measurements from a network of stations, the cost of the rockets had to be reduced considerably. The trend toward smaller meteorological rockets is evident in the reduction in the size and complexity of the rockets used. The V–2 rocket weighed some 12 700 kilograms, and the Aerobee weighed about 720 kilograms. In the present meteorological sounding-rocket programs, two-stage Nike-Cajun or Nike-Apache rockets are used, which weigh about 770 kilograms, but the cost is about one-fifth that of the Aerobee. Also in use are two types of small single-stage rockets, the Arcas and the Loki, which weigh about 34 kilograms and 14 kilograms, respectively. To distinguish between them, the two-stage rockets are referred to as large meteorological sounding rockets and the one-stage rockets as small.

Large Meteorological Sounding Rockets and Techniques

The large meteorological sounding rockets (the Nike-Cajun class) are presently the best suited for experiments in the mesosphere; that is, altitudes above 50 kilometers. They possess sufficient thrust to carry payloads of 30 to 40 kilograms and 15- to 20-centimeter diameters to altitudes of 100

to 200 kilometers. The size and complexity permit synoptic observations at several sites with periodic launching. A crew of less than 10 can usually handle the launch operation from a not-too-complex rail launcher. Figure 66 shows a typical Nike-Cajun rocket configuration. This rocket can carry several different types of payload. One is the sodium-vapor ejection (cesium and other chemicals are also used). In this experiment, sodium vapor is ejected into the atmosphere between 70 and 200 kilometers during twilight conditions. The interaction of the sunlight with the sodium vapor causes the vapor trail to be luminous (fig. 67). The trail moves with the wind field, and it is tracked by an array of cinetheodolite cameras. The wind velocity is determined by triangulation of significant features on the photographs of the trail. A disadvantage of the sodium technique is that it can be used only during twilight, when the region above 70 kilometers is illuminated by the Sun. However, research is progressing on self-luminous vapors, which glow for a sufficient time and intensity to permit this type of wind measurement at night.

Above 50 kilometers, the direct measurement of temperature with extremely small resistance thermometers becomes unreliable. In the mesosphere, therefore, the rocket-grenade is the most commonly used technique. In this experiment, grenades are ejected and exploded at latitudes up to 90 kilometers at regular intervals during the ascent of the rocket. The average temperatures and winds in the medium between two grenade explosions are determined by measuring the time and position of each explosion and the time of arrival of each sound wave at various ground-based microphones. The grenade experiment requires highly accurate tracking systems. A network of ballistic cameras, or Doppler tracking stations, or a high-precision radar of FPS–16 type, is used to determine the coordinates of the explosions. An array of microphones records the arrival of the sound waves (ref. 82). A schematic diagram of the essential components of the grenade experiment is shown in figure 68.

In this altitude region, the simplest method of measuring density is by the falling-sphere technique. The sphere is ejected from the rocket, and the drag force on the sphere as it goes through the atmosphere is determined. From this force, the density is computed. Falling spheres have been used in many different configurations, as rigid shells (fig. 69), or as inflatable balloons with built-in accelerometers, or as passive, radar-reflective inflatable spheres tracked by precision radar. From the radar tracking of the passive sphere, wind can also be computed. This technique can provide measurement in the region from 30 to 120 kilometers.

Another technique is to make pressure measurements while the rocket is in flight. In general, the pressure measurement is performed at two aerodynamically different locations along the surface of a pitot-static tube

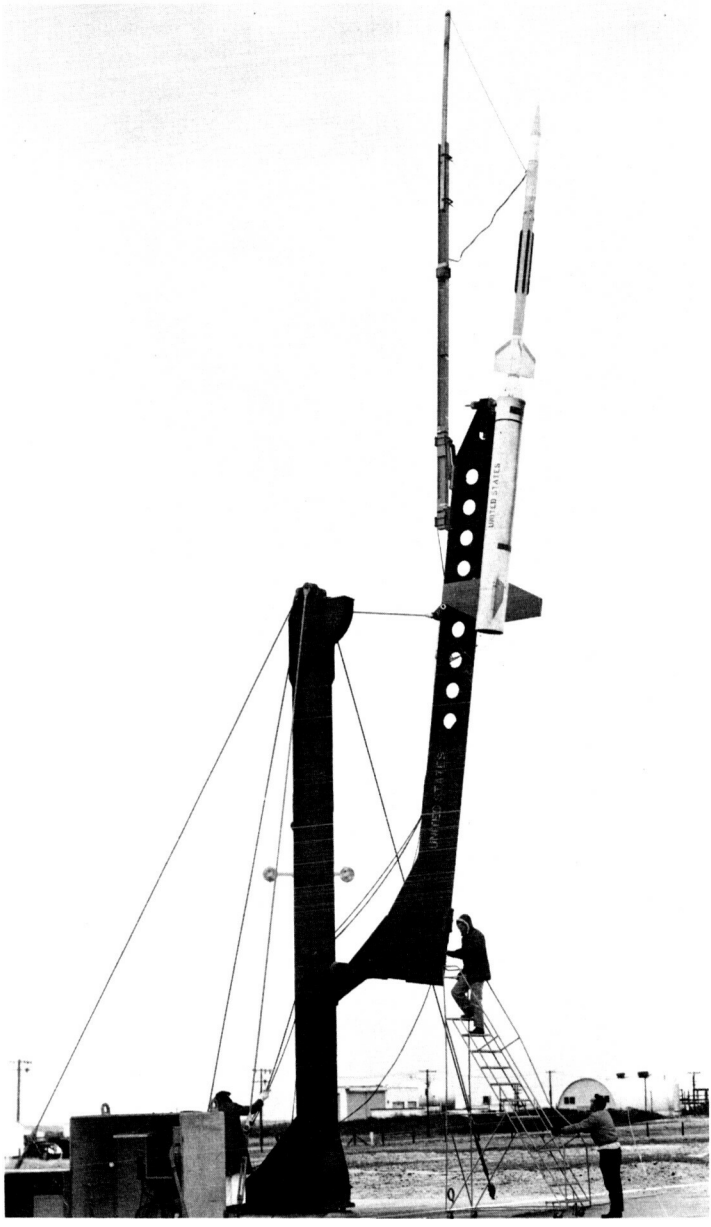

Figure 66.—Nike-Cajun rocket with grenade experiment ready for launch at Wallops Island, Va.

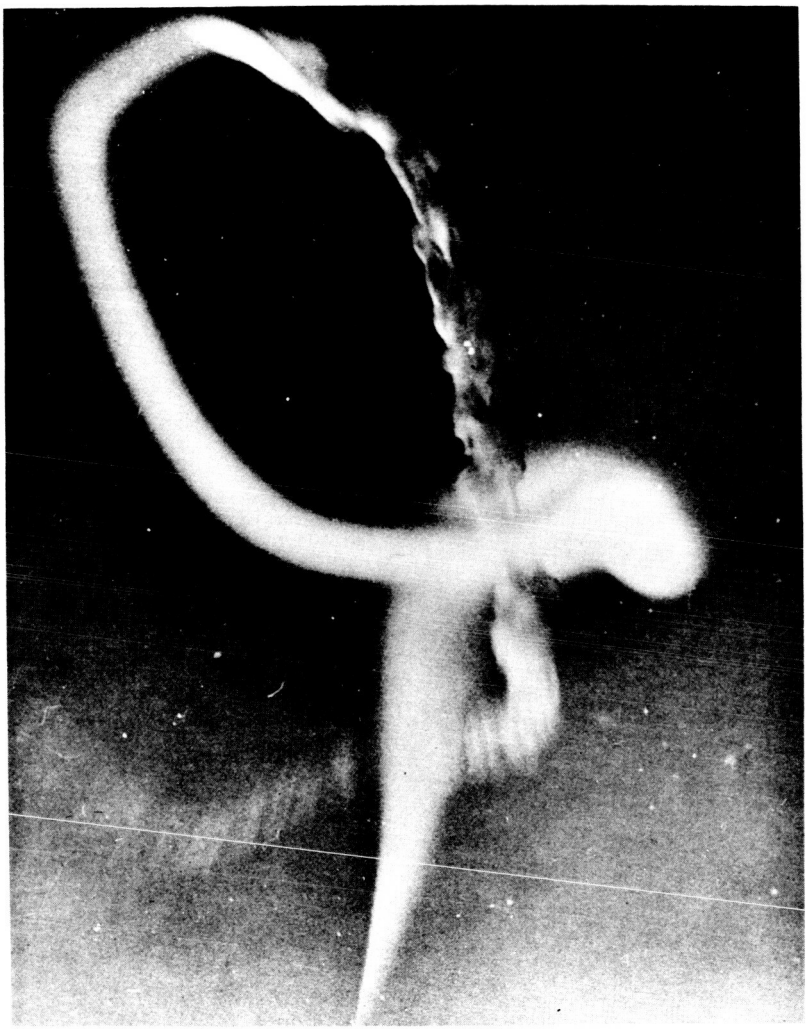

Figure 67.—Trail of a sodium-vapor release from a Nike-Cajun rocket.

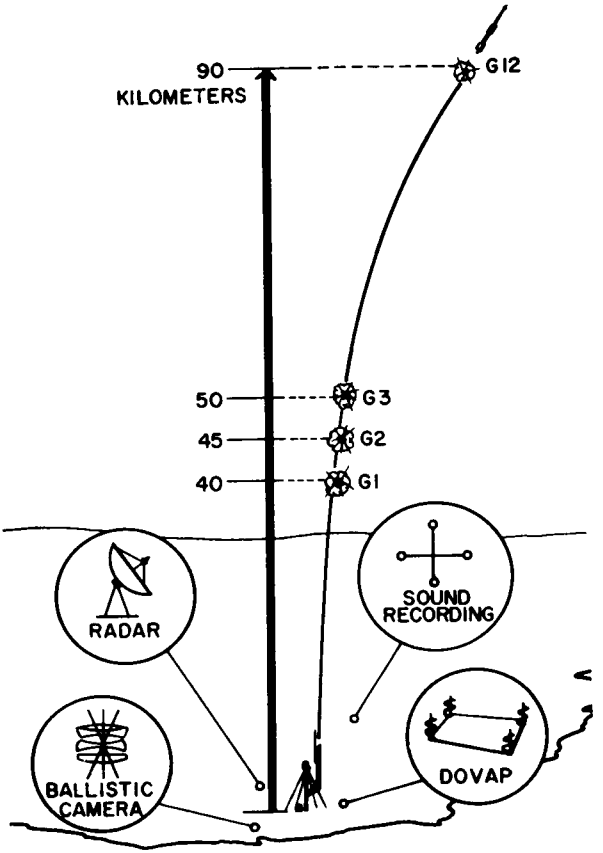

Figure 68.—Schematic diagram of the grenade-experiment system. Radar, ballistic camera, and DOVAP tracking systems are indicated. Each individual system or combination of systems suffices for the experiment. Sound-recording site is preferably located directly under the rocket trajectory. G1, G2, G3, and G12 indicate various altitudes of grenade explosions.

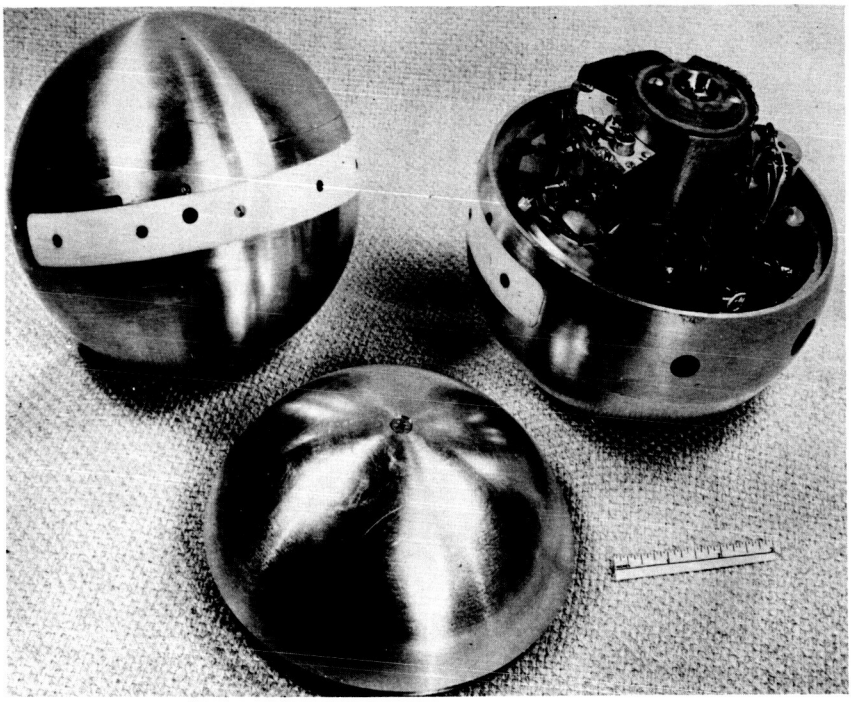

Figure 69.—**An active, rigid falling sphere for measuring density above 30 kilometers. The 7-inch-diameter sphere is shown fully assembled with the telemetering-antenna slot visible (upper left), and open to reveal a built-in accelerometer (upper right).**

carried at the tip of the rocket (fig. 70). Pressure sensors are usually placed in chambers exposed to the airflow by means of orifices in the skin of the rocket. The stagnation, or ram, pressure is measured at the tip of the pitot tube, and the ambient, or static, pressure is measured along the wall of the tube several calibers to the rear of the stagnation point. The ambient density is derived from these two pressure measurements. This technique can be used in the altitude interval of about 30–110 kilometers.

Present Large Meteorological Sounding-Rocket Program

Atmospheric rocket soundings should be conducted as worldwide programs at widespread geographical locations and at all seasons. However, range facilities, complexity, cost, and other factors impose severe limitations. During the IGY, the first measurements were made from which variations in the structure of the mesosphere could be derived. In fact, the four

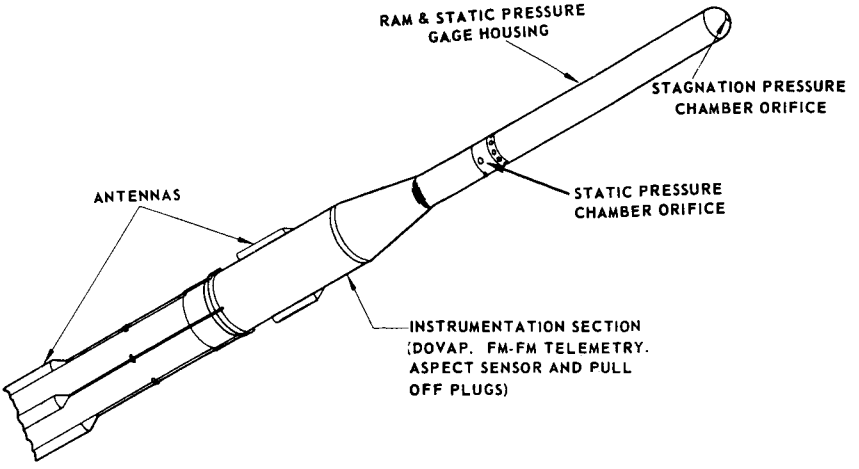

Figure 70.—Configuration of pitot-static-tube experiment.

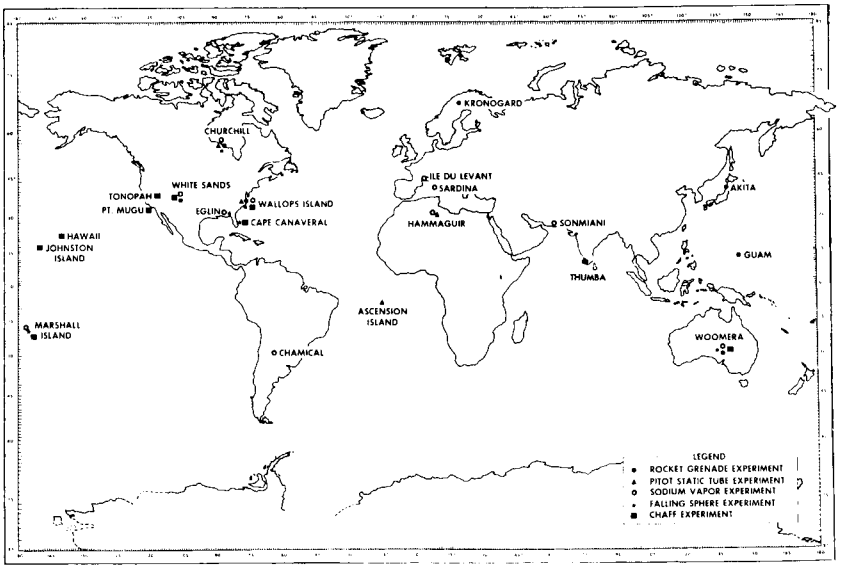

Figure 71.—Map of locations from which rocket soundings in the mesosphere have been conducted during and since IGY. The types of experiments performed are shown for each station.

methods mentioned—sodium release, grenade, pitot-static tube, and falling sphere—were successfully utilized during the IGY, and measurements of pressure, density, temperature, and wind in the 50–90-kilometer region still employ these four techniques.

Much progress has been made since the IGY in extending the geographical coverage of the soundings. The world map (fig. 71) indicates the sites at which rocket soundings have been conducted during and since the IGY. The types of experiments performed are also indicated for each site. Some of these soundings were internationally coordinated as a first attempt toward a synoptic program.

A NASA program of rocket soundings has been in progress since 1959. It is oriented toward the exploration of the mesosphere. The program started with two sodium soundings in August, and two in November 1959, and one each in May and December 1960 at Wallops Island, Va. One successful grenade sounding was conducted in July 1960 at Wallops Island. Between 1961 and 1963, a total of 22 successful grenade experiments were performed at Wallops Island, and 5 at Fort Churchill, Canada, during December 1962 and February and March 1963. Four of the grenade experiments were coordinated with similar experiments at Wallops Island. In the same period, 13 sodium releases were made at Wallops Island, 10 of which were simultaneous with grenade experiments. In addition, 4 pitot-static-tube experiments were launched at Wallops Island. As indicated in table VI, the geographical coverage in 1964 was extended to 5 locations with a total of 45 successful launches, many of which were accomplished simultaneously or within a short time of one another.

During November 1962, an international series of sodium releases was conducted at various sites around the world. On several occasions, coordinated sodium releases were made from Wallops Island and Italy, and also from Wallops Island, France, and North Africa. Four grenade experiments were conducted in July and August 1963, and three in August 1964, in northern Sweden. Half of these were during a display of noctilucent clouds, and the others during their absence.

In addition to using the persent sites, this sounding-rocket program will be extended by the addition of a launch site at Point Barrow, Alaska, and the use of shipboard launches.

Small Meteorological Sounding Rockets and Techniques

From the sporadic soundings of the upper atmosphere with expensive complex rockets, it became apparent that there was much still to be learned in order to achieve a complete understanding of the Earth's atmosphere, and that the available rocket systems were unsuitable for use on a synoptic scale. This provided the impetus for the development of a small rocket

Table VI.—*Monthly and Geographical Distribution of Successful Large Meteorological Sounding-Rocket Launches, 1960–64*

Year	Location	Jan.	Feb.	Mar.	Apr.	May	June	July	Aug.	Sept.	Oct.	Nov.	Dec.
1960	Wallops Island, Va					Na		G					Na
1961	Wallops Island		2G		G, 3Na	2G		3G		G, 2Na			
1962	Wallops Island			4G, 4Na	G, Na		2G, Na, P						2G, 2P
	Fort Churchill, Canada												2G
1963	Wallops Island		2G, 2Na	G									G, P
	Fort Churchill		2G	G									
	Kronogaard, Sweden							2G	2G				
1964	Wallops Island	2G, 3Na	3G	G	G			4Na	4G			5G, 2Na	
	Fort Churchill	2G	2G		G				3G				
	Ascension Island	G	G, P		2P				2G				
	Kronogaard								3G				
	Shipboard[a]											3Na	

[a] Off the east coast of the United States, in vicinity of Wallops Island.

G indicates grenade; Na, sodium-vapor release; P, pitot-static tube; and the numeral indicates the number of launches when greater than 1.

vehicle for meteorological experiments. From this development, several rockets evolved, of which the Arcas and Loki are now in general use. Both are single-stage, solid propellant rockets, which can be handled by two or three men and carry a 1- to 5-kilogram payload to 60-kilometer altitude. The Arcas motor, developed specifically for meteorological use, weighs about 35 kilograms and has a payload capacity of about 5 kilograms. It is an end-burning motor, and produces a sustained thrust for 30 seconds. Consequently, it has a relatively low acceleration and is sensitive to launch-wind conditions. This can be partially compensated for by a wind-weighting procedure and an adjustment of the launch angle. The Arcas rocket and its closed-breech launcher are shown in figure 72.

The Loki rocket was adapted from a tactical-weapon system. It weighs about 15 kilograms, with a payload capability of 3 kilograms. It has an internal-burning motor with a sustained thrust for about 2 seconds. When the burning phase is completed, the motor and payloads separate, as a result of differential drag. This rocket can be fired from an open-ended launch tube and can use a fixed launch angle, since it is insensitive to wind conditions. Figure 73 shows, in the foreground, a Loki rocket and launch tube.

The second part of a meteorological-rocket system consists of sensors and instrumentation. The two basic techniques are the passive and the active. In the passive technique, radar is used to track the movement of a target through the atmosphere. The velocity of the wind can be derived directly,

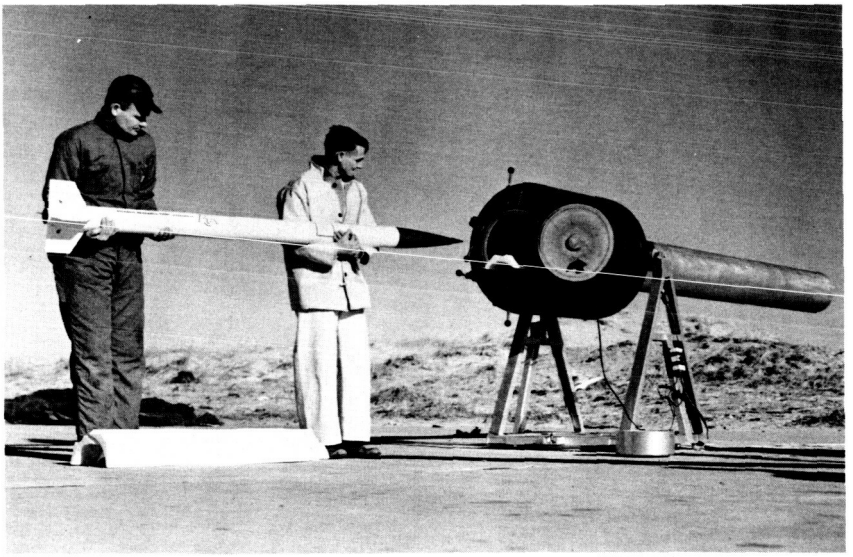

Figure 72.—Arcas sounding rocket and launcher.

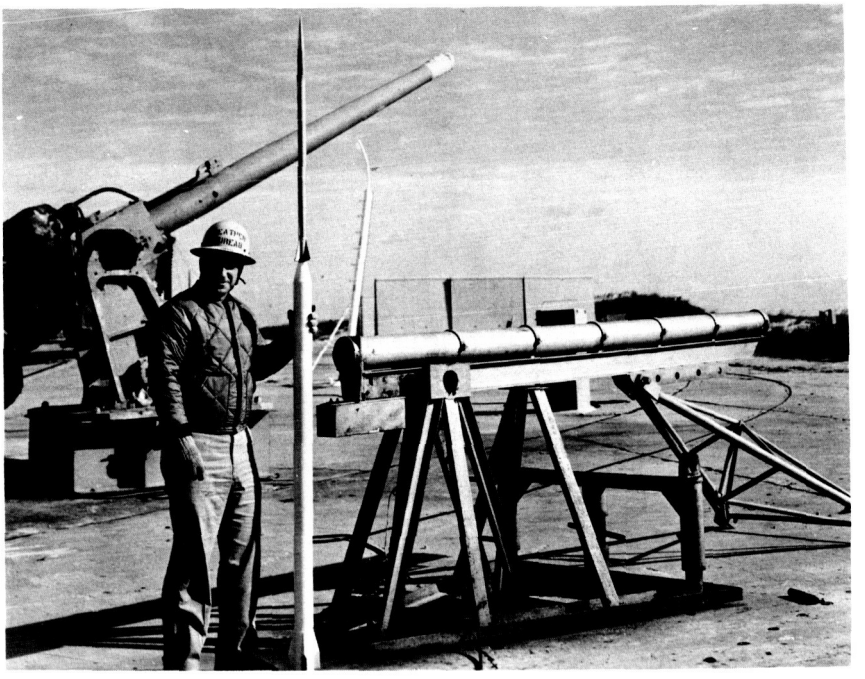

Figure 73.—**Loki sounding rocket and launcher.**

and the density of the atmosphere may be computed from the drag coefficients of the target. In the active technique, such parameters as temperature and pressure are measured *in situ* by a sensing element, and the data are telemetered to a ground station and recorded. Winds and density may be measured by the active technique with a transponder carried by a descending parachute or inflated sphere.

Atmospheric motion, or wind, was the first parameter measured with the present rocket vehicles as carriers for chaff or dipoles, which were released and tracked by radar. Although the chaff cloud is not a truly discrete target, as is a metalized parachute or an inflated radar-reflective sphere, chaff has now been so improved that reliable wind data may be obtained at altitudes from 60 kilometers to less than 30 kilometers.

The wind-sensing parachute was the logical successor of chaff. The metalized parachute has been developed to eject and deploy from the meteorological rocket at maximum altitude without the use of mechanical deployment, such as inflated tubing or springs. Apparently the highest altitude at which parachutes can be deployed without a complex mechanism is about 70 kilometers. The average effective maximum altitude for the 4.5-

meter parachute, deployed from the Arcas rocket, appears to be 55 to 60 kilometers. Parachutes have also been successfully deployed from the dart of the Loki system. Wind data derived from the tracking of the metalized parachute comprise a large portion of the rocket wind measurements made in the 55- to 30-kilometer-altitude interval.

The Robin (rocket balloon instrument) is an inflated Mylar sphere with an internal radar-corner reflector, ejected from a rocket. It is used to measure atmospheric density and wind velocity. The wind data may be obtained from the radar plot board, or by computer reduction of the radar data.

The current measurement of temperature in the stratosphere and the mesosphere is an extension of the basic radiosonde technique using the thermistor. A number of groups associated with missile-range meteorology have worked extensively on the calibration, mounting, and exposure of the rocketsonde thermistor, and current temperature measurements in the stratosphere show a marked improvement over the first measurements made in 1960.

Figure 74 illustrates the various techniques used on the small meteorological sounding rockets.

Present Small Meteorological Sounding-Rocket Program

The magnitude of a synoptic program dictated that it be a joint effort of the various groups or agencies engaged in upper-atmospheric research. The support requirements for even a small meteorological sounding rocket are such that a majority of the developmental firings occurred at established rocket-test ranges. Also, the meteorological data provided by the rockets were most needed at these ranges for missile and satellite research and development. Since the meteorological groups at the various ranges were the principals in this field, it was natural that they should form the basis for a cooperative network. The Chief Signal Officer of the Department of the Army initiated coordination with the government agencies involved. The Meteorological Working Group of the Inter-Range Instrumentation Group was the forum for coordination necessary for the program, which was initiated in 1959 as a joint effort of the Army, Navy, Air Force, NASA, and the Atomic Energy Commission (refs. 83 and 84). These represented the principal users of meteorological-rocket data. Each agency had its own specific mission, but the cooperation within the limitations of their missions greatly enhanced the collection of rocket data.

The first attempt at the synoptic launching of meteorological sounding rockets was made in October 1959 from Fort Churchill, Canada, and Point Mugu, Calif. A total of 18 successful observations of the wind profile were accomplished in this series. The second series began in January 1960, with

207-342 O-66—9

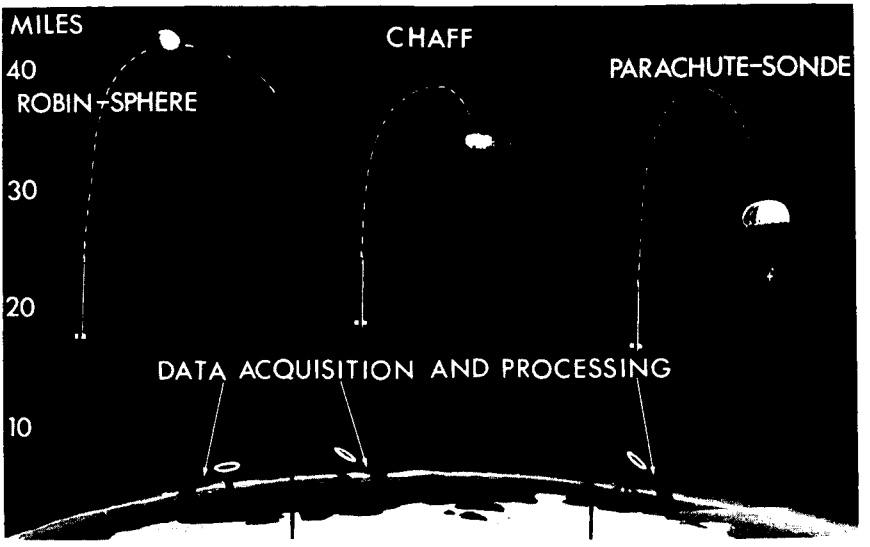

Figure 74.—**Various techniques for making meteorological experiments with small sounding rockets.**

launchings from three sites, with Wallops Island, Va., being the third. A total of 42 rocket wind soundings were made, including 3 with temperature measurements. A third series began in April 1960, with the addition of the Atlantic Missile Range (now Eastern Test Range); Eglin AFB, Fla.; and Tonopah, Nev. A total of 70 rocket soundings were made. These data, as well as those from subsequent launches, are collected in reference 85.

From October 1959 to April 1961, the launches were on a seasonal basis, but in the summer of 1961 a regular schedule of several times per week was initiated, with the various ranges participating as their commitments and resources permitted. There has been a steady growth in the number of launches and in the number of stations. Figure 75 is a cumulative graph of the successful launches from the cooperative network. Through the middle of 1964, almost 3500 successful upper-atmospheric soundings have been made with the small meteorological sounding rockets. However, most of these have obtained only wind data.

Figure 76 indicates the locations from which small meteorological sounding rockets have been launched by U.S. organizations since 1959. Some of them have launched rockets for short periods only, in connection with specific operations or research projects. Others are only recent additions to the network and are related to operations along the Eastern and Western Test Ranges. The selection of these sites has been guided by mission re-

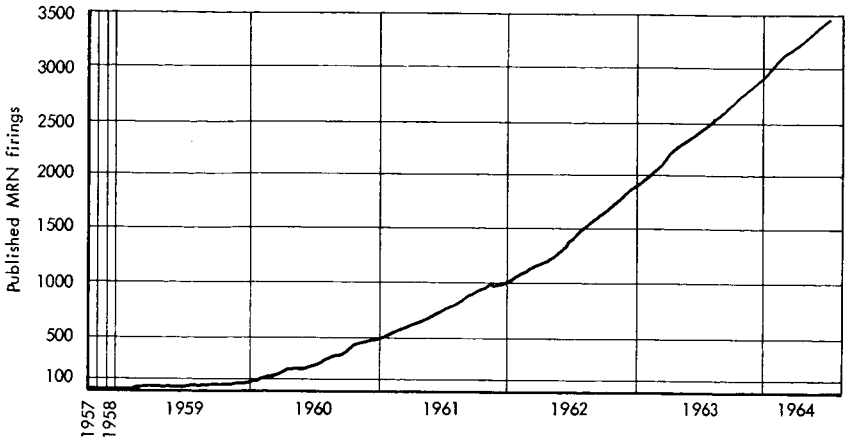

Figure 75.—**Cumulative graph of small meterological sounding-rocket launches by the Meteorological Rocket Network (MRN) (as published in IRIG documents).**

quirements and the availability of range real estate, since for safety reasons, the rockets must be fired from ranges or in restricted areas. Thus, the sites are not necessarily optimum for upper-air research, and large areas remain unobserved. It is highly fortuitous that the sites provide such a wide latitudinal and longitudinal range.

Since 1959, the requirement for upper-atmosphere meteorology has extended beyond the present altitude capability and reliability of the small meteorological rockets (ref. 86). In the latter part of 1963, as a result of the experience gained by participating in the above meteorological sounding-rocket activities, and its national objectives, NASA initiated a small-meteorological-rocket program. The objective was the development of a small, inexpensive, and reliable rocket system for routine observations. The system development is directed toward the measurement of the atmosphere in the 30- to 100-kilometer range by the improvement and development of a system for the 30- to 70-kilometer range and the progressive evolution of successive models to attain the 100-kilometer objective.

The program has resulted in measurements on board the Arcas rocket motor, such as longitudinal acceleration and spin rate; and the improvement of its performance and reliability. One problem was the premature ignition of the forward propellant grain by hot gases and high pressure, causing an explosion at the forward end. This type of failure was analyzed by high-speed film records and recovered motor casings, and the problem was solved by developing another method of sealing the forward end of the

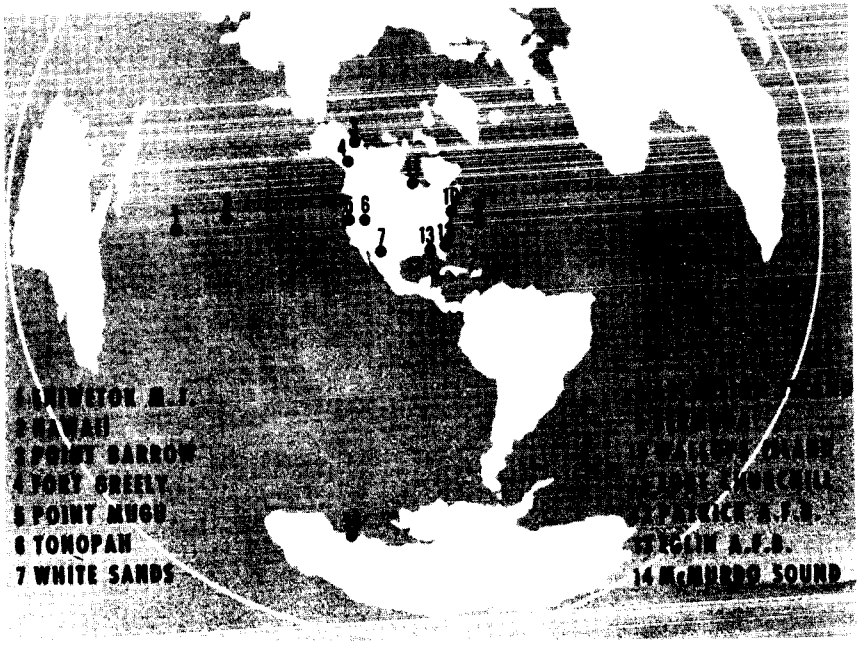

Figure 76.—Location of sites from which small meteorological sounding rockets have been launched since 1959.

motor grain. An analytical study is underway to define the most feasible rocket vehicle for synoptic rocket-sounding purposes, which will be followed by the development of the vehicle defined. In addition, there is a cooperative study with the U.S. Army Missile Command on methods of eliminating the falling-mass hazard associated with small rocket systems. The solution to this problem is a prerequisite of an operational vehicle free from severe launch-site limitations.

Parachute performance is undergoing intensive study, theoretically and also empirically, by photographing the parachute behavior in flight with cameras substituted for the payloads. Some improvement in the parachute performance has been achieved by a reduction in the high spin rate of the vehicle before ejection of the parachute, and by the addition of a swivel between the payload package and the suspension lines of the parachute. High shock loads and hot sparks from the ejection charge also adversely affected the parachute performance. A change in the composition of the propellant reduced the separation load and effectively eliminated the hot sparks. In addition, a design study is underway to develop a parachute with rapid deployment, improved descent rate, and aerodynamic stability,

based on the concept of geometric porosity using a disk-gap-band configuration.

The payload performance has been improved in several areas. A thermistor mounting for the Arcasonde has been developed with leads more resistant to vibration and shock, and reduced aerodynamic and radiofrequency heating of the thermistor. The data telemetry has been made more reliable through the development of a more rugged transmitter tube. The tube now has a greater life expectancy and gives a more stable carrier frequency under acceleration. A new battery pack has been designed with a performance life of 6½ hours, and a shelf life increased six to eight times; that is, the shelf life is about 3 to 4 years. To improve payload performance further, laboratory evaluation of available payload packages is being conducted in the areas of temperature calibration; reaction to spin, shock, and vibration; and antenna field strength.

The complete rocket systems are flight tested at Wallops Island, Va., on a regular basis to provide field-performance data for system development and meteorological data for use by the range and the meteorological community.

RESULTS OF ROCKET PROGRAMS

Large Meteorological Sounding Rockets

The gross features of the mesosphere, such as the steadily declining temperature between 50 and 90 kilometers, were known before the systematic exploration of the upper atmosphere with sounding rockets. During recent years, the rocket-borne experiments have clarified many characteristics of this region and of the stratosphere and thermosphere. It has been learned that there are consistent exceptions to the steady decline of temperature with altitude in the mesosphere, and that the persistent large-scale circulation systems characteristic of the lower mesosphere change their behavior rather abruptly at higher altitudes (refs. 78 and 87).

A large variation in the temperature profile in the 60–90-kilometer region exists between high and low latitudes and between winter and summer in the temperate and northern latitudes (refs. 88–90). Figure 77 is a comparison among typical temperature profiles for high-latitude winter and summer and low-latitude atmospheres. The average temperatures for summer and winter over Wallops Island and their variability from day to day are shown in figure 78. As observed at Fort Churchill, the temperatures above 60 kilometers are higher during the winter than during the summer.

A remarkable, sharp boundary seems to separate the circulation below 80 kilometers from the circulation in the regions where ionization of the atmosphere and dissociation of oxygen set in. This boundary, near 80 kilometers, suggests that the physical causes of atmospheric motions are

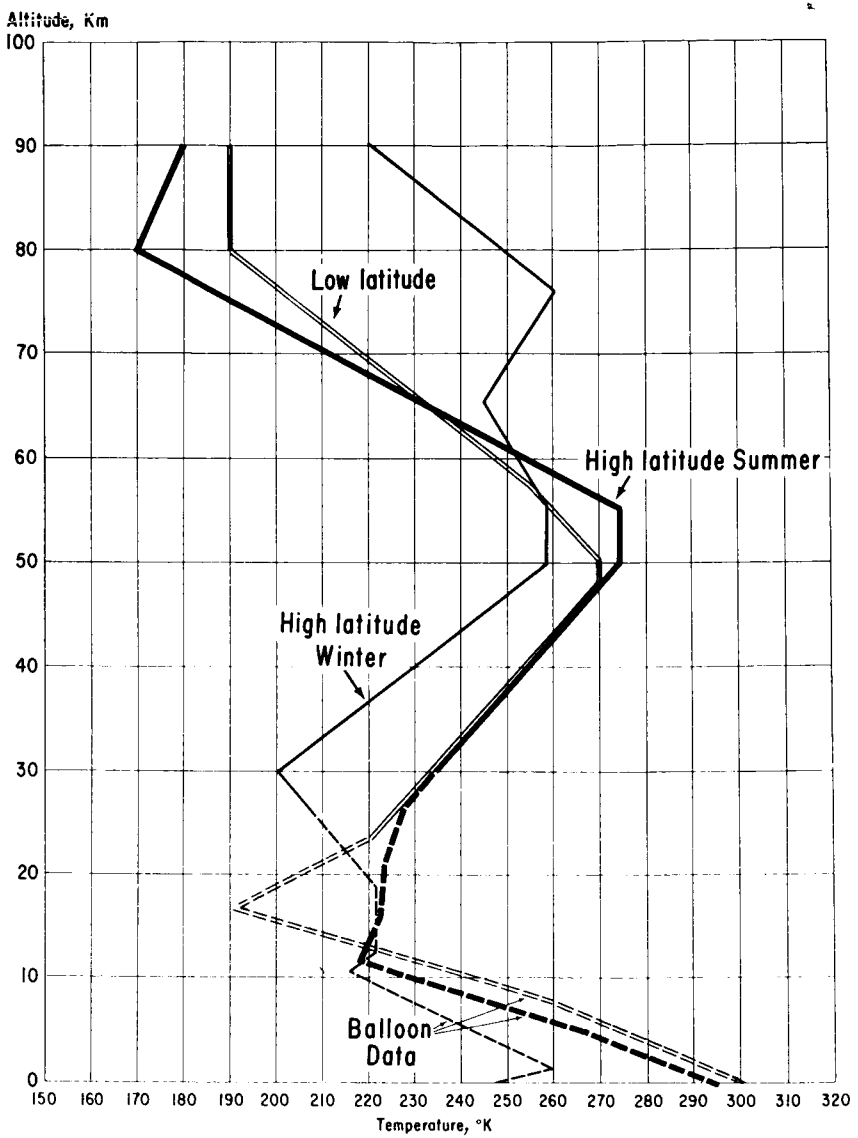

Figure 77.—Comparison of temperature profiles for high-latitude winter and summer atmospheres and low-latitude atmospheres.

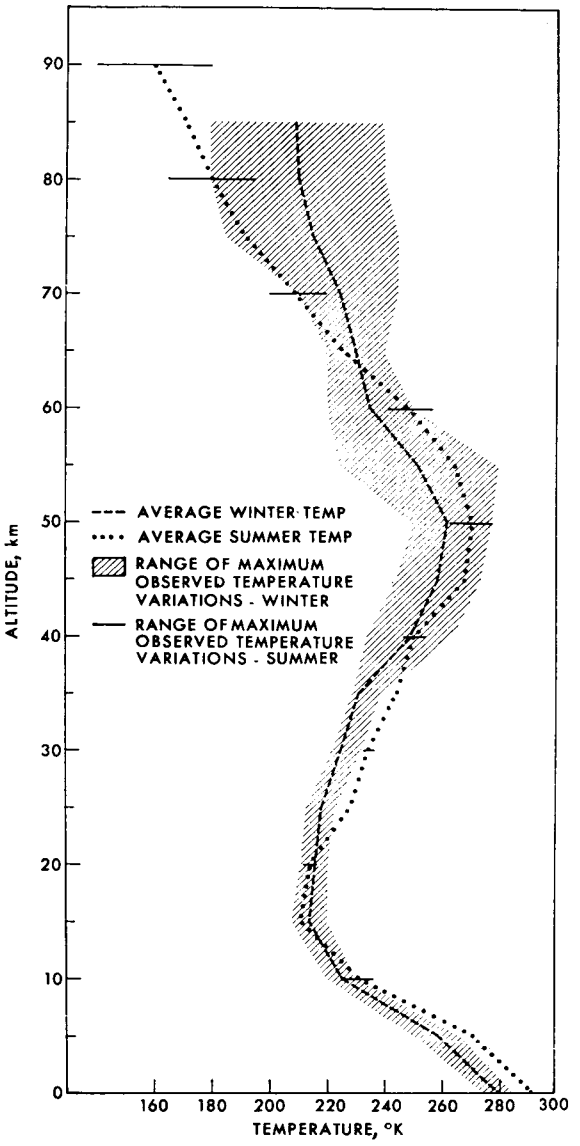

Figure 78.—Average profiles of temperature versus altitude for winter and summer over Wallops Island (38° N). Maximum variation in temperature between soundings is indicated by shading for winter and by horizontal bars for summer soundings.

quite different in the two regions. The winds below 80 kilometers conform to the pattern of uniform zonal flow, and reverse regularly with the season, interrupted only by occasional breakdowns during the spring transition. Above this altitude, however, the flow is no longer uniform and exhibits no regular seasonal pattern. Some features are common, nevertheless, to most of the wind profiles taken above 80 kilometers; namely, the strong but highly variable winds sandwiched between zones of relative calm, resulting in extreme wind shears. Thus far, every sounding conducted has shown these wind shears between 90 and 110 kilometers. Above 120 kilometers, greater uniformity seems to return, but observations at these altitudes are too few to derive any definite circulation patterns.

From the rocket soundings it was observed that at Fort Churchill a breakdown of the winter circulation in the mesosphere and upper statosphere precedes sudden warmings at lower levels. Also, there is a systematic seasonal variation of pressure, temperature, and density at high latitudes, with variations by a factor of 2 in density between winter and summer at 60 kilometers.

During the summers of 1963 and 1964, at Kronogaard, Sweden (66° N), the thermal structure of the atmosphere was measured with acoustic grenades during the presence and absence of noctilucent clouds. These observations indicated a very large variation in temperature at the height of the noctilucent clouds, which could be related to the occurrence of these clouds. For example, on July 29, 1963, a temperature of 130° K was observed at 85 kilometers, which was the height of the noctilucent clouds. This temperature was the lowest ever observed in the atmosphere and was 35° K lower than the temperatures at the same height 3 days later, in the absence of noctilucent clouds.

Small Meteorological Sounding Rockets

With the formation of the cooperative meteorological-rocket network in 1959, the altitude limit for synoptic analysis rose to twice that possible with the existing rawinsonde network. Less than 3 years earlier, as a part of the IGY program, an equally significant upward extension of the hemispheric rawinsonde network was achieved through the application of greatly improved balloons, instruments, and tracking techniques. The upper-air charts up to the 10-millibar (31-kilometer) level that could be constructed with the new rawinsonde data have provided a firm foundation for the analysis of the sparse rocketsonde information.

The major findings from the meteorological-rocket soundings are discussed in reference 91.

The vertical shear of the zonal winds through the 25- to 55-kilometer layer requires a generally decreasing temperature in the horizontal from the

summer pole across the Equator to the winter pole. In the layers above 55 kilometers, the region of the polar night remains warmer than the sunlit regions to the south. Several mechanisms have been proposed to explain this, such as heating by recombination of atomic oxygen, compressional heating by subsidence in polar regions, or horizontal heat transport by eddies in the mesospheric circulation (ref. 92).

The semiannual temperature maximum observed in recent years at 30° N near the 45-kilometer level still demands explanation. However, there is a possibility that this phenomenon will not appear in the monthly averages for 1962 and 1963, in view of the powerful mixing forces that characterized the midwinter circulation of those years.

At rocket altitudes, diurnal and semidiurnal changes of temperature and wind have been shown to increase with height, becoming an order of magnitude larger than those at high rawinsonde levels (ref. 93).

The annual cycle in zonal winds includes a summer period of east winds and a slightly longer winter period of substantially stronger west winds. The autumnal reversal from east to west winds may take place very gradually, with the westerly flow appearing first at high latitudes near the present maximum level of the Meteorological Rocket Network (MRN) soundings and thereafter spreading southward and downward. After the winter westerlies are fully established, they are sometimes replaced within 1 or 2 days over limited areas by easterlies associated with anticyclogenesis at high latitudes. When such interruption by anticyclogenesis takes place before mid-February, the westerlies are generally restored once again. However, in April or May there is a final reversal to the summer easterlies. This spring reversal tends to be more abrupt than that of autumn, taking place in about 10 days, sometimes in the form of a merging of polar anticyclogenesis with the northward-spreading belt of subtropical easterlies.

Marked changeovers to strong easterlies were observed in late January or early February of 1961, 1962, and 1963, but with increasing intensity leading to the huge maximum of 1963. Thus, while the 1961 wind reversal, observed at Wallops Island, scarcely affected the 30-kilometer circulation, the great 1963 reversal dominated the hemisphere, and extended downward to upset the circulation in the low layers of the stratosphere. This year-to-year variation in the amount of cellular activity indicates that the degree of horizontal mixing, and thus, for example, the resulting meridional exchange of tracers like ozone and radionuclides, may vary markedly from one winter to the next (refs. 94–96).

The recent extension of the synoptic stratosphere to 55 or 60 kilometers has revealed other interesting features of the transient systems that move through the upper stratosphere and lower mesosphere. On summer maps, the relatively slight perturbations superimposed upon the circumpolar east-

erly flow are almost undetectable. During the changeover seasons, the winds themselves are weak, but show a relatively large percentage variability. In winter the winds are stronger and the variations, though larger in absolute value, are less on a percent basis. In late January, the variability is particularly large, because of the tendency for a middle-latitude wind reversal, with maximum intensity near 45 kilometers.

There is increasing evidence that 45 kilometers is the source level of the circulation breakdown and sudden heating observed at and below the 10-millibar level during several winters since 1952. Interestingly, this layer of maximum activity coincides with the portion of the ozone layer heated most strongly by solar radiation. The development of strong perturbations at this level is necessary for a large horizontal heat transport from low to high latitudes. This influence of the high stratosphere on the circulation of the lower stratosphere appears to be important in the transport of heat and ozone to the lower stratosphere and their concentration at high latitudes in the colder months of the year.

There is increasing evidence of a close similarity, in vertical motion and horizontal transport, between the tropopause- and stratopause-level jet-streams. Extension of this similarity suggests that the same countergradient heat flux found in the layers just above the tropopause-level jet will be found just above its counterpart at the stratopause. The existence of such a countergradient heat flux in the mesosphere might explain the warmth of the wintertime pole in the layers above 55 kilometers, partially or entirely without recourse to heating by subsidence and recombination.

chapter 4

Summary and Conclusions

METEOROLOGICAL SATELLITES

The achievements of the past 6 years have demonstrated that the meteorological satellite is an important scientific tool. These achievements have been in several areas: (1) meteorological research, using cloud pictures and radiometric data; (2) the technological achievements represented by the capabilities of the spacecraft systems; (3) the application of the data to operational meteorology; and (4) the interest and participation of the world meteorological community in the meteorological-satellite program.

Satellites cloud pictures have been the basis of numerous research projects. This early work confirmed the general existence of highly organized cloud patterns, although specific examples had been seen in rocket photographs. The cloud vortex was the most dramatic of these patterns. Most important, the cloud patterns were found to be characteristic of local atmospheric conditions and could be used, particularly the vortices, to identify and locate storms and frontal systems. Other results are as follows:

Cloud-producing severe local storms were correlated with areas of negative relative vorticity.

Modifications to theoretical cyclone models were made necessary because the vertical-motion field of the atmosphere was shown to be much finer in structure than the fields computed from previous models.

Satellite pictures were used to identify and position jetstreams and associated clouds in data-sparse areas.

Hurricanes appear to be ringed by "outer convective bands" or "pre-hurricane squall lines," separated from the storm itself by clear areas. This fact is important in hurricane-model considerations.

Cloud spirals and cycloids, never before observed, were found in the lee of Madeira and the Canary Islands; some have been shown to be mechanical eddies, but others are yet to be explained.

Research on the so-called cellular patterns has shown that the characteristic width-to-height ratios differ significantly from laboratory results, indicating that all the factors involved have not yet been determined.

Wave patterns observed in clouds do not always agree with theoretically calculated values of wavelength, indicating the inadequacy of current theory.

The radiation measurements provide information on the global distribution of energy sources and sinks and the heat budget of the Earth-atmosphere system. The data permit the following:

(1) Derivation of the time variations in the latitudinal averages of the net energy balance in the atmosphere.
(2) Mapping of the large-scale distribution of cloud patterns, both day and night, along with cloud-top height.
(3) Estimation of the distribution of water vapor in the upper troposphere, and almost global measurements of mean stratospheric temperatures.

The TV and radiometer data from the meteorological satellites form a vast body of information for current and future meteorological research. The TV pictures are being used in many investigations, including the following:

(1) Formation and development of tropical storms.
(2) Circulation patterns and vortex formation in the extratropical regions.
(3) Relation between large-scale vertical motion and cloud systems.
(4) Large-scale circulation in both tropical and extratropical regions.

In addition to macroscale research, the data are being utilized in mesoscale analyses—

(1) Of mesoscale flow patterns, in conjunction with laboratory simulation.
(2) Of eddy flow patterns in the lee of obstacles.
(3) Of orographic cloud systems.
(4) In conjunction with cloud physics research.

The satellite data from areas of sparse conventional data are incorporated into research through correlation of satellite and conventional data in areas where the conventional data are adequate.

The technological capabilities of the spacecraft systems are reflected in the successful launches and operations in orbit and in the measurements obtained. There have been nine successful satellite launches and operations in nine attempts; that is, eight Tiros and one Nimbus. Tiros VII and VIII have exceeded expectations in length of performance. As of December 1964, they have been operating continuously for 18 and 12 months, respectively, and are still operating.

Moreover, the technological capabilities of the meteorological satellite have been improved. The first meteorological satellite was spin-stabilized and provided cloud pictures between about 48° N and 48° S latitudes, while the cameras were facing the Earth, during the daylight hours. Tiros *I*, however, is planned to have an almost-polar orbit and a cartwheel mode, spinning about an axis at right angles to the orbital plane. This mode will

provide global TV cloud-picture coverage daily. The Tiros *I* flight will test the feasibility of this concept for the TOS system. The flight of Nimbus I in a polar orbit established the practicability of a stabilized, Earth-oriented spacecraft and the use of an HRIR system to observe cloud cover during the night.

Real-time accessibility of cloud-cover information was provided by the APT system, which was flown on Tiros VIII and Nimbus I. The radiation characteristics of the Earth and atmosphere have been measured by several types of radiation sensors. LRIR measured the radiation reflected from the Earth and atmosphere and the total infrared emission of the Earth and atmosphere. The five-channel MRIR measured, with a 50- to 60-kilometer resolution, reflected and emitted radiation in five spectral regions, some of which overlapped. Both LRIR and MRIR were flown on Tiros II, III, IV, and VII. The MRIR on Tiros VII for the first time had a radiometer channel responsive to the 15-μ carbon dioxide region and measured stratospheric temperatures. The HRIR aboard Nimbus I operated with an 8-kilometer resolution, providing night cloud-cover pictures and temperatures of the radiating surfaces (Earth and cloud top), with an accuracy of 2° K.

The meteorological-satellite data have also been applied to operational meteorology. Within 60 hours after Tiros I was launched, cloud analyses based on the satellite cloud pictures were used in weather analyses and forecasts. Furthermore:

(1) Where conventional meteorological data are available, the satellite data serve to modify the interpretation of the analyses already prepared.

(2) In data-sparse areas, the satellite data are used on an equal basis with other observations.

(3) Cloud pictures have been used to detect and locate tropical storms and typhoons, and have tracked them and aided in the forecast of their movement.

(4) Satellite pictures have been used to show jetstreams and shear lines, which are of importance in the identification of areas likely to contain clear-air turbulence.

(5) Satellite pictures have shown mesoscale cloud features not discernible from single-station observations, or not deductible from the combined data from several neighboring stations.

The satellite TV pictures have been used to follow in detail many nonmeteorological features, including the location and movement of sea ice, the freezeup and the breakup of ice in major rivers and lakes, the extent of snow cover, the height of the snowline, and variations in the extent of

swamps and flooded areas. The synoptic weather patterns from Tiros nephanalyses, and the satellite pictures themselves, have been used on several occasions in conjunction with surface meteorological observations to forecast the migration of swarms of the desert locust. The Nimbus I HRIR data have been used to estimate sea-surface temperatures in cloud-free areas. Undoubtedly, the nonmeteorological applications, such as the detection of forest fires and volcanic activity, will continue to increase.

From the outset of the meteorological-satellite program, the results have been shared with other countries. The analyzed results of the picture data are transmitted internationally to assist forecasters everywhere. In November 1961, an International Meteorological Satellite Workshop was conducted, in which about 40 representatives from some 30 countries participated. At the workshop, the results of the satellite activity and the possibilities for the future were presented. It was also expected that the participants might acquire a working knowledge of meteorological-satellite data for use in research and operations.

A workshop on the Uses of Weather Satellite Data in Tropical Meteorology was conducted at Florida State University in February 1963, with 60 persons attending. The material presented concerned both operations and basic research in tropical meteorology. Laboratory sessions were conducted in which satellite data were used by the participants under the supervision and guidance of investigators experienced in that phase of work. The large ocean areas and the general sparsity of data in the Tropics make satellite data particularly valuable for such studies.

Under the auspices of the World Meteorological Organization (WMO), an Interregional Seminar on the Interpretation and Use of Meteorological Satellite Data was held in Tokyo, November 27 through December 8, 1964. The conventional TV pictures, APT pictures, and radiometric data were discussed and studied. The participants came from many of the Asian countries and those bordering the Pacific Ocean. Especially keen interest was shown in the APT system, which provides direct readout from the satellite to the users, and in the HRIR, which provides cloud-cover pictures from the dark side of the Earth.

The flight of APT on Tiros VIII and Nimbus I provided an opportunity for active participation in the meteorological-satellite experiments. Some 12 countries purchased or built APT receivers, and obtained real-time pictures of local cloud cover for use in their meteorological services and research.

Meteorological Sounding Rockets

During recent years, meteorological sounding-rocket activity has clarified many characteristics of the atmosphere between 30 and 100 kilometers.

The large meteorological sounding rockets for exploring the atmosphere in the 50- to 100-kilometer region have improved, from the complex V–2 and Aerobee to the more easily handled and less expensive Nike-Cajun. These, although still too large and complex for routine synoptic observations, permit periodic observations from several sites. The program has developed a capability for observations from four sites, ranging from the Arctic to the Tropics, supplemented by special launches from other countries and from aboard ship.

These soundings have shown—

(1) The existence of large variations in the 60–90-kilometer temperature profile between high and low latitudes, and between winter and summer in the temperate and the northern latitudes, along with higher winter temperatures in the northern areas than at lower latitudes.

(2) The existence of different circulation patterns below and above 80 kilometers, suggesting that the physical causes of the motions may be quite different in the two regions.

(3) That a breakdown in the winter circulation in the mesosphere and upper stratosphere precedes the occurrence of sudden warming phenomena at lower levels.

The small meteorological sounding rockets that now provide measurements of the atmosphere in the 30- to about 60-kilometer range have potential for the development of a truly synoptic network. From the initial 2 launch sites in 1959, there has evolved a cooperative network of 8 to 10 sites, using mainly Arcas- and Loki-type sounding rockets. There has been considerable improvement in rocket technology which has made the coordination of the launches feasible.

The analyses of the wind data from these soundings indicate that—

(1) The vertical shear of the zonal winds from 25 to 55 kilometers requires a generally decreasing temperature in the horizontal from the summer pole across the Equator to the winter pole.

(2) In the midlatitudes the annual cycle in the zonal winds includes a summer period of east winds and a slightly longer winter period with stronger west winds.

(3) The autumn reversal may take place gradually, appearing first in high latitudes and altitudes and spreading southward and downward, but the spring reversal tends to be more abrupt.

(4) In recent years, there has been a semiannual temperature maximum near the 45-kilometer level at 30° N.

(5) The 45-kilometer level may be the source of the circulation breakdown and sudden heating that has been observed at and below the 10-millibar level during several winters since 1952.

There is increasing evidence of a similarity in vertical-motion and horizontal transport between the tropopause- and stratopause-level jetstreams. Extension of this similarity suggests that the same countergradient heat flux found in the layers just above the tropopause jet will be found just above its counterpart at the stratopause.

Significant Questions and Outlook

Despite the wealth of data that meteorological satellites and sounding rockets have yielded, there are many questions in research and operations that remain unanswered because of inadequate information. Both operations and research require a three-dimensional picture of the atmosphere and its motions. Fortunately, both operations and research require, in general, information on the same parameters, with operations having the added requirement of timeliness of the data.

A recent WMO document (ref. 97) identified some of the areas in meteorology that require extensive investigations. There is a strong demand for improved detailed knowledge of the space and time variations in the structure of the atmosphere. This is related to the problems of the interaction between upper and lower atmospheric layers and the interaction of the Earth's surface and the atmosphere. The problem of the general circulation has great practical importance, and involves consideration of the budgets of energy, momentum, and water vapor.

The Sun's variability produces fluctuations in the motions and physical state of the atmosphere above 70 kilometers, and research on the influence of variable solar activity on the lower levels of the atmosphere is essential. Numerical prediction and atmospheric model development depends on these previously mentioned areas and on the provision of a better network of data. Weather modification also depends on these research areas, for it is only when our understanding of changes in energy sources, albedo, etc., and of the ocean-atmosphere linkage is much improved over the present, in a fully quantitative manner, that any real prospect of large-scale artificial modification will be opened up.

Some of the requirements will be met through the improvement of the spacecraft as an observation platform; for example, its mode of operation, sensor developments to extend the observational capabilities, increased power supply, digitization and compression of the data, increased memory capacity, and direct-readout capability. The cartwheel configuration in a polar orbit is a step toward an operational capability that will lead to further improvements, along with the operations of and experiments aboard the Nimbus satellites. The utilization of synchronous meteorological satellites is another means of improving the satellite operation.

A greater geographic and time coverage will evolve naturally from the improvement of the satellite as an observation platform. Combining this with timely acquisition of the data, as was demonstrated with the APT system on Tiros VIII and Nimbus I, will give the operational meteorologists direct access to information on the current state of the atmosphere.

The Nimbus I satellite as a meteorological observatory is the means of developing, testing, and improving sensors for extending the capabilities of the meteorological satellites. The development of satellite-borne grating and interference spectrometers will permit the measurement of the thermal structure of the atmosphere. The microwave region holds promise for the measurement of cloud water content, ocean temperature and possibly the sea state, and thermal structure. Radiometers operating in the ultraviolet region will provide measurements of ozone distribution and information on incoming solar radiation.

The use of meteorological satellites for the detection, location, and measurement of such phenomena as sferics will supplement other data on the location and intensity of storm activity. This combination of the meteorological satellite with fixed and mobile platforms at the surface of the Earth and immersed in the atmosphere is another valuable technique. The sensors aboard the platforms will measure the atmosphere parameters, while the satellite will locate and interrogate the platforms and record the measurements for transmission.

The data from the meteorological sounding rockets have added greatly to the knowledge and description of the upper atmosphere. This knowledge is based on sparse data coverage and relatively infrequent observations, and most of the basic questions still remain to be answered. The interactions between and among the regions of the atmosphere, the circulation and thermodynamics of the atmosphere, the relationship between solar-energy input and its meteorological effects, and other questions still require research and more data.

In the field of atmospheric physics, the cause of the high temperatures and their great variability above 60 kilometers during the wintertime remains one of the most outstanding questions.

Thus, one of the tasks is to increase the geographic coverage with the meteorological-rocket soundings, by soliciting the cooperation of more individual launch sites all over the globe. More synoptic soundings throughout the atmosphere will also enable us to determine the interaction between various circulation regimes in the atmosphere, and may possibly lead to discovery of a mechanism for the downward propagation of solar-terrestrial energy. The similarities and differences in the upper-atmospheric circulation patterns and changes in patterns between the Northern and Southern Hemispheres are importat manifestations of the dynamics of the atmosphere,

207-342 O-66—10

and are related to the development of global atmospheric models. The approximate 26-month cycle in the upper-air tropical winds still remains an open question. As yet there is not sufficient evidence to determine properly the variation in amplitude of this oscillation above the balloon altitudes or its longitudinal variation. The amplitude is known to increase up to 25 kilometers, but there is presently only fragmentary evidence. Speculation is that this increase may not continue beyond 30 kilometers and may possibly decrease above this altitude.

However, before there can be an adequate increase in the meteorological sounding-rocket observations, which is a prerequisite to the research and development of atmospheric models, an inexpensive sounding-rocket system must be developed that is capable of reliable routine observations.

When one views the significant contributions made by meteorological satellites and sounding rockets to date and the advancements in technology, there is every reason to believe that an orderly and well-planned, progressive program will lead to early answers to many of the still unanswered questions. Most certainly, an objective of making the satellite a meteorological observatory in space will result in more and better data, with improved sensors, instrumentation, and measuring techniques. A continuing R&D program will push technology forward, with a corresponding advance in scientific achievements. Also, the initiation of a worldwide, operational meteorological-satellite system and a worldwide, operational meteorological sounding-rocket network will result in a wealth of data to upgrade weather prediction and forecasting.

References

1. GREENFIELD, S. M.; AND KELLOGG, W. W.: Inquiry Into the Feasibility of Weather Reconnaissance From a Satellite Vehicle. Rand Corp., Aug. 1960.
2. HUBERT, L. F.; AND BERG, O.: A Rocket Portrait of a Tropical Storm. Monthly Weather Rev., vol. 83, June 1955.
3. FRITZ, SIGMUND: Pictures From Meteorological Satellites and Their Interpretation. Space Science Reviews, vol. 3, 1964, pp. 541–580.
4. STAMPFL, R. A.; AND STROUD, W. G.: The Automatic Picture Transmission (APT) TV Camera System for Meteorological Satellites. NASA X–650–63–77, Apr. 1963.
5. ANON.: Tiros—A Story of Achievement. Astro-Electronics Division, Radio Corp. of America, Feb. 28, 1964.
6. ANON.: Proc. International Meteorological Satellite Workshop (Washington, D.C., Nov. 13–22, 1961). NASA and U.S. Dept. of Commerce, Weather Bureau, 1962.
7. TEPPER, M.: Meteorological Satellites. Space Exploration (D. P. LeGalley and J. W. McKee, eds.), McGraw-Hill Book Co., 1964, pp. 386–427.
8. BARTKO, F.; ET AL.: The Tiros Low Resolution Radiometer. NASA TN D–564, 1964.
9. NORDBERG, W.; ET AL.: Preliminary Results of Radiation Measurements From the Tiros III Meteorological Satellite. NASA TN D–1338, 1962.
10. DAVIS, J. F.; ET AL.: Telemetering Infrared Data From the Tiros Meteorological Satellites. NASA TN D–1293, 1962.
11. ALLISON, L. J.; AND NEIL, E. A., EDS.: Final Report on the Tiros I Meteorological Satellite System. NASA TR R–131, 1962.
12. ANON.: Mission Operation Report, Nimbus A Meteorological Satellite Project. NASA Hq. Rept. No. S–604–64–01, July 28, 1964.
13. PRESS, H.; ET AL.: Proceedings of the Nimbus Program Review. NASA TM X–650–62–226, Nov. 1962.
14. JOHNSON, D. S.; HALL, W. F.; AND BRISTOR, C. L.: Nimbus Data in Operational Meteorology. Astronaut. Aerospace Eng., vol. 1, no. 3, Apr. 1963.
15. NORDBERG, W.; AND PRESS, H.: The Nimbus I Meteorological Satellite. Bull. Am. Meteorol. Soc., vol. 45, no. 11, Nov. 1964.
16. JONES, JAMES; and MACE, LEE M.: Tiros Meteorological Operations. Astronaut. Aerospace Eng., vol. 1, no. 3, Apr. 1963, p. 32.
17. WEXLER, H.; AND JOHNSON, D. S.: Meteorological Satellites. Bull. At. Scientists, vol. 17, nos. 5–6, May–June 1961.
18. JONES, J. B.: A Western Atlantic Vortex Seen by Tiros I. Monthly Weather Rev., vol. 89, Oct. 1961.
19. RUTHERFORD, G. T.: Synoptic Applications of Nephanalyses From Artificial Satellites. Australian Meteorol. Mag., no. 32, Mar. 1962, pp. 1–17.

20. ANON.: Research Progress and Plans, Meteorological Satellite Activities, U.S. Weather Bureau, FY 1962. U.S. Dept. of Commerce-Weather Bureau, 1961.
21. ANON.: Research Progress and Plans of the U.S. Weather Bureau, FY 1963. U.S. Dept. of Commerce-Weather Bureau, 1962.
22. TEPPER, M.: Meteorological Satellite Flight Program. NASA Program Management Rept., Sept. 1964.
23. WIEGMAN, ELDON J.; ET AL.: Atlas of Cloud Vortex Patterns Observed in Satellite Photography. Stanford Research Institute, Apr. 1964.
24. ANON.: Research Progress and Plans of the U.S. Weather Bureau, FY 1964. U.S. Dept. of Commerce-Weather Bureau.
25. ANON.: Reduction and Use of Data Obtained by Tiros Meteorological Satellites. World Meteorological Organization Tech Note 49, 1963.
26. KRUEGER AND FRITZ: Cellular Cloud Patterns Revealed by Tiros I. Tellus, vol. 13, 1961, pp. 1–7.
27. GRAHAM: Shear Patterns in an Unstable Layer of Air. Phil. Trans. Roy. Soc. London (A), vol. 232, 1934.
28. ROY, D.; AND SCORER, R. S.: Studies of Cellular Convection With Special Reference to the Atmosphere. Imperial College, London, 1962.
29. HUBERT, L. F.; AND KRUEGER, A. F.: Satellite Pictures of Mesoscale Eddies. Monthly Weather Rev., vol. 90, 1962.
30. FRITZ, S.: Satellite Pictures and Origin of Hurricane Anna. Monthly Weather Rev., vol. 90, no. 12, Dec. 1962, pp. 507–513.
31. FRITZ, S.: Research With Satellite Cloud Pictures. Astronaut. Aerospace Eng., vol. 1, no. 3, Apr. 1963, pp. 70–74.
32. ERICKSON, C. O.: An Incipient Hurricane Near the West African Coast. Monthly Weather Rev., vol. 91, no. 2, Feb. 1963.
33. YANAI, M.: A Detailed Analysis of Typhoon Evolution. J. Meteorol. Soc. Japan, ser. 3, vol. 39, 1961.
34. FALLER, A. J.: An Experimental Analogy to and Proposed Explanation of Hurricane Spiral Bands. Proc. Second Tech. Conf. on Hurricanes, June 27–30, 1961 (Miami), Rept. 50, Part II, Hurricane Research Project, U.S. Weather Bureau, Mar. 1962.
35. DÖÖS, B. R.: A Theoretical Analysis of Lee Wave Clouds Observed by Tiros I. Tellus, vol. 14, 1962, pp. 301–309.
36. OLIVER, V. J.; ET AL.: Some Examples of the Detection of Jet Streams From Tiros Photographs. Monthly Weather Rev., vol. 92, no. 10, Oct. 1964, pp. 441–448.
37. BYERS, H. R.; AND BATTAN, J. L.: Some Effects of Vertical Wind Shear on Thunderstorm Structure. Bull. Am. Meteorol. Soc., vol. 30, no. 5, May 1949, pp. 168–175.
38. BYERS, H. R.; AND BRAHM, R. R., JR.: The Thunderstorm. U.S. Weather Bureau, June 1949.
39. MALKUS, J. S.: Effects of Wind Shear on Some Aspects of Convection. Trans. Am. Geophysical Union, vol. 30, no. 1, Feb. 1949, pp. 19–25.
40. MALKUS, J. S.: The Slopes of Cumulus Clouds in Relation to the External Wind Shear. Quart. J. Roy. Meteorol. Soc., vol. 78, no. 338, Oct. 1952, pp. 530–542.
41. ERICKSON, C. O.: Satellite Photographs of Convective Clouds and Their Relation to the Vertical Wind Shear. Monthly Weather Rev., vol. 92, no. 6, June 1964, pp. 283–296.
42. FETT, R. W.: Aspects of Hurricane Structure: New Model Considerations Suggested by Tiros and Project Mercury Observations. Monthly Weather Rev., vol. 92, no. 2, Feb. 1964, pp. 43–60.

43. FRITZ, S.: U.S. Special Meteorological Studies for the IGY. Geophysics and the IGY (Hugh Odishaw and Stanley Ruttenberg, eds.), Geophysics Monograph No. 2, Am. Geophys. Union, 1958, pp. 161–168.
44. MALONE, T. F., ED.: Compendium of Meteorology. Am. Meteorol. Soc., 1951.
45. WEINSTEIN, M.; AND SOUMI, V. E.: Analysis of Satellite Infrared Radiation Measurements on a Synoptic Scale. Monthly Weather Rev., vol. 89, no. 11, Nov. 1961.
46. NORDBERG, W.; ET AL.: Stratospheric Temperature Patterns Based on Radiometric Measurements From the Tiros VII Satellite. NASA TN D–2798, 1964.
47. BANDEEN, W. R.; ET AL.: A Radiation Climatology in the Visible and Infrared From the Tiros Meteorological Satellites. NASA Goddard Space Flight Center, Rept. X–651–64–218, Aug. 1964.
48. NORDBERG, W.: Research with Tiros Radiation Measurements. Astronaut. Aerospace Eng., vol. 1, no. 3, Apr. 1963, pp. 76–83.
49. FRITZ, S.; AND WINSTON, J. S.: Synoptic Use of Radiation Measurements From Satellite Tiros II. Monthly Weather Rev., vol. 90, no. 1, 1962.
50. NORDBERG, W.; BANDEEN, W. R.; CONVATH, B. J.; ET AL.: Preliminary Results of Radiation Measurements From the Tiros III Meteorological Satellite. J. Atmos. Sci., vol. 19, no. 1, Jan. 1962, pp. 20–29.
51. WINSTON, J. S.; AND RAO, P. K.: Temporal and Spatial Variations in the Planetary Scale Outgoing Long-Wave Radiation as Derived From Tiros II Measurements. Monthly Weather Rev., vol. 91, Oct.–Dec. 1963, pp. 641–657.
52. FUJITA, T.; ET AL.: Meteorological Interpretation of Convective Nephsystems in Tiros Cloud Photographs. Res. Rept. No. 9, Univ. of Chicago, Apr. 1962.
53. FUJITA, T.; AND ARNOLD, J.: The Decaying Stage of Hurricane Anna of July 1961, as Portrayed by Tiros Cloud Photographs and Infrared Radiation From the Top of the Storm. Mesometeorology Project, Res. Paper No. 28, Univ. of Chicago, Nov. 1963.
54. PEDERSEN, F.; AND FUJITA, T.: Synoptic Interpretation of Tiros III Measurements of IR Radiation. Res. Paper No. 19, Univ. of Chicago, Oct. 1963.
55. MÖLLER, F.; AND RASCHKE, E.: Evaluation of Tiros III Radiation Data. Interim Rept. No. 1, Ludwig-Maximilians-Universität, Meteorologisches Institut, München, Germany, July 1963.
56. MÖLLER, F.: Some Preliminary Evaluation of Tiros II Radiation Measurements. Universität München, Meteorologisches Institut, Jan. 15, 1962.
57. MANABE, S.; AND MÖLLER, F.: The Radiative Equilibrium and Heat Balance of the Atmosphere. Monthly Weather Rev., vol. 89, no. 12, Dec. 1961, pp. 503–532.
58. LONDON, J.: A Study of the Atmospheric Heat Balance. Final Rept., Contract No. AF 19(122)–165, Dept. of Meteorology and Oceanography, N.Y. Univ., 1957.
59. MÖLLER, F.: Atmospheric Winter Vapor Measurements at 6–7 Microns From a Satellite. Planet. Space Sci., vol. 5, 1961, pp. 202–206.
60. MÖLLER, F.; AND RASCHKE, E.: Evaluation of Tiros III Radiation Data. Interim Rept. No. 1, 1963 and Final Rept., 1964. NASA Research NsG–305, Meteorolog. Institut der Universität München.
61. GOLDBERG, I. L.; ET AL.: Nimbus High Resolution Infrared Measurements. Proc. Third Sym. on Remote Sensing of Environment. Inst. of Sci. and Tech., Univ. of Michigan (Ann Arbor, Mich.), Oct. 1964.
62. KENNEDY, J.: Nimbus I Preliminary Results. Paper presented at the American Geophysical Union Meeting (Seattle), Dec. 1964.

63. ANON.: The Use of Meteorological Satellite Data in Analysis and Forecasting. USWB Tech. Note No. 13, Nov. 1963.
64. ANON.: First Report on the Advancement of Atmospheric Sciences and Their Application in the Light of Developments in Outer Space. Secretariat, World Meteorological Organization, Geneva, Switzerland, 1962.
65. ANON.: Second Report on the Advancement of Atmospheric Sciences and Their Application in the Light of Developments in Outer Space. Secretariat, World Meteorological Organization, June 1963.
66. ANON.: An Outline of International Programs in the Atmospheric Sciences. Report by the Ad Hoc Committee on International Programs in Atmospheric Sciences and Hydrology. Nat. Academy of Sci.-Nat. Res. Council Pub. No. 1085, 1963.
67. SINGER, S. F.; AND POPHAM, R. W.: Non-Meteorological Observations From Weather Satellites. Astronaut. Aerospace Eng., Apr. 1963.
68. WARK, D. Q.; AND POPHAM, R. W.: Ice Photography From the Meteorological Satellites Tiros I and Tiros II. Rept. No. 8, Meteorological Satellite Lab., Mar. 1962.
69. SINGER, S. F.: Forest Fire Detection From Satellites. J. Forestry, vol. 60, no. 12, Dec. 1962.
70. AUFM KAMPE, H. J.: Evolution of Upper Air Meteorology. J. Am. Rocket Soc., vol. 31, no. 8, Aug. 1961, pp. 1047–1059.
71. TEWELES, S.: Time Section and Hodograph Analysis of Churchill Rocket and Radiosonde Winds and Temperature. Monthly Weather Rev., vol. 19, no. 4, Apr. 1961, pp. 125–136.
72. TEWELES, S.; ET AL.: Circulation at 10-mb Constant Pressure Surface Over N. America and Adjacent Areas, July 1957 Through June 1958. Monthly Weather Rev., vol. 88, no. 4, Apr. 1960, pp. 137–149.
73. HARE, F. K.: The Disturbed Circulation of the Arctic Stratosphere. J. Meteorol., vol. 17, 1960, pp. 36–51.
74. VIEZEE, W.: The Mean Circulation of the Equatorial Stratosphere. Final Rept., Contract No. AF 19(604)–2134, Inst. of Geophysics, Univ. of Calif., Aug. 1958.
75. REED, R. J.; ET AL.: Evidence of a Downward Propagating Annual Wind in the Equatorial Stratosphere. J. Geophys. Res., vol. 66, no. 3, Mar. 1961, pp. 813–818.
76. ANGELL, J. K.; AND KORSHOVER, J.: Biennial Wind and Temperature Oscillations of the Equatorial Stratosphere and Their Possible Extension to Higher Latitudes. Monthly Weather Rev., vol. 90, no. 4, Apr. 1962, pp. 127–132.
77. THE ROCKET PANEL: Pressures, Densities, and Temperatures in the Upper Atmosphere. Phys. Rev., vol. 88, 1952, pp. 1027–1032.
78. STROUD, W. G.; ET AL.: Rocket-Grenade Measurements of Temperature and Winds in the Mesosphere Over Churchill, Canada. J. Geophys. Res., vol. 65, 1960, pp. 2307–2323.
79. JONES, L. M.; AND BARTMANN, F. L.: Simplified Falling-Sphere Method for Upper-Air Density. Univ. of Mich. Eng. Research Inst. Rept. 2215–10–T, 1956.
80. LA GOW, H. E.; ET AL.: Rocket Measurements of the Arctic Upper Atmosphere. Nat. Acad. Sci. IGY Rocket Rept., ser. 1, 1958, pp. 27–37.
81. NORDBERG, W.; AND STROUD, W. G.: Results of IGY Rocket Grenade Experiments to Measure Temperatures and Wind Above the Island of Guam. J. Geophys. Res., vol. 66, Feb. 1961, pp. 455–464.

82. NORDBERG, W.; AND SMITH, W.: The Rocket Grenade Experiment. NASA TN D–2107, 1964.
83. ANON.: Initiation of the Meteorological Rocket Network, Revised August 1961. Inter-Range Instrumentation Group-Meteorological Working Group Report No. 105–60, Aug. 1961.
84. WEBB, W. L.; ET AL.: Inter-Range Instrumentation Group Participation in the Meteorological Rocket Network. Bull. Am. Meteorol. Soc., vol. 43, no. 12, Dec. 1962, pp. 640–649.
85. ANON.: Data Reports of the Meteorological Network Firings. Inter-Range Instrumentation Group-Meteorological Working Group Series, U.S. Army Electronics Research and Development Activity, White Sands Missile Range, Docs. 109–62, 1960–1964.
86. ANON.: The USAF Meteorological Rocket Network, a Status Report. USAF Fourth Weather Group Rept. 105–7–4, July 1963.
87. NORDBERG, W.: Rocket Soundings in the Mesosphere. Meteorological Observations Above 30 km. NASA SP–49, 1964, pp. 37–57.
88. NORDBERG, W.; AND STROUD, W. G.: Seasonal, Latitudinal, and Diurnal Variations in the Upper Atmosphere. NASA TN D–703, 1961.
89. NORDBERG, W.; AND SMITH, W.: Preliminary Measurements of Temperatures and Winds Above 50 km Over Wallops Island, Va. NASA TN–1694, 1963.
90. NORDBERG, W.; AND SMITH, W.: Rocket Measurements of the Structure of the Upper Stratosphere and Mesosphere. NASA TM X–651–63–66, 1963.
91. TEWELES, S.: Application of Meteorological Rocket Network Data. Meteorological Observations Above 30 km, NASA SP–49, 1964, pp. 15–36.
92. KELLOGG, W. W.: Chemical Heating Above the Polar Mesopause in Winter. J. Meteorol., vol. 18, 1962, pp. 373–381.
93. LENHARD, R. W.: Variation of Hourly Winds at 35 to 65 km During One Day at Eglin AFB, Fla. J. Geophys. Res., vol. 68, no. 1, 1963, pp. 227–234.
94. BELMONT, A. D.: The Reversal of Stratospheric Winds Over North America during 1957, 1958, and 1959. Berträge zur Physik der Atmosphäre, vol. 35½, 1962, pp. 126–140.
95. FINGER, F. G.; ET AL.: Synoptic Analysis Based on Meteorological Rocketsonde Data. J. Geophys. Res., vol. 68, no. 5, 1963, pp. 1377–1399.
96. FINGER, F. G.; AND TEWELES, S.: The Mid-Winter 1963 Stratospheric Warming and Circulation Change. J. Meteorol., vol. 3, no. 1, 1964, pp. 1–15.
97. ANON.: Third Report on the Advancement of Atmospheric Sciences and Their Application in the Light of Developments in Outer Space. World Meteorological Organization, Aug. 1964.

U.S. GOVERNMENT PRINTING OFFICE: 1966 O—207–342

"The aeronautical and space activities of the United States shall be conducted so as to contribute . . . to the expansion of human knowledge of phenomena in the atmosphere and space. The Administration shall provide for the widest practicable and appropriate dissemination of information concerning its activities and the results thereof."

—NATIONAL AERONAUTICS AND SPACE ACT OF 1958

NASA SCIENTIFIC AND TECHNICAL PUBLICATIONS

TECHNICAL REPORTS: Scientific and technical information considered important, complete, and a lasting contribution to existing knowledge.

TECHNICAL NOTES: Information less broad in scope but nevertheless of importance as a contribution to existing knowledge.

TECHNICAL MEMORANDUMS: Information receiving limited distribution because of preliminary data, security classification, or other reasons.

CONTRACTOR REPORTS: Technical information generated in connection with a NASA contract or grant and released under NASA auspices.

TECHNICAL TRANSLATIONS: Information published in a foreign language considered to merit NASA distribution in English.

SPECIAL PUBLICATIONS: Information derived from or of value to NASA activities. Publications include conference proceedings, monographs, data compilations, handbooks, sourcebooks, and special bibliographies.

TECHNOLOGY UTILIZATION PUBLICATIONS: Information on technology used by NASA that may be of particular interest in commercial and other nonaerospace applications. Publications include Tech Briefs; Technology Utilization Reports and Notes; and Technology Surveys.

Details on the availability of these publications may be obtained from:

SCIENTIFIC AND TECHNICAL INFORMATION DIVISION

NATIONAL AERONAUTICS AND SPACE ADMINISTRATION

Washington, D.C. 20546